



FLUORESCENCE
FOUNDATION

Principles of Fluorescence Techniques

Urbana-Champaign, Illinois

April 15-18, 2024

Basic Fluorescence Principles I: David Jameson
Overview, Excitation and Emission Spectra,
Quantum Yields, Polarization/Anisotropy

What is fluorescence?

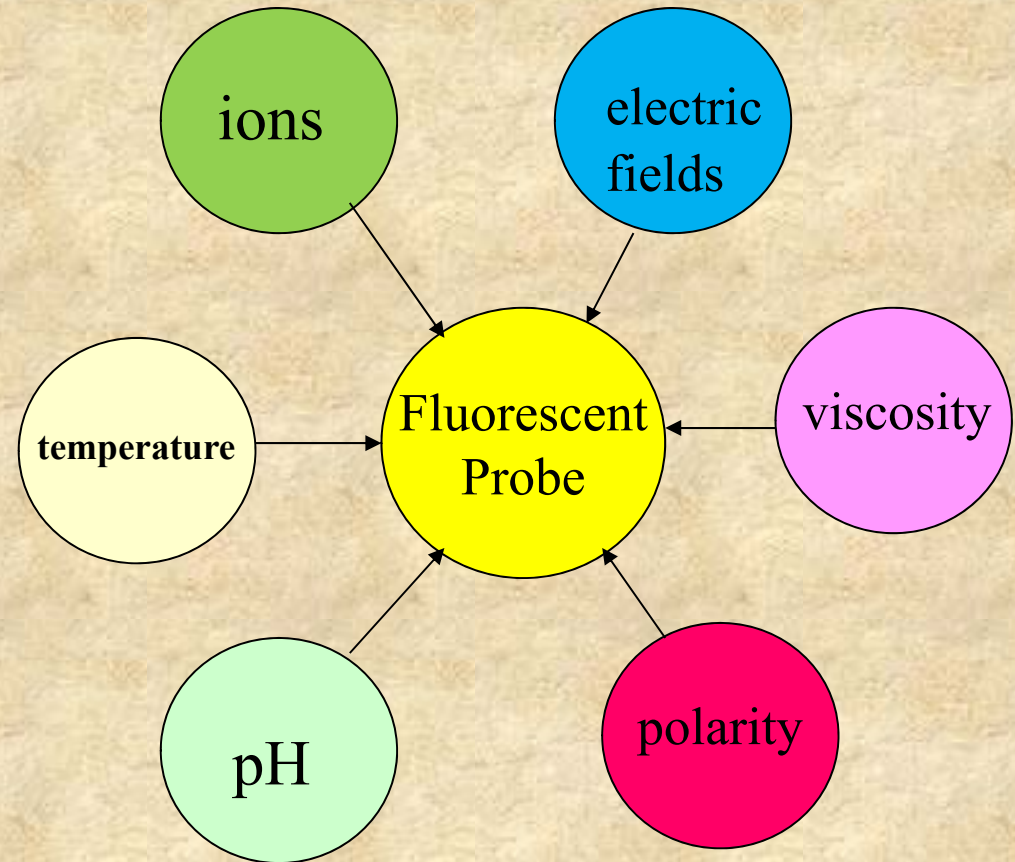
FLUORESCENCE is the light emitted by an atom or molecule after a finite duration subsequent to the absorption of electromagnetic energy.

Specifically, the emitted light arises from the transition of the excited species from its first excited electronic singlet level to its ground electronic level. (**usually**)

The development of highly sophisticated fluorescent probe chemistries, new laser and microscopy approaches and site-directed mutagenesis has led to many novel applications of fluorescence in the chemical, physical and life sciences. Fluorescence methodologies are now widely used in the biochemical and biophysical areas, in clinical chemistry and diagnostics and in cell biology and molecular biology.

Why fluorescence?

- its pretty!
- it provides information on the molecular environment
- it provides information on dynamic processes on the nanosecond timescale



Fluorescence Probes are essentially molecular stopwatches which monitor *dynamic* events which occur during the excited state lifetime – such as movements of proteins or protein domains

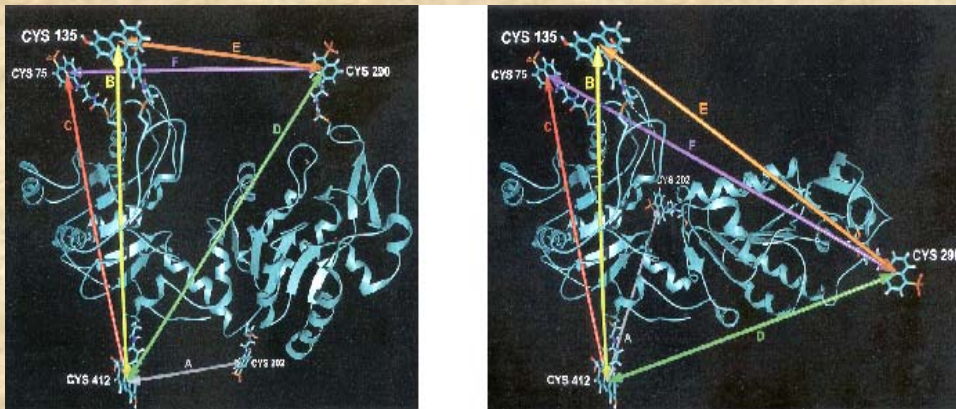
Coupled with modern fluorescence microscopy (confocal, multiphoton, etc) and fluorescent proteins (such as GFP, etc) fluorescence is also providing extremely detailed spatial information in living cells – as well as information on the dynamics of cellular components

Also fluorescence is very, very, very sensitive!

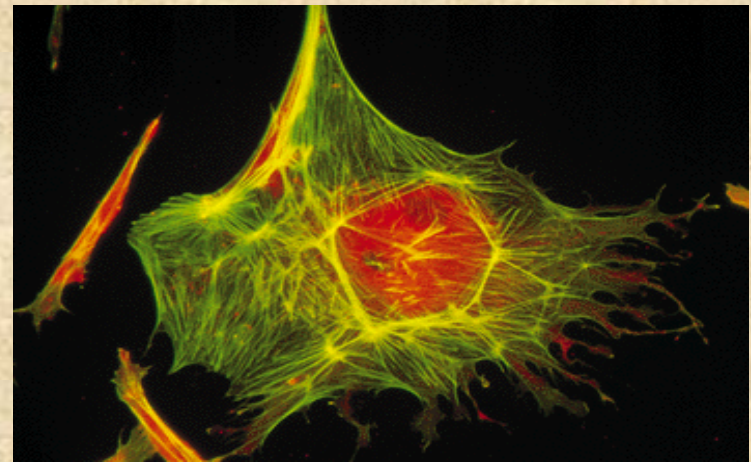
**Work with subnanomolar concentrations is
routine while femtomolar
and even SINGLE MOLECULE studies are
possible with some effort**

Experimental Systems Accessible to Fluorescence

Molecular structure and dynamics



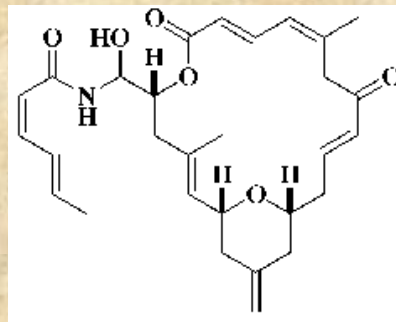
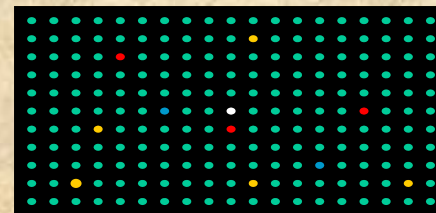
Cell organization and function



Live Animals



Engineered surfaces



High throughput
Drug discovery

Instrumentation

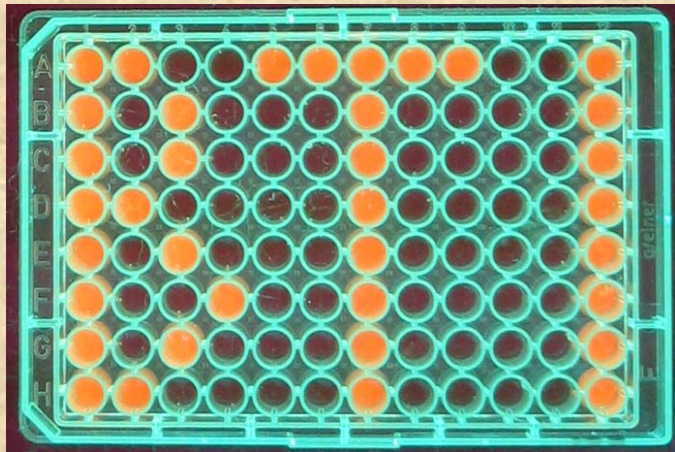
Fluorimeters



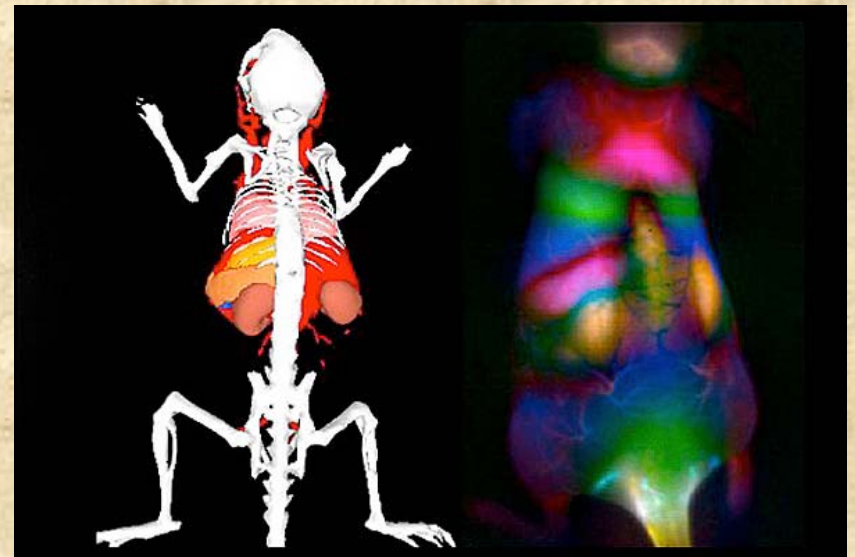
Microscopes



High throughput Plateraders



Intravital Imaging



Virtually all fluorescence data required for any research project will fall into one of the following categories.

- 1. The fluorescence emission spectrum**
- 2. The excitation spectrum of the fluorescence**
- 3. The quantum yield**
- 4. The polarization (anisotropy) of the emission**
- 5. The fluorescence lifetime**

In these lectures, we examine each of these categories and briefly discuss historical developments, underlying concepts and practical considerations

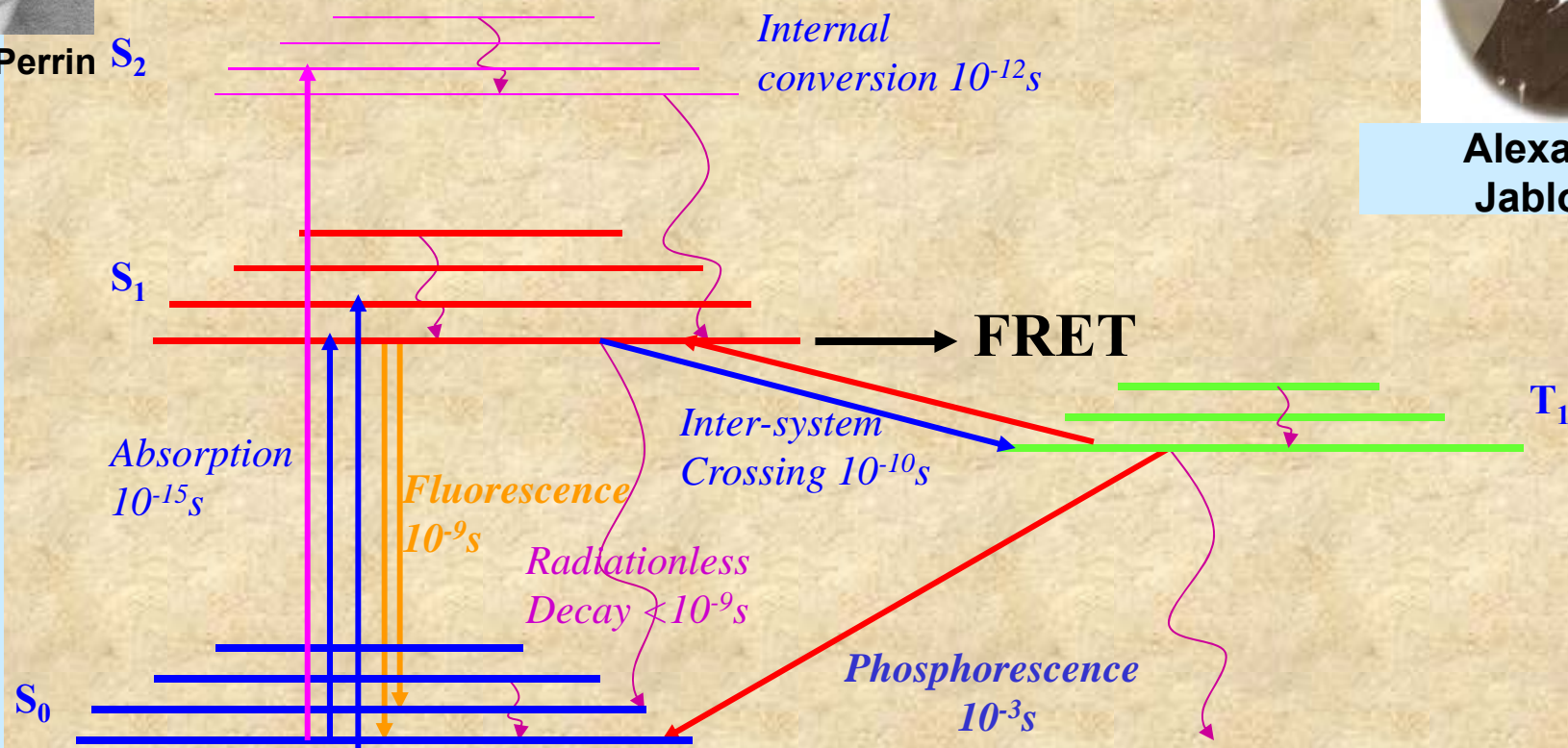


Francis Perrin



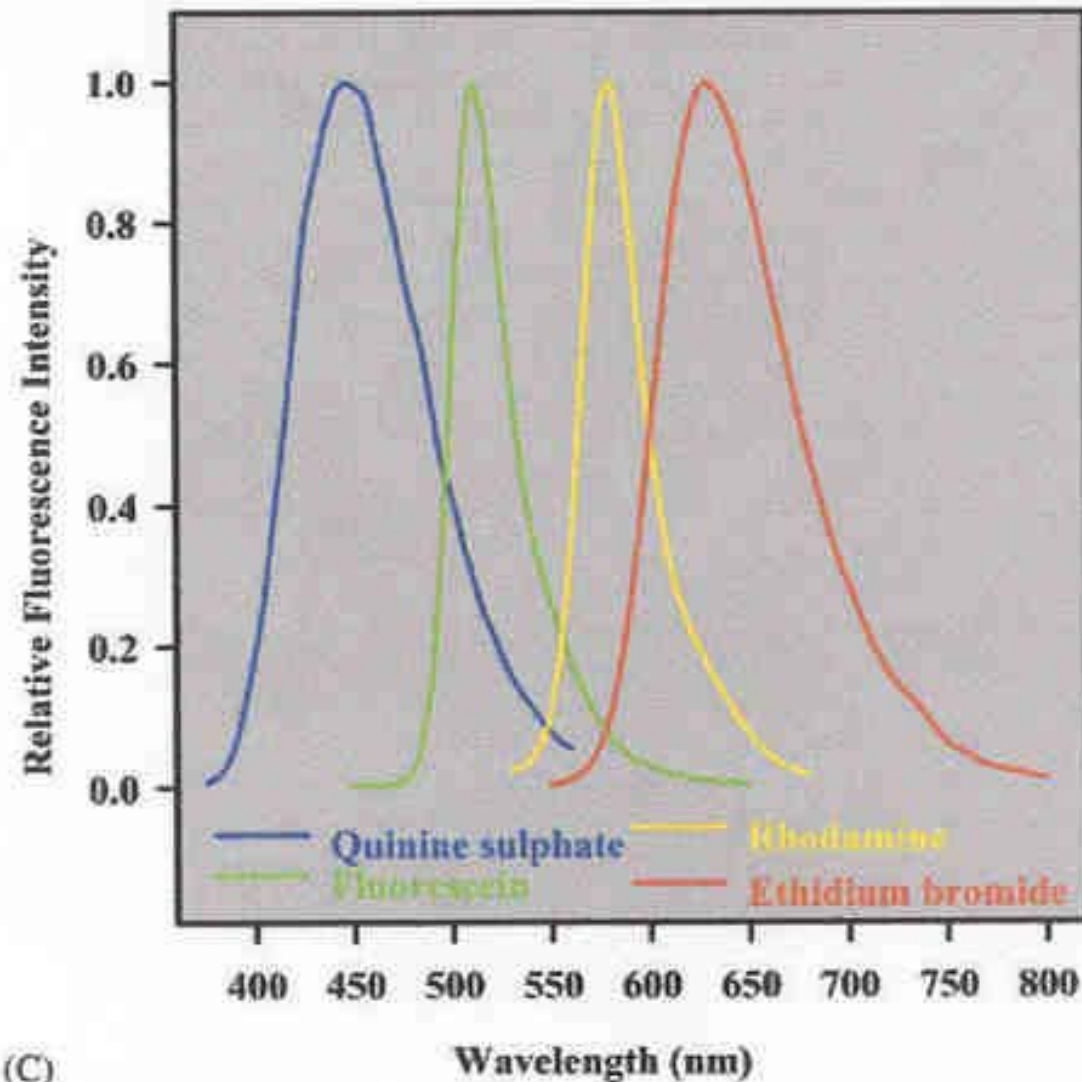
Alexander Jablonski

The Perrin-Jablonski Diagram

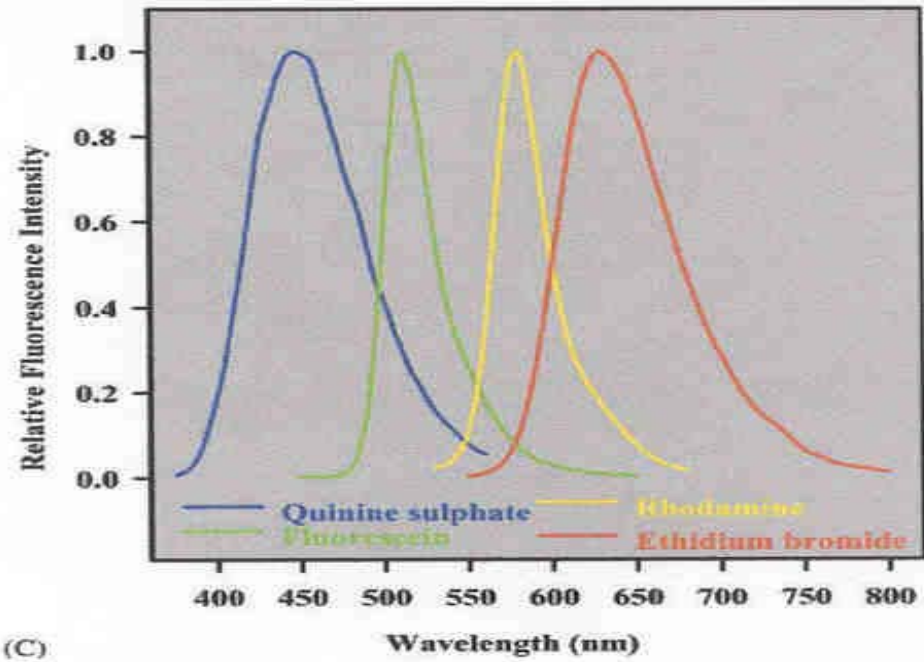
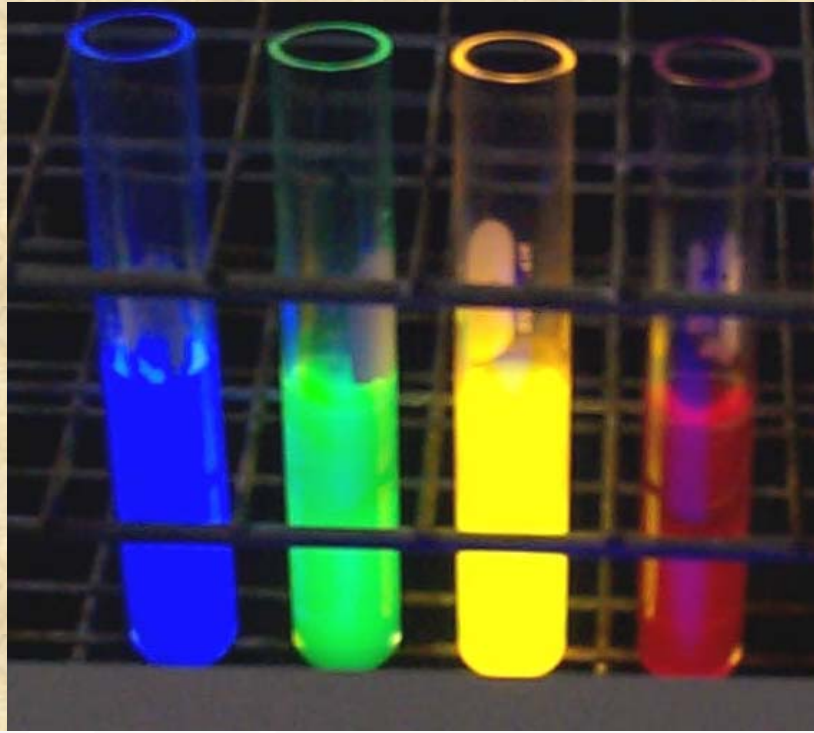


The fluorescence emission spectrum

In a typical emission spectrum, the excitation wavelength is fixed and the fluorescence intensity versus wavelength is obtained



(C)



(C)

Early examination of a large number of emission spectra resulted in the formulation of certain general rules:

- 1) In a pure substance existing in solution in a unique form, the fluorescence spectrum is invariant, remaining the same independent of the excitation wavelength*
- 2) The fluorescence spectrum lies at longer wavelengths than the absorption*
- 3) The fluorescence spectrum is, to a good approximation, a mirror image of the absorption band of least frequency*

1) *In a pure substance existing in solution in a unique form, the fluorescence spectrum is invariant, remaining the same independent of the excitation wavelength*

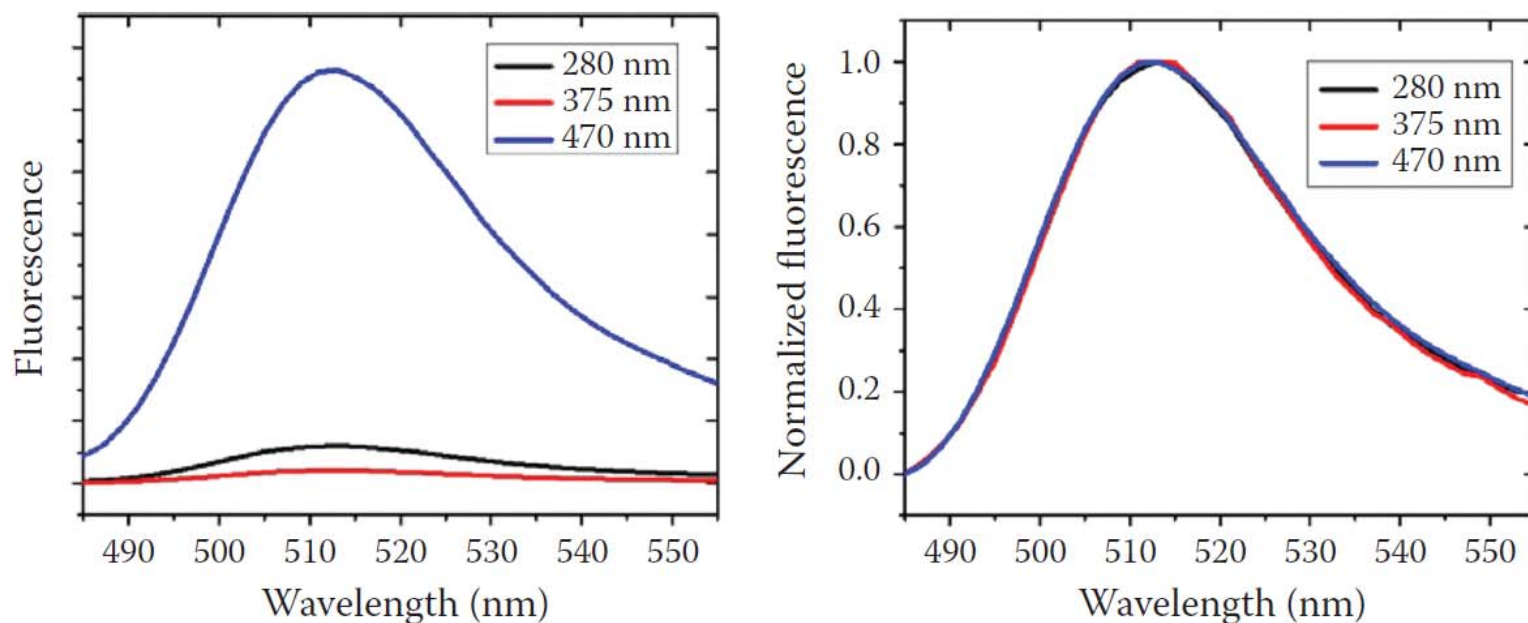


FIGURE 4.5 Comparison of fluorescein emission spectra excited at 280, 340, and 470 nm. Left: not normalized. Right: normalized.

The normalized spectra illustrate the fact that the shape of the emission spectrum and its maximum are independent of the excitation wavelength. If the emission maximum actually changes with excitation wavelength it usually means that the fluorescent sample is not pure, that is, more than one fluorescing molecule is present which has a different absorption spectrum and/or emission spectrum than the target fluorophore.

2) *The fluorescence spectrum lies at longer wavelengths than the absorption*

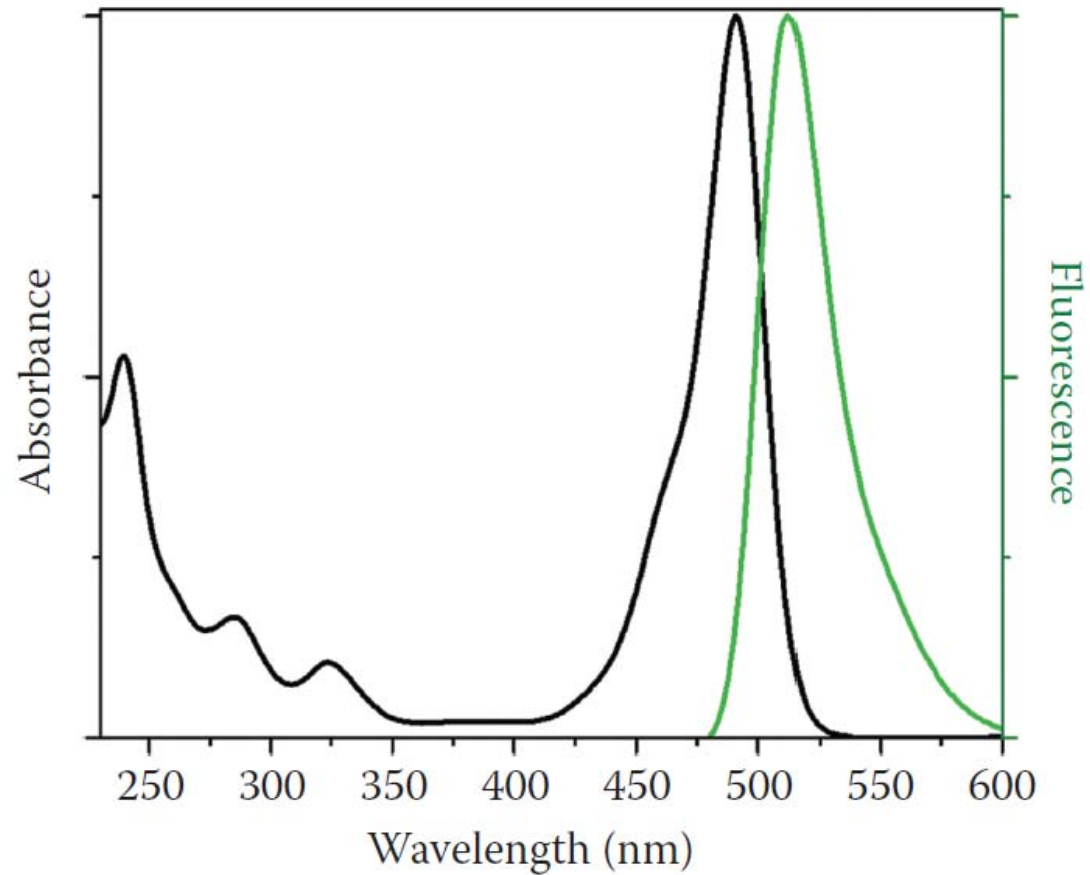
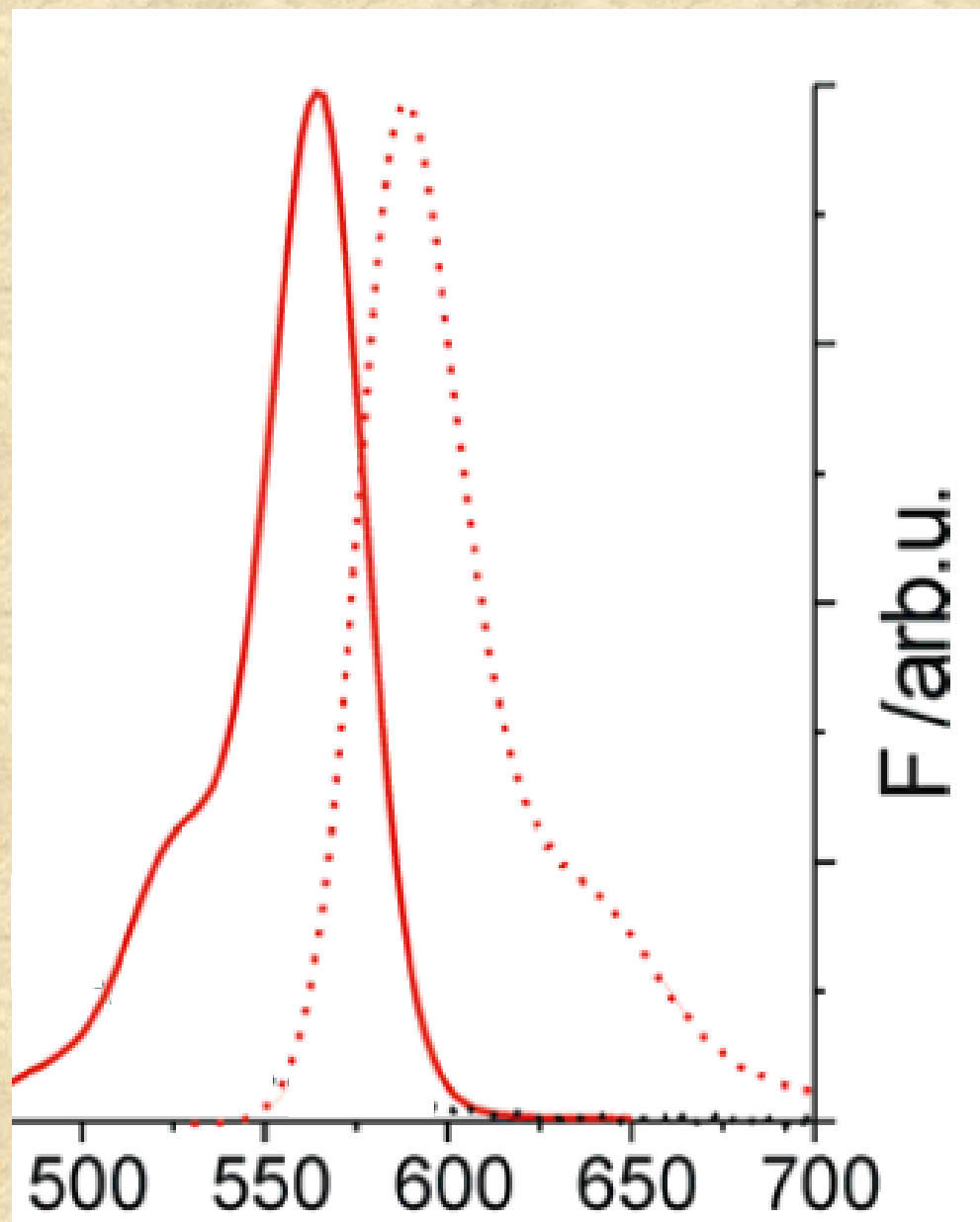


FIGURE 4.3 Absorption and emission spectra of fluorescein in alkaline solution.

3) The fluorescence spectrum is, to a good approximation, a mirror image of the absorption band of least frequency

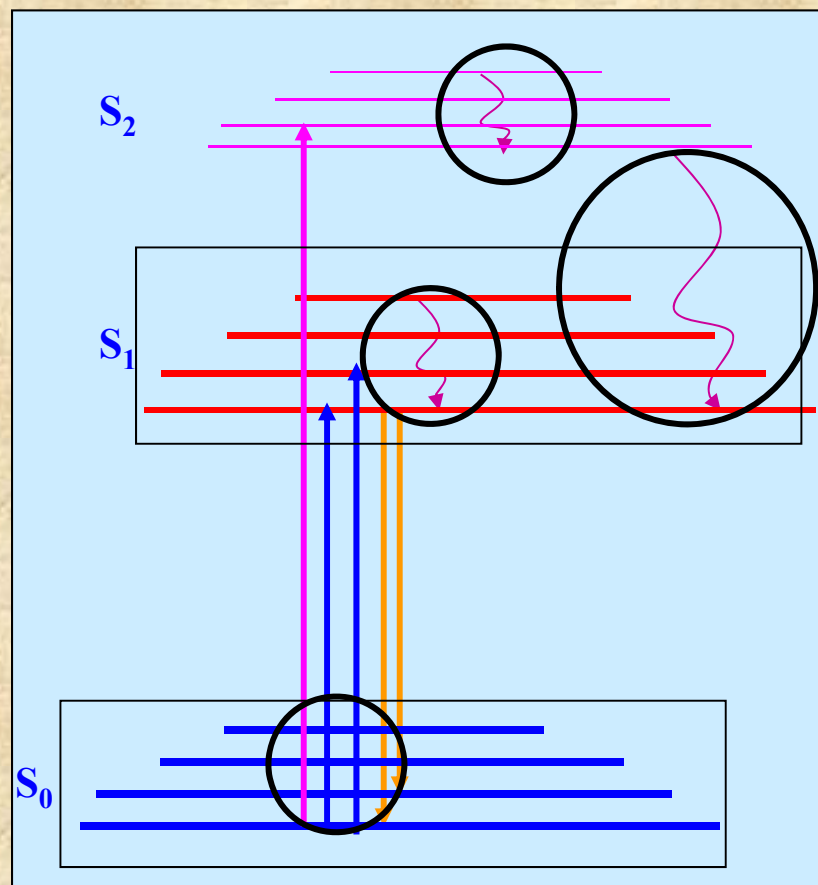
**Rhodamine
101 in ethanol**



These general observations follow from consideration of the Perrin-Jabłoński diagram shown earlier

Specifically, although the fluorophore may be excited into different singlet state energy levels (e.g., S_1 , S_2 , etc) rapid thermalization invariably occurs and emission takes place from the lowest vibrational level of the first excited electronic state (S_1). This fact accounts for the independence of the emission spectrum from the excitation wavelength.

The fact that ground state fluorophores, at room temperature, are predominantly in the lowest vibrational level of the ground electronic state (as required from Boltzmann's distribution law) accounts for the Stokes shift.

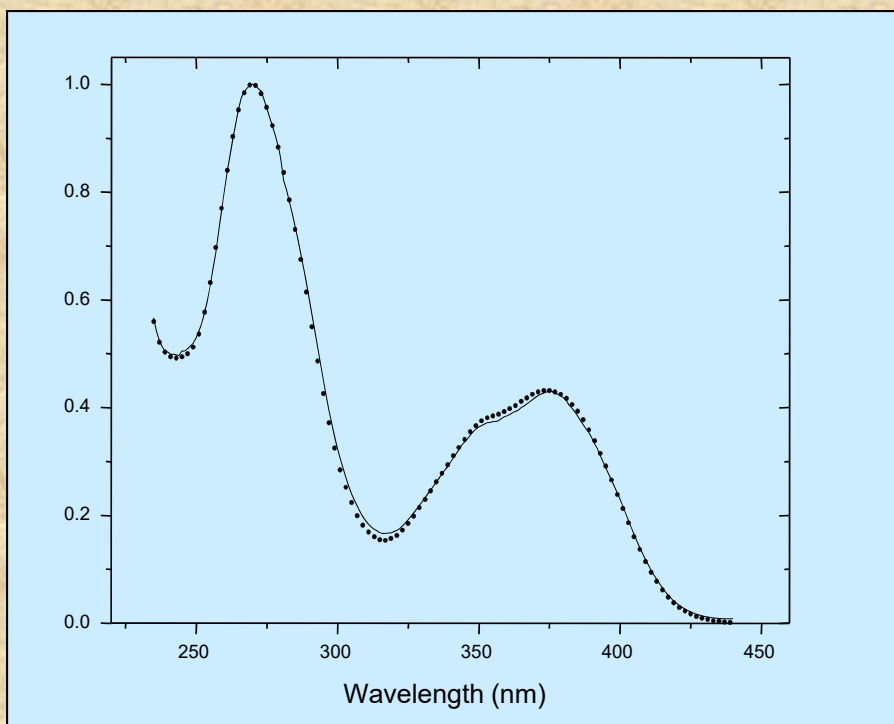


Finally, the fact that the spacings of the energy levels in the vibrational manifolds of the ground state and first excited electronic states are usually similar accounts for the fact that the emission and absorption spectra (plotted in energy units such as reciprocal wavenumbers) are approximately mirror images

The fluorescence excitation spectrum

The relative efficiencies of different wavelengths of incident light to excite fluorophores is determined as the excitation spectrum. In this case, the excitation monochromator is varied while the emission wavelength is kept constant if a monochromator is utilized - or the emitted light can be observed through a filter.

If the system is “well-behaved”, i.e., if the three general rules outlined above hold, one would expect that the excitation spectrum will match the absorption spectrum. In this case, however, as in the case of the emission spectrum, corrections for instrumentation factors are required.



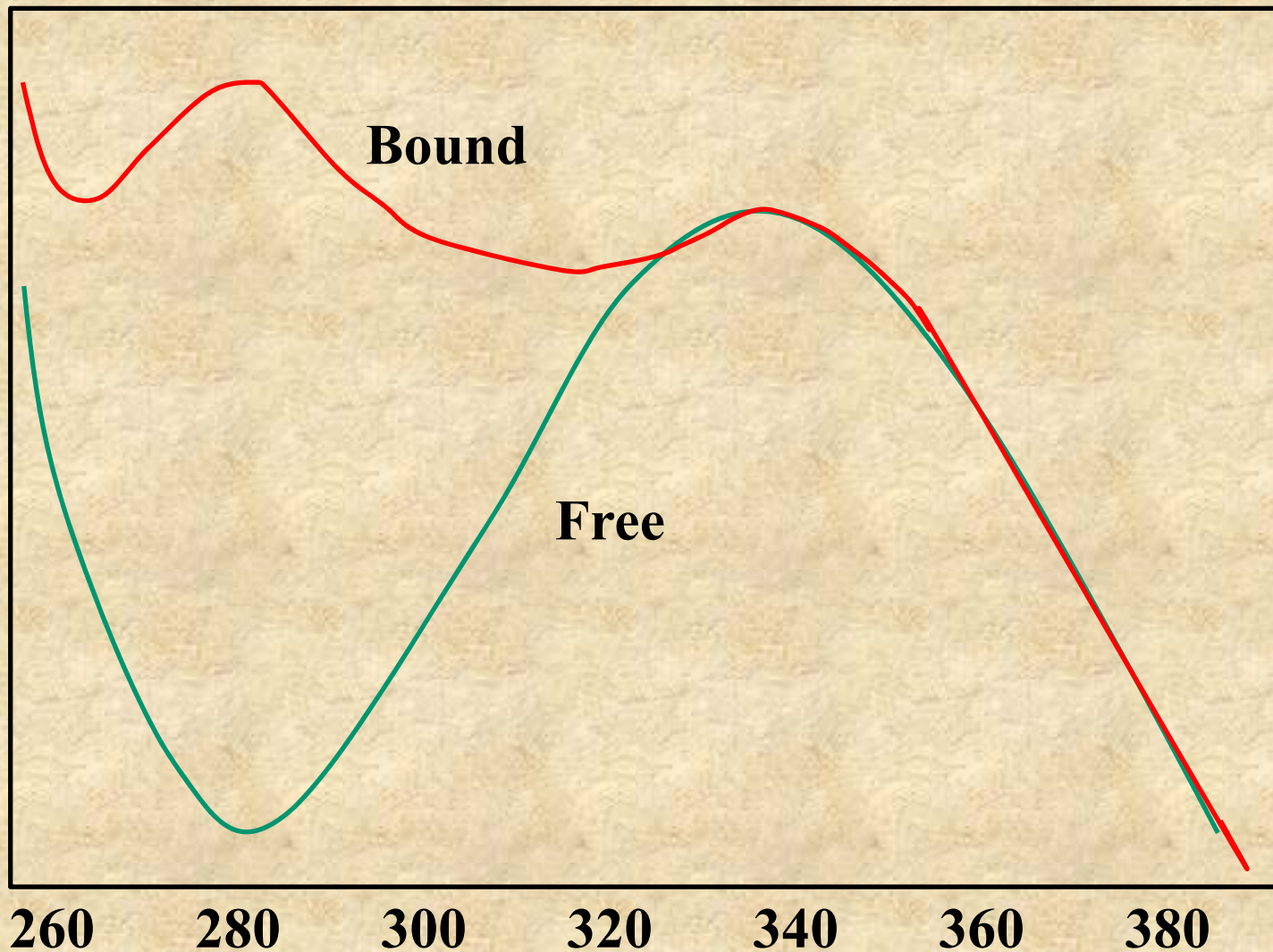
Overlay of Absorption Spectrum and Corrected Excitation Spectrum for ANS in ethanol

Why should we want excitation spectra?

- 1) Can be used to obtain absorption spectrum in a system wherein only one absorbing molecule emits fluorescence**
- 2) Can obtain absorption spectrum at very low concentrations**
- 3) Can be used to detect energy transfer**

Consider the excitation spectra below for a fluorophore free in solution and then bound to a protein

As we will discuss in more detail later, the increase in the excitation spectrum around 280nm indicates energy transfer from the protein's tryptophan residues to the bound fluorophore



A method which has become very popular in analytical chemistry applications is the Excitation Emission Matrix (EEM)

This approach was conceived by Gregorio Weber as a method to elucidate the number of fluorescing compounds in mixtures of fluorophores by variation of the excitation and emission wavelengths and construction of a matrix of the resulting intensities.

(Reprinted from *Nature*, Vol. 190, No. 4770, pp. 27-29, April 1, 1961)

ENUMERATION OF COMPONENTS IN COMPLEX SYSTEMS BY FLUORESCENCE SPECTROPHOTOMETRY

By DR. G. WEBER

Department of Biochemistry, University of Sheffield

THE constancy of the spectral distribution of the fluorescence for a given substance excited with light of different wave-lengths permits the development of a simple quantitative criterion for the determination of the number of independent fluorescent components in a mixture and also results in an interesting extension of the concept of resolution as commonly applied in spectroscopy.

In fluorescence spectrophotometry a number of fluorescence intensity measurements are made, following excitation with different wave-lengths. Both fluorescence observation and excitation cover discrete wave-bands. Continuously recorded fluorescence and fluorescence-excitation spectra are to be considered here as finite series of measurements with effective band-widths determined by the conditions used¹. In either case the results may be set down as an $m \times n$ matrix, where the m columns are determined by the wave-lengths of excitation and the n rows by the wave-lengths of observation. The matrix elements, F_{ij} , are numbers proportional to the response of the detector, that is, photocurrents in the ordinary case. The i, j element of this EF matrix, as I propose to call it, is the fluorescence omitted at wave-length j on excitation with light of wave-lengths i . When several components are present in a mixture the EF matrix may be written as :

$$|EF|_{mn} = \begin{vmatrix} \sum_k F_{11}^k & \sum_k F_{12}^k & \dots & \sum_k F_{1m}^k \\ \sum_k F_{21}^k & \sum_k F_{22}^k & \dots & \sum_k F_{2m}^k \\ \dots & \dots & \dots & \dots \\ \sum_k F_{n1}^k & \sum_k F_{n2}^k & \dots & \sum_k F_{nm}^k \end{vmatrix} \quad (1)$$

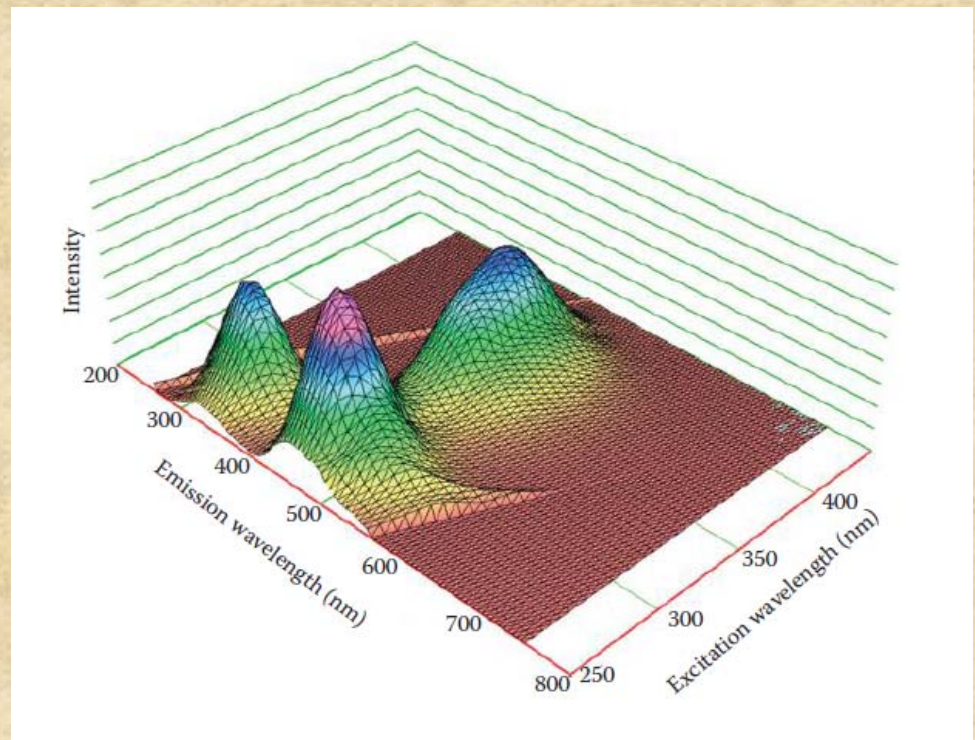
The superscript k refers to the different components. Of the quanta absorbed in the solution from the

With the advent of computer-controlled instrumentation and data analysis, Weber's EEM approach would become widely utilized in Analytical Chemistry.

Typically, in analytical applications, EEMs are used to obtain a unique "fingerprint" of a mixture, which can be used for sample characterization or even forensic purposes. The EEM method has, in fact, found wide application in environmental issues such as organic matter in water (including waste water), soil, and oils.

An example of an EEM is ANS is bound to BSA. One notes three peaks: BSA, ANS excited directly by mid-UV, ANS excited near 280 nm as well as ANS excited via energy transfer from BSA.

(EEM taken on an ISS PC)



Other ways to depict EEM spectra are shown here

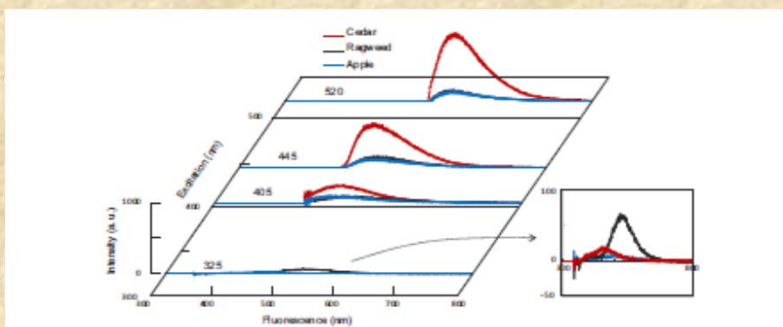


Fig. 3. Raw fluorescence spectrum of cedar, ragweed and apple pollens measured by the fluorescence lidar. Data are not corrected with excitation power. The spectrum for 325 nm excitation is shown in the figure to the right.

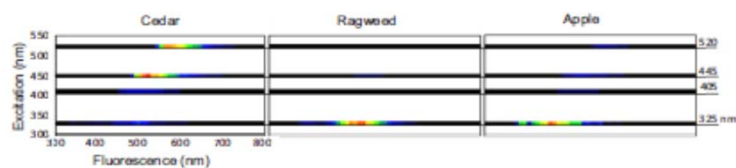


Fig. 4. EEM fluorescence of cedar, ragweed and apple pollen measured in the fluorescence lidar simulation experiment. Each is expressed relatively to its maximum intensity.

Vol. 30, No. 11/23 May 2022/ Optics Express 19922

Environmental Science and Pollution Research (2018) 25:34777–34787

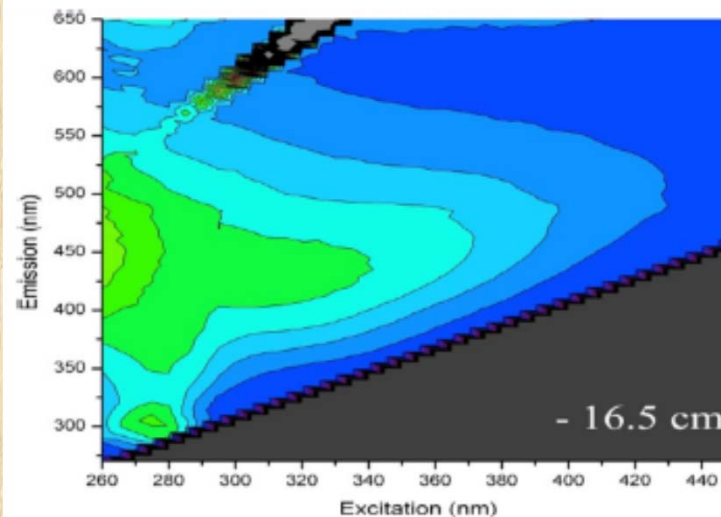
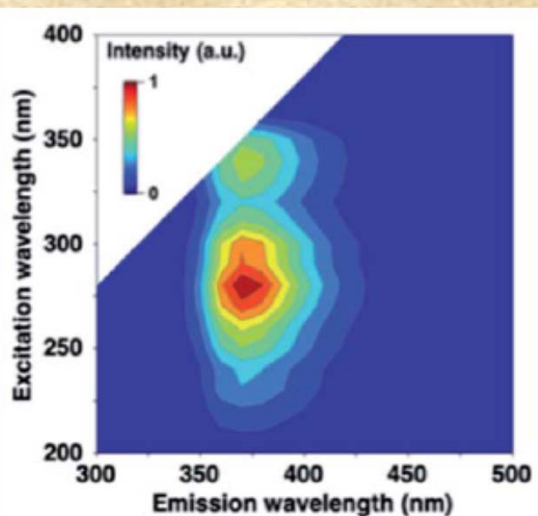
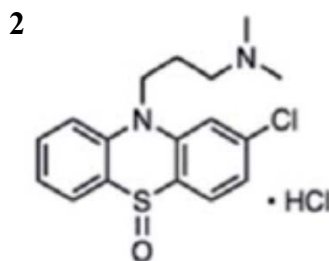


Fig. 1 EEM of chromophoric dissolved organic matter in a porewater sample at a depth of 16.5 cm below the sediment surface in a Southern Californian salt marsh in the vicinity of an oil well (Bowen et al. 2017). The feature in the EEM with excitation between 260 and 280 nm and emission at 320 nm was attributed to a component of crude oil. The remaining features are peaks A and C (Coble 1996) due to terrestrial humic materials



EEM of isolated photodegradation products of 2 in CH₃OH



RSC Adv., 2022, 12, 20714–20720

PARAllel FACtor analysis (PARAFAC)

PARAllel FACtor analysis (PARAFAC) is used to decompose fluorescence excitation emission matrices (EEMs) into their underlying chemical components.

The first step is to transfer the data from the instrument to software supporting PARAFAC analysis. Analysis is frequently performed with the commercial MATLAB (Mathworks, Inc.) software which efficiently handles data arrays.

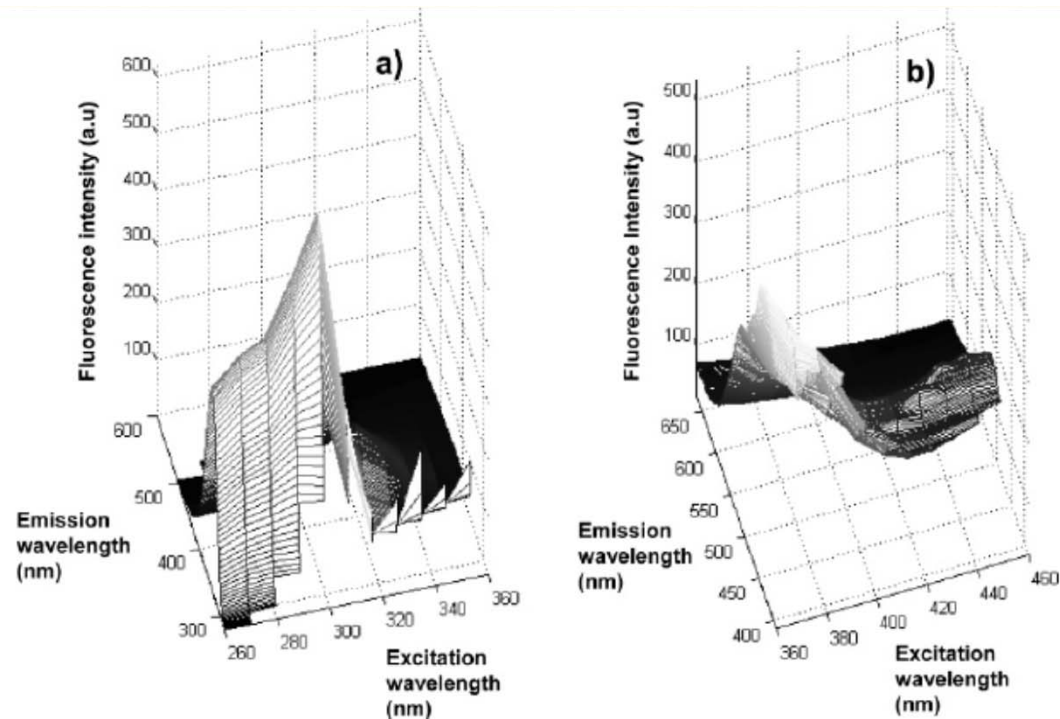


Figure 1. Raw excitation–emission matrices: (a) excitation, 260–360 nm; emission, 280–600 nm; (b) excitation, 360–460 nm; emission, 390–650 nm.

Application of Fluorescence Spectroscopy in the Evaluation of Light-Induced Oxidation in Cheese

CHARLOTTE M. ANDERSEN,^{*,†} METTE VISHART,[§] AND VIBEKE K. HOLM[§]

J. Agric. Food Chem. **2005**, *53*, 9985–9992

This study examines how fluorescence spectroscopy can be used to evaluate the quality of semihard cheese (Danbo cheese) packaged in modified atmosphere and exposed to light for up to 84 days. The cheeses were stored in the light or dark with variations in oxygen availability provided by oxygen scavengers and the packaging materials as described by Holm et al. (*§*).

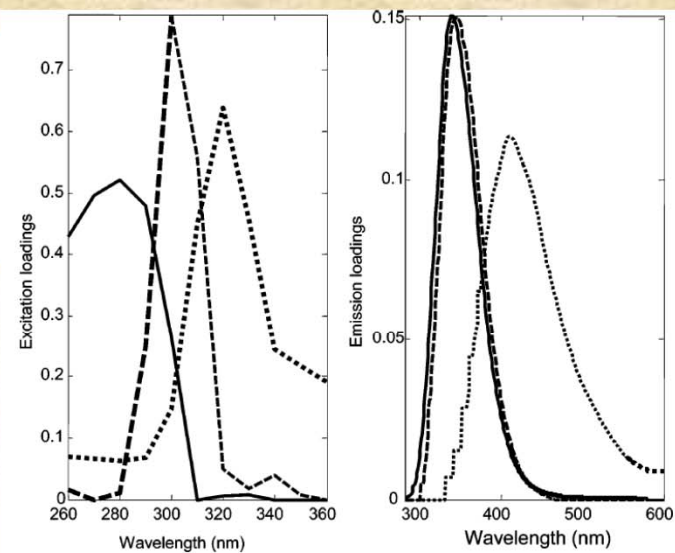


Figure 2. Excitation and emission loadings of the PARAFAC model with excitation from 260 to 360 nm: (solid line) component 1; (dashed line) component 2; (dotted line) component 3.

Synchronous Scanning

This method is also used to examine mixtures of fluorophores but the approach is quite different from the EEM method. In synchronous scanning, both excitation and emission monochromators are scanned simultaneously with a particular wavelength interval ($\Delta\lambda$) between the excitation and emission wavelengths.

The resulting spectrum will vary depending on the $\Delta\lambda$ value and, of course, on the spectral characteristics of the components of the sample. Each mixture will have a unique spectroscopic “signature” or “fingerprint” using this method, which can be very useful for analytical purposes.

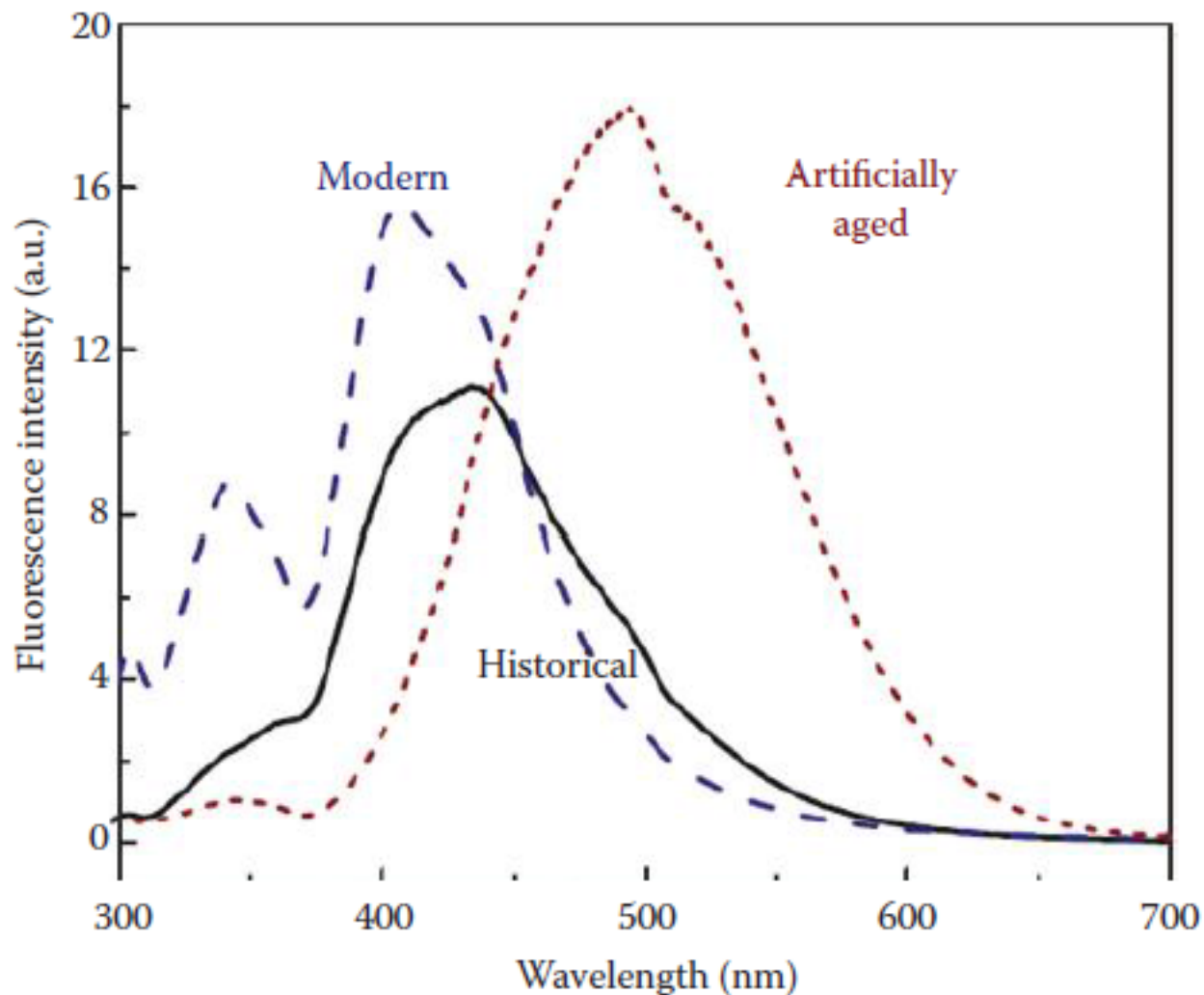


FIGURE 4.14 Synchronous scans of modern, historical, and artificially aged parchment samples. The wavelength difference between excitation and emission was 70 nm. (From B. Dolgin, V. Bulatov, and I. Schechter, 2009. *Anal. Bioanal. Chem.* 395: 2151.)

Here is another example of synchronous scanning – a three dimensional plot presentation is used.

The system is Benzo(a)pyrene Diolepoxide-DNA Adducts

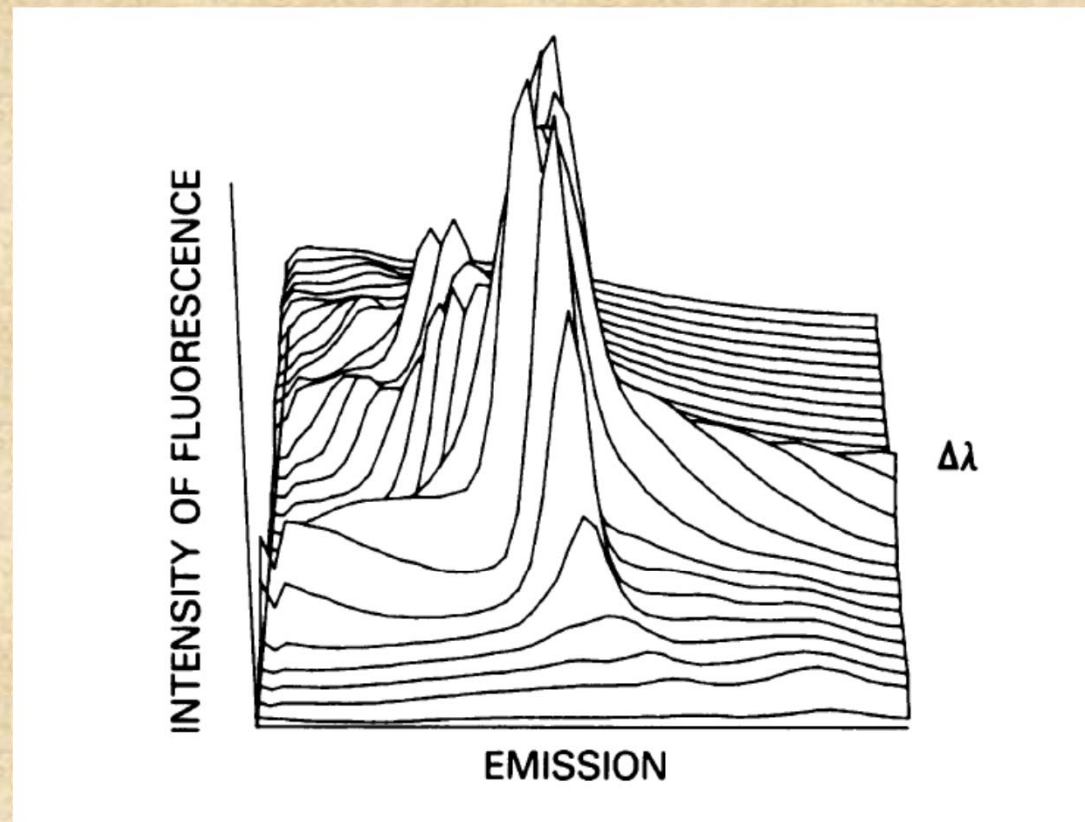


FIGURE 5. Three-dimensional synchronous spectrum of BPDE-DNA (BP-DNA). For the first scan $\Delta\lambda$ of 10 nm was used. Total of 28 scans with an increment of 4 nm.

Environmental Health Perspectives
Vol. 62, pp. 101-104, 1985

Spectral Center of Mass

In some cases, changes in the position of the emission maxima, which accompany some process such as ligand binding, oligomerization, or denaturation, are of great interest. The most common way to determine an emission maximum is to look at the recorded spectrum and estimate the wavelength corresponding to the highest signal, that is, estimate λ_{\max} .

Such “eyeball” estimates may be adequate for many purposes, especially if the wavelength shifts are significant. In some cases, however, one may desire a less subjective and more sensitive method. In such cases, one may consider determining the spectral center of mass, $\langle \nu_g \rangle$, defined by the relation:

$$\nu_g = \frac{\sum \nu_i F_i}{\sum F_i}$$

where F_i is the emission at a wavenumber, ν_i , and the sum is carried over all wavenumbers where $F_i > 0$.

This approach offers a very precise and reproducible measure of spectral shifts. Apparently, the term “center of mass” dates back to the days of spectroscopy before computer interfaced equipment, when spectra were recorded on chart paper, and people would cut out the spectrum and weigh the paper to get the area, and then cut the spectrum into parts and weigh the pieces to find the “center of mass”.

An example of the use of this approach is in the article by Silva et al. (1986) (*Biochemistry* 25:5780–5786), which followed the dissociation of the tryptophan synthase dimer induced by elevated hydrostatic pressure. The dissociation into monomers leads to a red shift in the intrinsic protein fluorescence, as shown in Figure 4.10a, which can be quantified using the center of mass. A plot of the center of mass versus applied pressure (Figure 4.10b), for example, allows one to readily follow the dimer dissociation process.

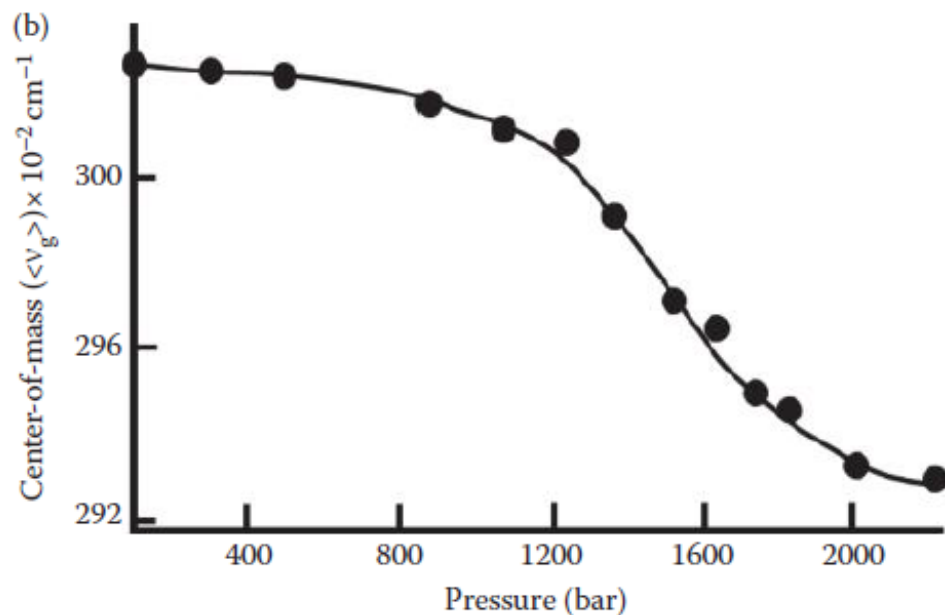
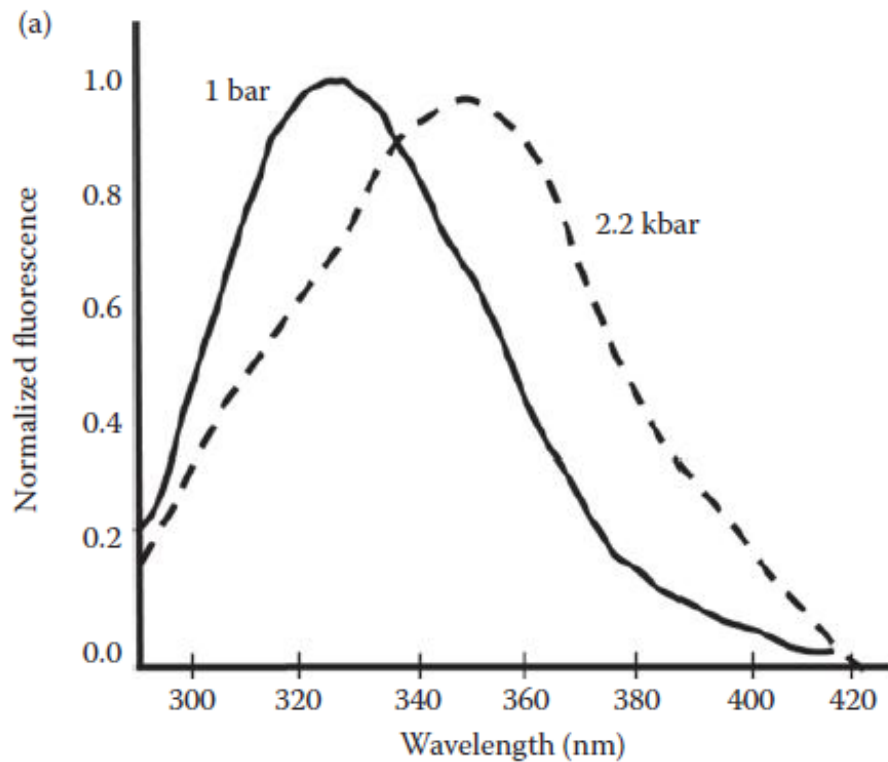


FIGURE 4.10 (a) Emission spectra of the holo form of tryptophan synthase at pressures of 1 bar and 2.2 kbars. (b) Illustration of center-of-mass used for quantification of wavelength shifts. (Adapted with permission from J.L. Silva et al., 1986. *Biochemistry* 25: 5780. Copyright 1996 American Chemical Society.)

Quantum Yield

The fluorescence quantum yield was a concept introduced in 1924 by Sergey Ivanovich Vavilov



Perhaps the simplest definition of quantum yield (QY) is that it represents the number of photons emitted divided by the number of photons absorbed:

$$\text{QY} = \text{photons emitted as fluorescence} / \text{photons absorbed}$$

So, if a fluorophore absorbs 100 photons and emits 100 photons, its quantum yield is 1.0 or 100% whereas if it absorbs 100 photons and emits only 20 photons then its quantum yield is 0.20 or 20%.

Quantum Yield

A more insightful definition of QY would be that the QY equals the *rate of the emission process* divided by the sum of the *rates of all other deactivation processes*.

$$\text{QY} = k_f / \sum k_d$$

where k_f is the rate of fluorescence, and $\sum k_d$ designates the sum of the rate constants for the various processes, in addition to fluorescence, that depopulate the excited state.

These non-radiative deactivation processes may include photochemical and dissociative processes in which the products are well characterized chemical species (electrons, protons, radicals, molecular isomers). Also, we may have less well characterized changes that result in a return to the ground state with the simultaneous dissipation of the excited state energy as heat. These latter processes are collectively called ‘radiationless transitions

Quantum yields are usually determined using either "absolute" or "relative" methods.

Absolute methods include:

- 1) Actinometry**
- 2) Calorimetric methods**
- 3) Optical methods**
- 4) Photoacoustic Spectroscopy*
- 5) Thermal Lensing*

Actinometry

Chemical actinometry involves measuring the radiant flux from a sample via the yield from a chemical reaction. Specifically, a chemical system (fluid, gas or solid) containing a chromophore that undergoes a light-induced reaction is used. To use this approach, the quantum efficiency of the reaction must be known.

In 1834, John Herschel described the first chemical actinometer for use in meteorology which used temperature changes induced by light absorption by a copper sulfate solution (hence his approach was calorimetric).

Herschel, J. F. W. (1834) Explanation of the principle and construction of the actinometer. Report of the Third Meeting of the British Association for the Advancement of Science. Vol. 379–381

In 1929, Allmand and Webb introduced the potassium ferrioxalate actinometer [$\text{K}_3\text{Fe}(\text{C}_2\text{O}_4)_3$].

Allmand, A. J. and W. W. Webb. (1929) The photolysis of potassium ferrioxalate solutions. Part I. Experimental. *J. Chem. Soc.* 1518-1531; 1531-1537.

Calorimetry

Calorimetric approaches try to measure the amount of excitation energy that is not emitted by the fluorophore but converted into heat and dissipated into the surrounding medium. This conversion efficiency is 100 % for an entirely nonfluorescent compound and correspondingly lower for an emitter with a certain quantum yield.

In calorimetric measurements, the heating effect of the fluorophore under consideration is usually compared to that of a non-emissive dye in the same solvent and absorbing at the same wavelength.

Photochemistry and Photobiology. 1969. Vol. 9, pp. 229-242.

PAUL G. SEYBOLD†, MARTIN GOUTERMAN and JAMES CALLIS

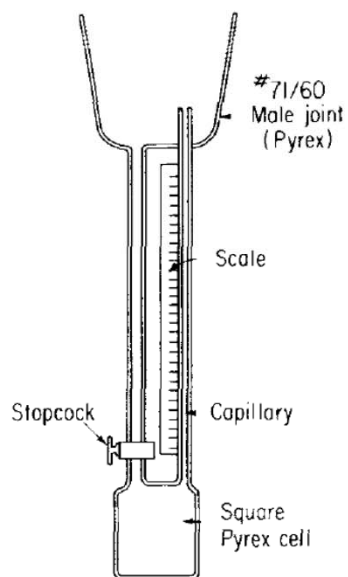
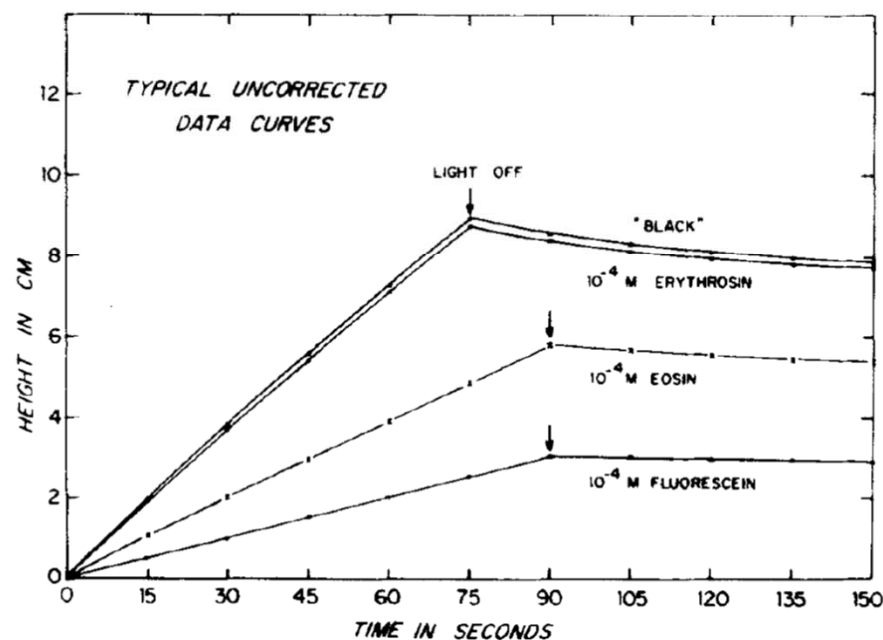
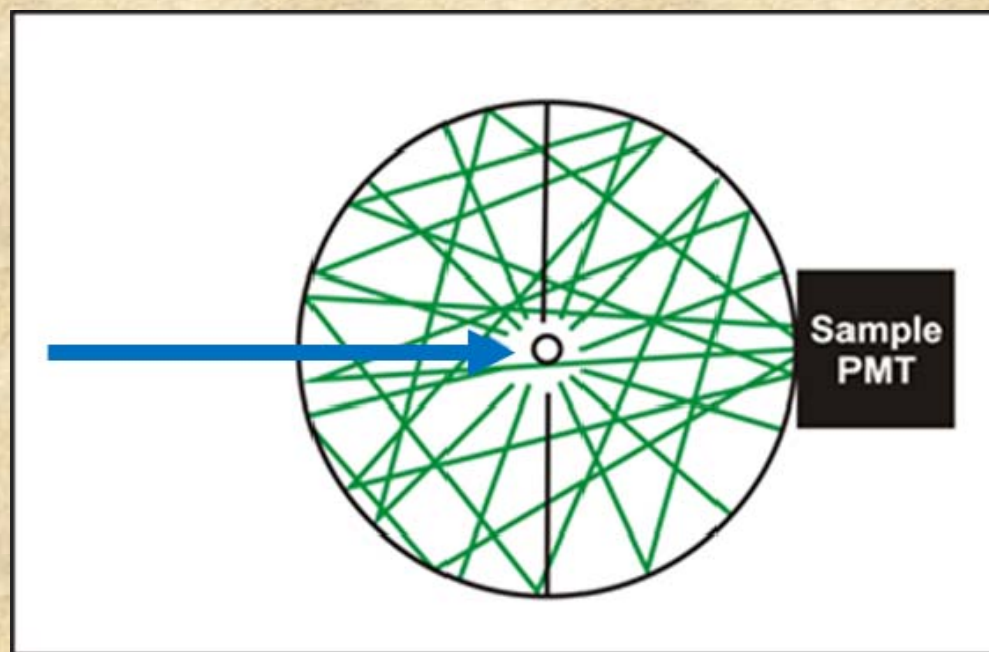


Fig. 2. Detail of cell used in calorimetric study.



Optical methods

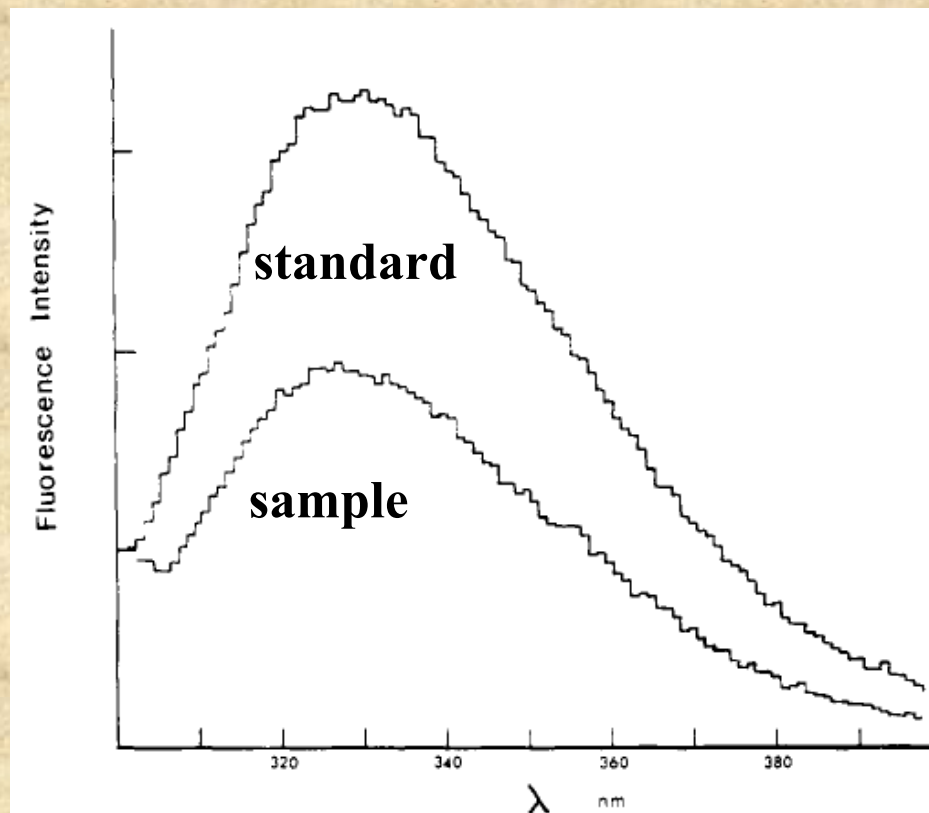
The main absolute optical method uses an integrating sphere (often termed an Ulbricht sphere in honor of Richard Ulbricht who built the first integrating sphere in 1894). The fluorescing sample is placed in the sphere's interior, which is coated with a highly reflective material such that the emitted light will reflect many times, but will eventually reach the detector. Polytetrafluoroethylene is a typical modern coating material due to its high, flat reflectance over a wide range of wavelengths, as well as its chemical inertness. These multiple diffuse reflections ensure that the light becomes uniform and independent of polarization and spatial properties. Hence, essentially all of the emitted light can be measured and quantified relative to a highly scattering sample.



Relative Approaches

The classic approach for determination of a quantum yield using the "relative" method was introduced by Parker and Rees (Parker, C. A., Rees, W. T. *Analyst* 1960, 85:587). In this approach, one selects a fluorophore, a standard, which has absorption and emission properties that roughly match those of your sample. For example, tryptophan or N-acetyltryptophanamide (NATA) are common standards for proteins, while quinine sulfate and fluorescein are often used when the excitation is in the mid-UV or visible regions, respectively.

Then, one makes up solutions of the standard and sample such that the optical densities are similar. Now, one simply measures the emission spectra of both standard and sample, applies correction factors to get true molecular spectra, and integrates the area under the spectra to get the total intensity of the emitted light.



Wavelength Invariance

The Kasha-Vavilov Rule (named for Michael Kasha and Sergey Vavilov) states that the quantum yield of a fluorophore is independent of the excitation wavelength. Generally, this rule holds since, as stated earlier, regardless of the excitation wavelength the emission is from the lowest vibrational level of the first excited electronic state.

There are occasional exceptions to this rule, however. For example, the quantum yields of indole and tryptophan vary depending on whether they excited into the lowest energy electronic states (S_1) or the higher energy electronic levels (S_2). The yield of indole, for example, begins to drop as the excitation wavelength decreases below 240 nm, reaching a value about 60% lower than that upon excitation above 240 nm (Tatischeff and Klein (1975) *Photochem. Photobiol.* 22:221). The reason for this decreased quantum yield is thought to be due to electron ejection from the higher electronic excited state. Similar observations have been made for benzene and naphthalene derivatives.

The lifetime of tryptophan has, on the other hand, been shown to be independent of the excitation wavelength down to 200 nm (I actually reported those measurements in my PhD thesis), which means that excited tryptophans not quenched by electron ejection undergo the normal decay process.

One then uses the following equation to calculate the quantum yield of the sample:

$$QY_{\text{sample}} = QY_{\text{standard}} \left(\frac{I_{T \text{ sample}}}{I_{T \text{ standard}}} \right) \left(\frac{1 - 10^{-\text{Abs}(\text{standard})}}{1 - 10^{-\text{Abs}(\text{sample})}} \right) \left(\frac{n_{\text{sample}}}{n_{\text{standard}}} \right)^2$$

The term $(1 - 10^{-\text{Abs}})$ represents the fraction of light absorbed at the excitation wavelength.

In the literature, one often sees these terms replaced with absorbances or optical densities, which is only a good approximation if the optical densities are very low. The I_T terms are, of course, the total intensities (more about these terms soon), and n refers to the refractive index.

List of quantum yields from “Molecular Fluorescence” by Bernard Valeur

Tab. 6.1. Standards for the determination of fluorescence quantum yields

Range	Compound	Temp. (°C)	Solvent	Φ_F	Ref.
270–300 nm	Benzene	20	Cyclohexane	0.05 ± 0.02	1
300–380 nm	Tryptophan	25	H ₂ O (pH 7.2)	0.14 ± 0.02	2
300–400 nm	Naphthalene	20	Cyclohexane	0.23 ± 0.02	3
315–480 nm	2-Aminopyridine	20	0.1 mol L ⁻¹ H ₂ SO ₄	0.60 ± 0.05	4
360–480 nm	Anthracene	20	Ethanol	0.27 ± 0.03	1, 5
400–500 nm	9,10-diphenylanthracene	20	Cyclohexane	0.90 ± 0.02	6, 7
400–600 nm	Quinine sulfate dihydrate	20	0.5 mol L ⁻¹ H ₂ SO ₄	0.546	5, 7
600–650 nm	Rhodamine 101	20	Ethanol	1.0 ± 0.02	8
				0.92 ± 0.02	9
600–650 nm	Cresyl violet	20	Methanol	0.54 ± 0.03	10

- 1) Dawson W. R. and Windsor M. W. (1968) *J. Phys. Chem.* 72, 3251.
- 2) Kirby E. P. and Steiner R. F. (1970) *J. Phys. Chem.* 74, 4480.
- 3) Berlman I. B. (1965) *Handbook of Fluorescence Spectra of Aromatic Molecules*, Academic Press, London.
- 4) Rusakowicz R. and Testa A. C. (1968) *J. Phys. Chem.* 72, 2680.
- 5) Melhuish W. H. (1961) *J. Phys. Chem.* 65, 229.
- 6) Hamai S. and Hirayama F. (1983) *J. Phys. Chem.* 87, 83.
- 7) Meech S. R. and Phillips D. (1983) *J. Photochem.* 23, 193.
- 8) Karstens T. and Kobs K. (1980) *J. Phys. Chem.* 84, 1871.
- 9) Arden-Jacob J., Marx N. J. and Drexhage K. H. (1997) *J. Fluorescence* 7(Suppl.), 91S.
- 10) Magde D., Brannon J. H., Cramers T. L. and Olmsted J. III (1979) *J. Phys. Chem.* 83, 696.

But you should be aware that quantum yields are notoriously difficult to measure. For example, “reliable” literature values for quinine sulfate range from ~0.50 – 0.70!

In Fluorescence Microscopy an important parameter is the Molecular Brightness

Brightness = Quantum Yield (Φ) x Molar Absorptivity (ϵ)

Essentially the photons emitted per molecule per second is the important factor.

Polarization



Polarizers have been in use for a very long time - the Vikings are believed to have used a “sunstone” (thought to have been composed either of the mineral cordierite or iceland spar – calcite – both of which are naturally polarizing materials) to observe the location of the sun on foggy or overcast days. Since scattered sunlight is highly polarized compared to light coming along the direction to the sun, the distribution of the sky’s brightness could be observed through the sunstone and hence the sun’s position could be localized and, if the time of day were known, the compass directions.



Etienne-Louis Malus (1775-1812)

In 1808, Malus observed sunlight reflected from the windows of the Luxemburg Palace in Paris through an Iceland spar (Calcite) crystal that he rotated.



(Erasmus Bartholin (1625-1698) discovered the double refraction of light by Iceland spar in 1669)

Malus discovered that the intensity of the reflected light varied as he rotated the crystal and coined the term “**polarized**” to describe this property of light.

He published his findings in 1809:

“Sur une propriété de la lumière réfléchiée par les corps diaphanes” (*Bull. Soc. Philomat.* 1:16)

Malus also derived an expression for calculating the transmission of light as a function of the angle (θ) between two polarizers. This equation (Malus’ Law) is now written as: $I_{\theta} = I_0 (\cos^2\theta)$

Sir David Brewster (1781-1868)



David Brewster studied the relationship between refractive index and angle of incidence on the polarization of the reflected light

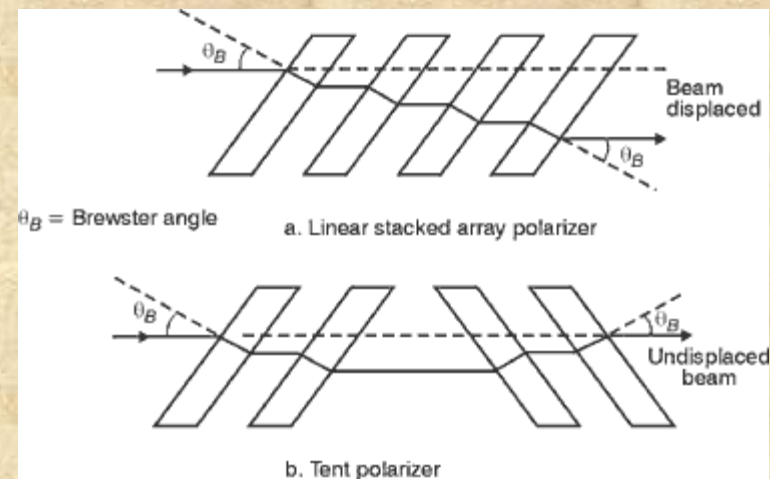
III. *On the law of the partial polarization of light by reflexion.* By
DAVID BREWSTER, LL.D. F.R.S. L. & E.

Read February 4, 1830.

He discovered that for normal glass and visible light, an incidence angle of ~56 degrees resulted in total reflection of one plane of polarization – this angle is now known as *Brewster's Angle*

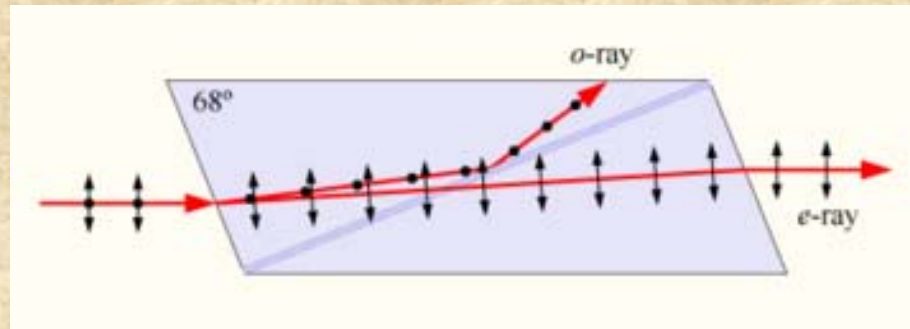
$$\theta_B = \tan^{-1} \left(\frac{n_2}{n_1} \right)$$

This discovery allowed Brewster to construct a polarizer composed of a “pile of plates”



William Nicol (1770-1851)

In 1828, Nicol joined two crystals of Iceland spar, cut at an angle of 68° , using Canada balsam.



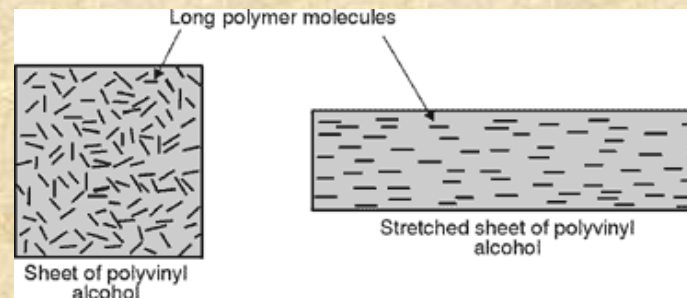
Other important calcite polarizers developed around this time include: Glan-Foucault; Glan-Thompson; Glan-Taylor; Wollaston; Rochon

But the Henry Ford of polarizers was.....

Edwin Herbert Land (1909-1991)

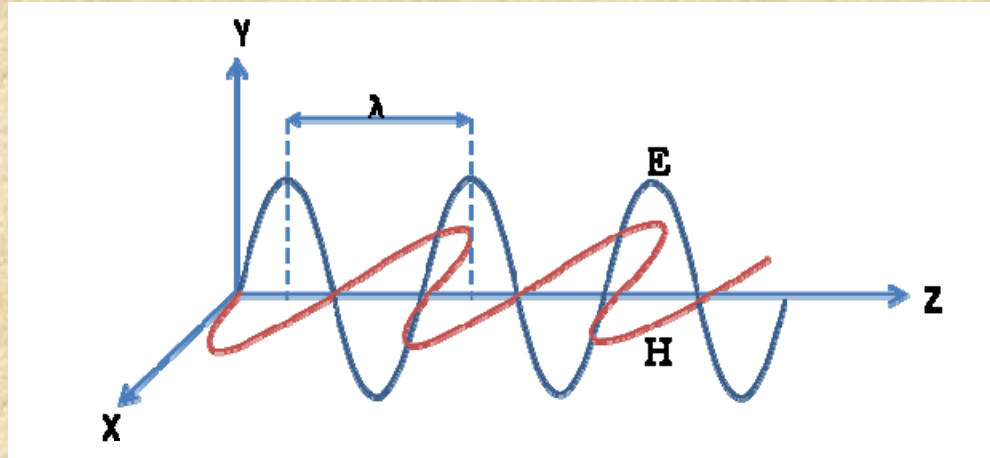


In 1929 Edwin Land patented the sheet polarizer (the J-sheet), consisting of crystals of iodoquinine sulfate embedded in nitrocellulose film followed by alignment of the crystals by stretching which led to dichroism. In 1938 he invented the H-sheet which was comprised of polyvinyl alcohol sheets with embedded iodine.



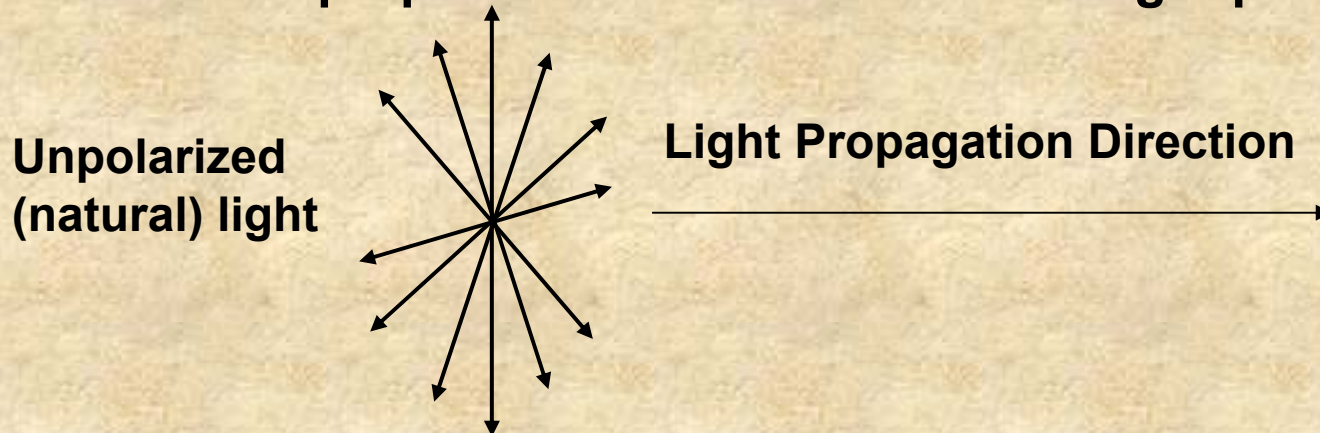
Polarization

Light can be considered as oscillations of an electromagnetic field – characterized by electric and magnetic components - perpendicular to the direction of light propagation.

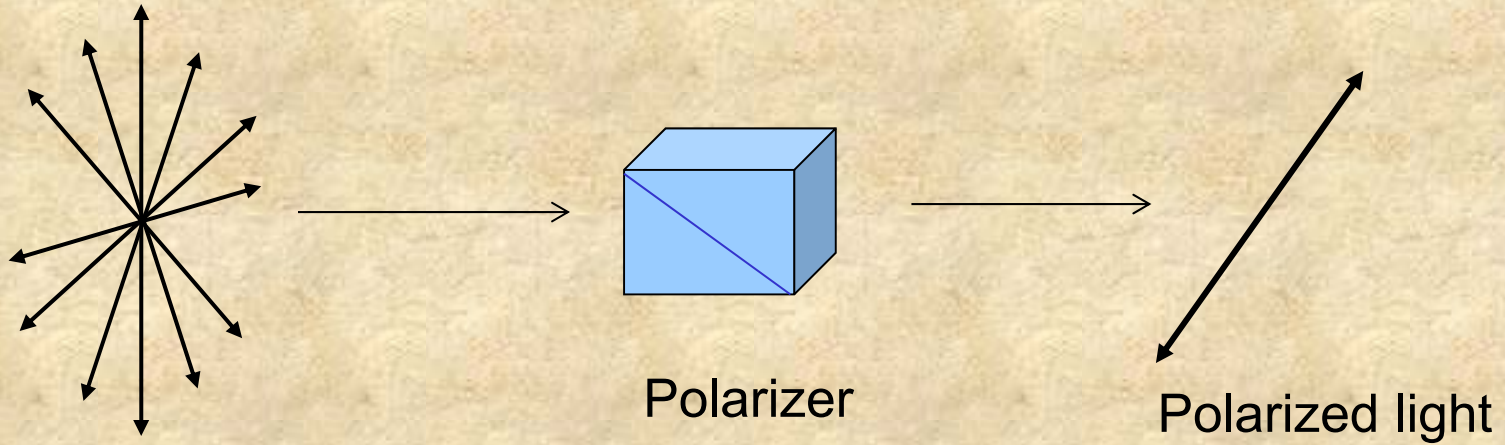


In these lectures we shall be concerned only with the electric component.

In natural light the electric field vector can assume any direction of oscillation perpendicular or normal to the light propagation direction.



Polarizers are optically active devices that can isolate one direction of the electric vector.

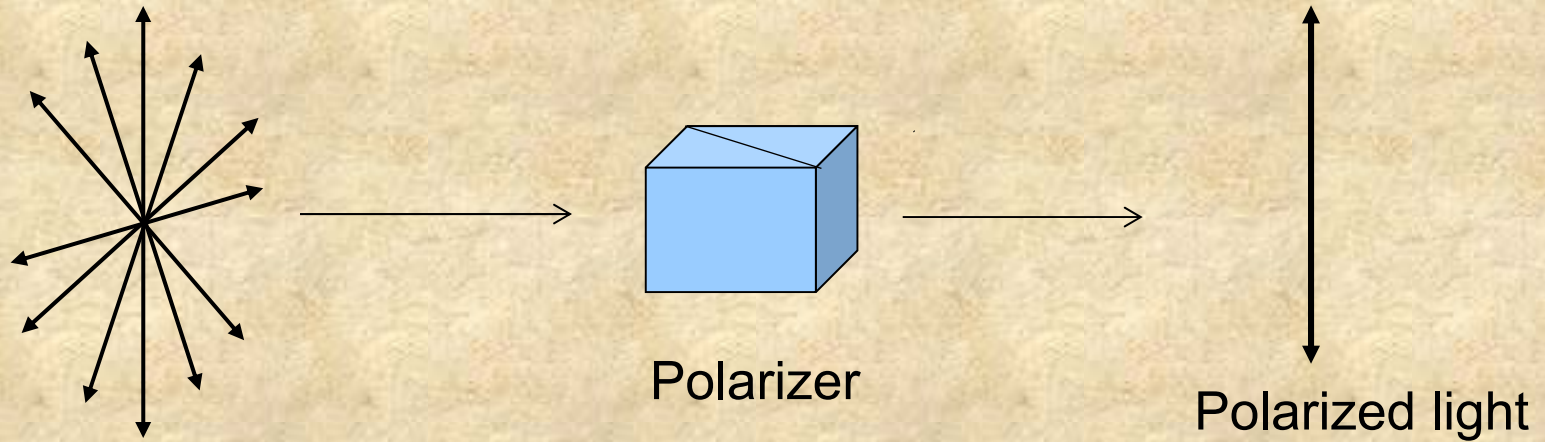


Unpolarized (natural) light

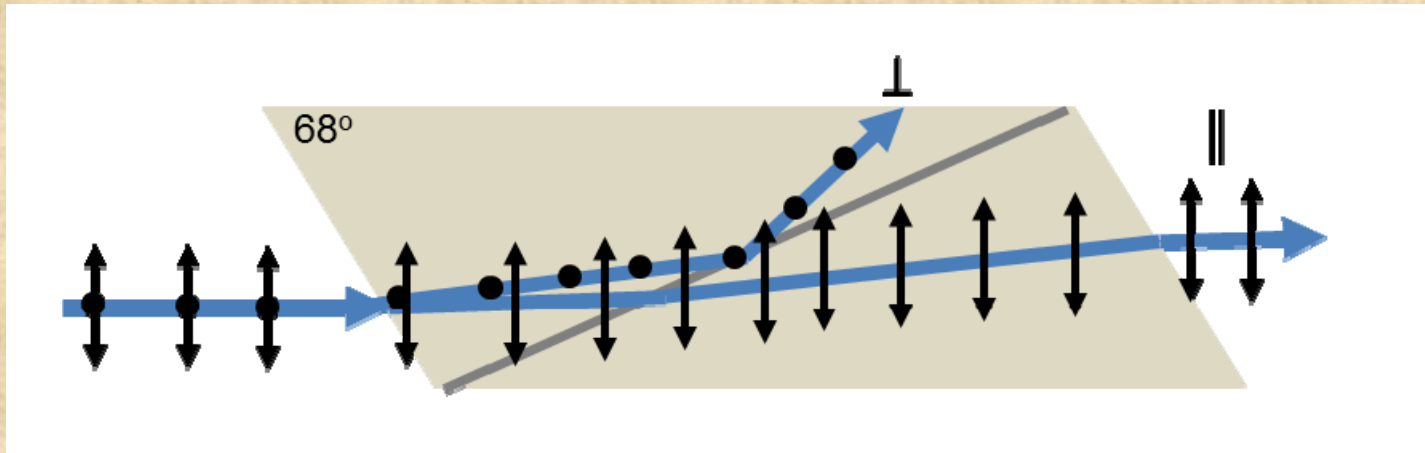
Polarizer

Polarized light

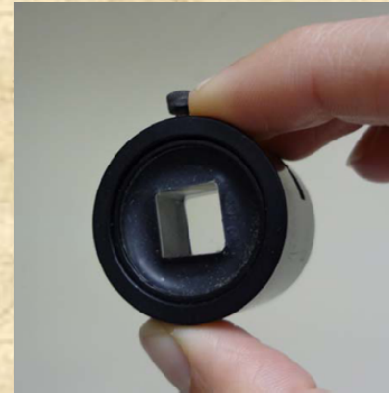
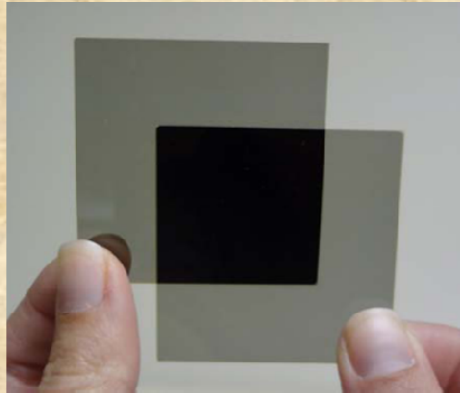
Polarizers are optically active devices that can isolate one direction of the electric vector.



Unpolarized (natural) light



The most common polarizers used today are (1) dichroic devices, which operate by effectively absorbing one plane of polarization (e.g., Polaroid type-H sheets based on stretched polyvinyl alcohol impregnated with iodine) and (2) double refracting calcite (CaCO_3) crystal polarizers - which differentially disperse the two planes of polarization (examples of this class of polarizers are Nicol polarizers, Wollaston prisms and Glan-type polarizers such as the Glan-Foucault, Glan-Thompson and Glan-Taylor polarizers)



Polarization of Fluorescence

In 1920, F. Weigert discovered that the fluorescence from solutions of dyes was polarized. Specifically, he looked at solutions of fluorescein, eosin, rhodamine and other dyes and noted the effect of temperature and viscosity on the observed polarization.

In Weigert's words "Der Polarisationsgrad des Fluorezenzlichtes nimmt mit wachsender Molekulargröße, mit zunehmender Viskosität des Mediums und mit abnehmender Temperatur, also mit Verringerung der Beweglichkeit der Einzelteilchen zu"

"The degree of the polarization increases with increasing molecular size, with increasing viscosity of the medium and with decreasing temperature, that is with the reduction of the mobility of the single particles."

He recognized that all of these considerations meant that fluorescence polarization increased as the mobility of the emitting species decreased.

In 1925 - 1926, Francis Perrin published several important papers describing a quantitative theory of fluorescence polarization including what is now considered his classic paper containing most of the essential information that we use to this day

J. de Physique 1926

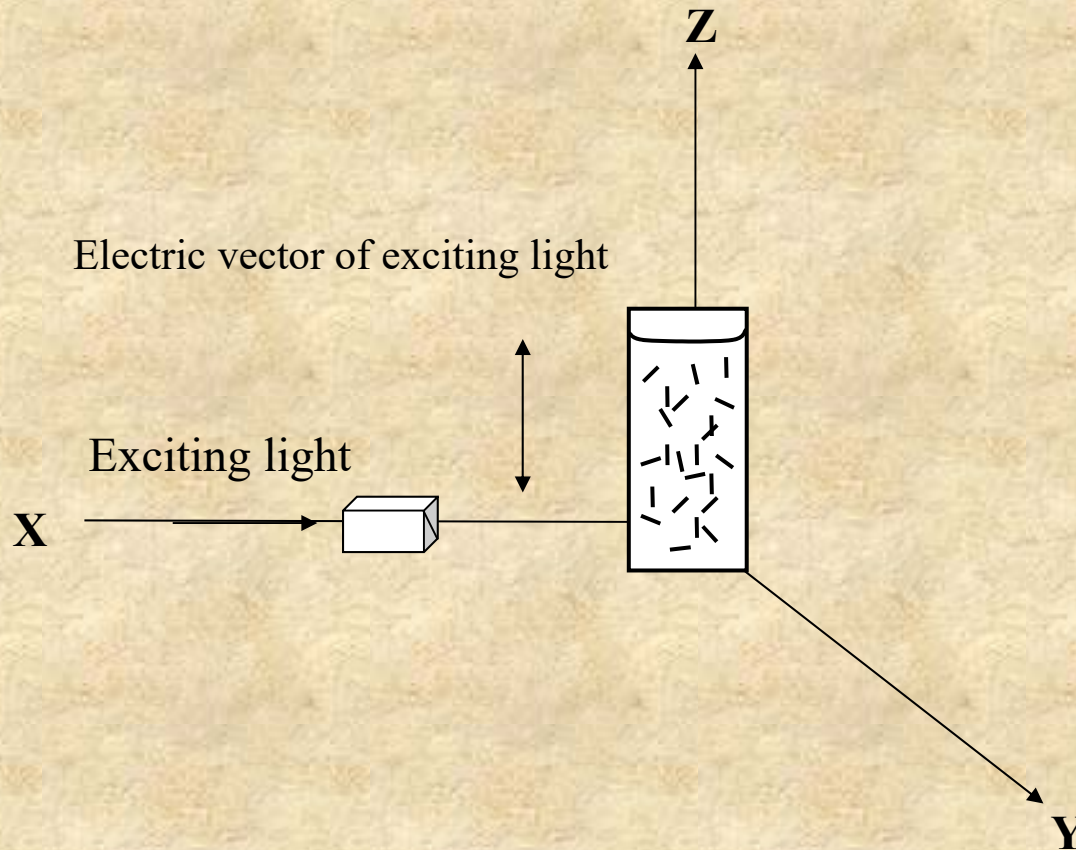
POLARISATION DE LA LUMIÈRE DE FLUORESCENCE. VIE MOYENNE DES MOLECULES
DANS L'ETAT EXCITE
par M. FRANCIS PERRIN.

$$P = P_0 \frac{1}{1 + \left(1 - \frac{1}{3} P_0\right) \frac{RT}{v\eta} \tau}$$

Polarization remained largely in the province of the physicists for almost two decades, until Gregorio Weber began his thesis.

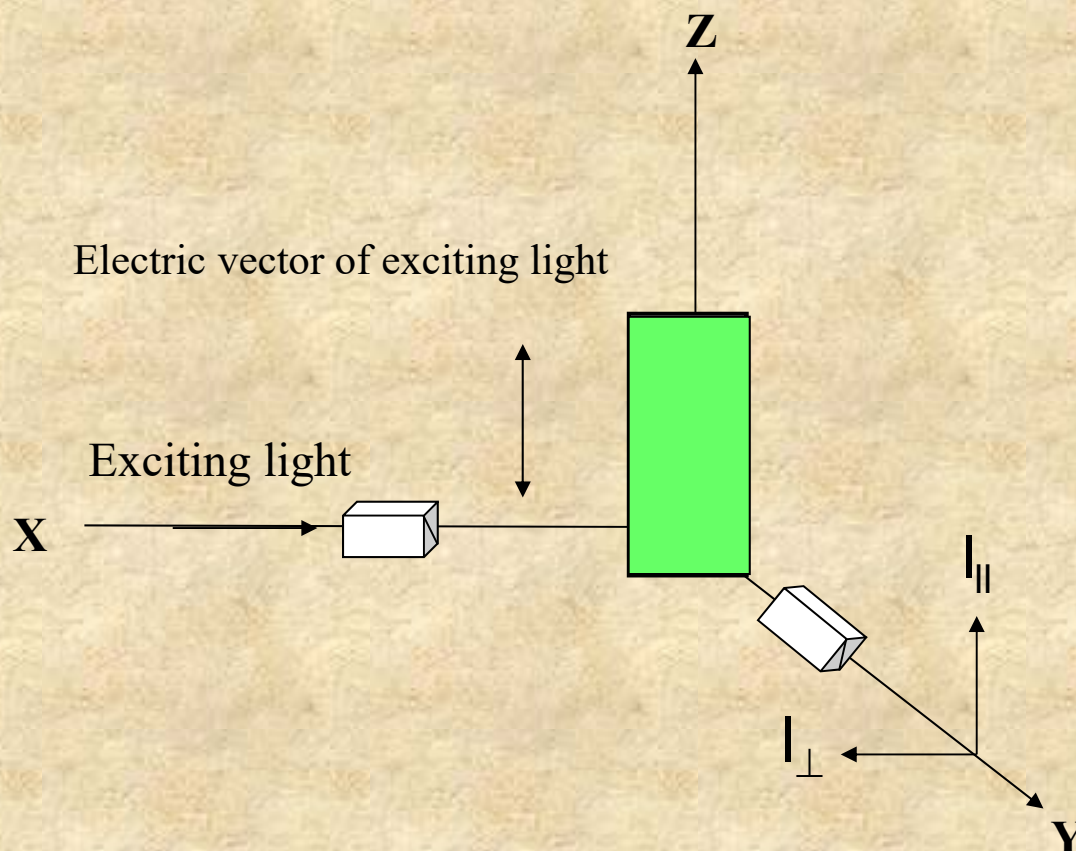
Weber's subsequent theoretical and experimental work – which extended Perrin's earlier contributions and also developed what became modern instrumentation - brought fluorescence polarization to the attention of the biochemical community, and so ushered in a new scientific discipline – quantitative biological fluorescence.

Consider an XYZ coordinate framework with a fluorescent solution placed at the origin, as shown below, where XZ is in the plane of the page.



In this system, the exciting light is traveling along the X direction. If a polarizer is inserted in the beam, one can isolate a unique direction of the electric vector and obtain light polarized parallel to the Z axis which corresponds to the vertical laboratory axis.

This exciting light will be absorbed by the fluorophore at the origin and give rise to fluorescence which is typically observed at 90° to the excitation direction, i.e., from along the Y axis.



The actual direction of the electric vector of the emission can be determined by viewing the emission through a polarizer which can be oriented alternatively in the parallel or perpendicular direction relative to the Z axis or laboratory vertical direction.

Polarization is then defined as a function of the observed parallel (I_{\parallel}) and perpendicular intensities (I_{\perp}) :

$$P = \frac{I_{\parallel} - I_{\perp}}{I_{\parallel} + I_{\perp}}$$

If the emission is completely polarized in the parallel direction, i.e., the electric vector of the exciting light is totally maintained, then:

$$P = \frac{1 - 0}{1 + 0} = 1$$

If the emitted light is totally polarized in the perpendicular direction then:

$$P = \frac{0 - 1}{0 + 1} = -1$$

The limits of polarization are thus +1 to -1

Another term frequently used in the context of polarized emission is anisotropy (usually designated as either A or r) which is defined as:

$$r = \frac{I_{\parallel} - I_{\perp}}{I_{\parallel} + 2I_{\perp}}$$

By analogy to polarization, the limits of anisotropy are +1 to -0.5.

A comment about the difference between polarization and anisotropy:

Given the definition of polarization and anisotropy, one can show that:

$$r = \frac{2}{3} \left(\frac{1}{P} - \frac{1}{3} \right)^{-1} \quad \text{or} \quad r = \frac{2P}{3 - P}$$

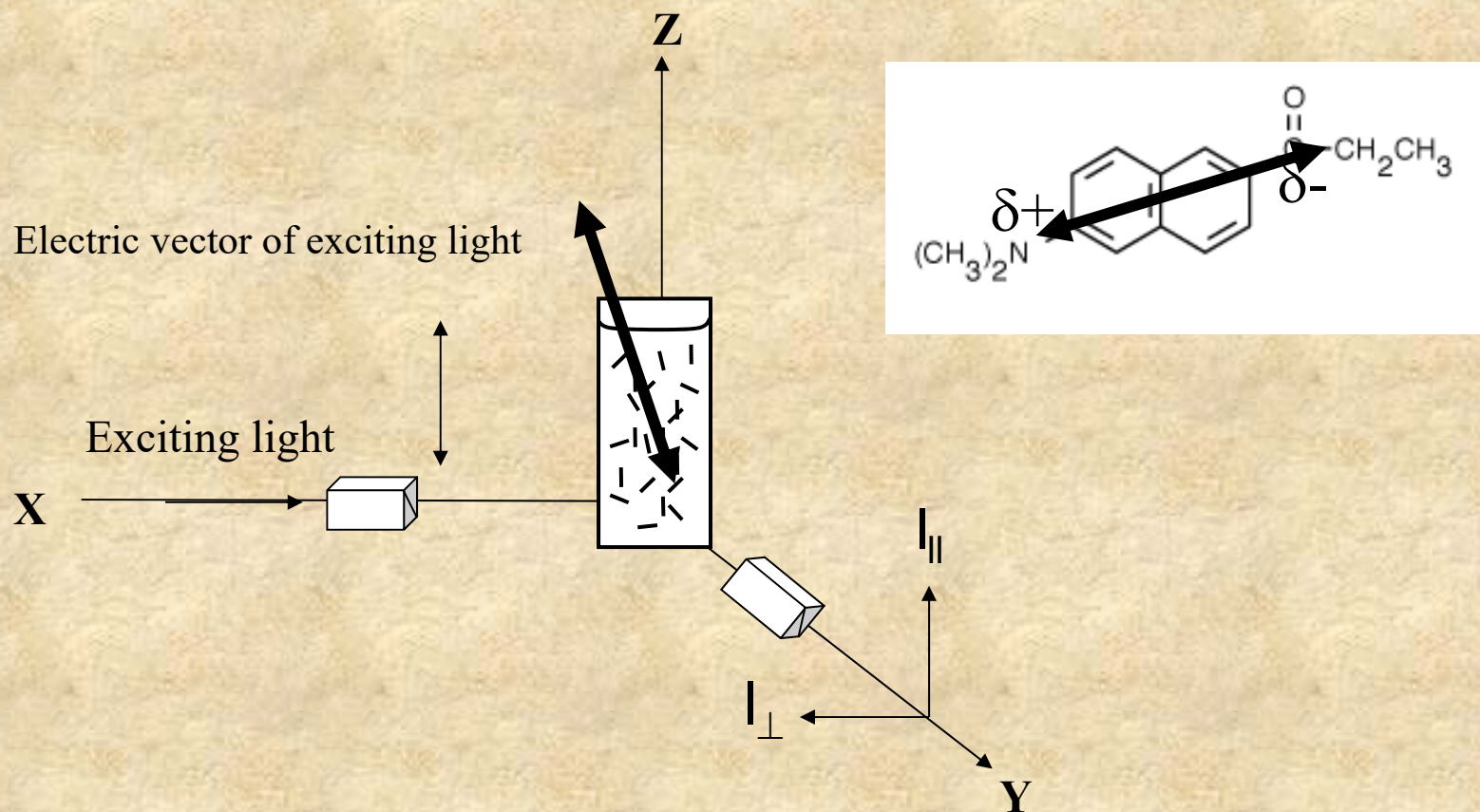
For example:

P	r
0.50	0.40
0.25	0.20
0.10	0.069
-0.10	-0.065

Clearly, the information content in the polarization function and the anisotropy function is identical and the use of one term or the other is dictated by practical considerations as will be discussed later.

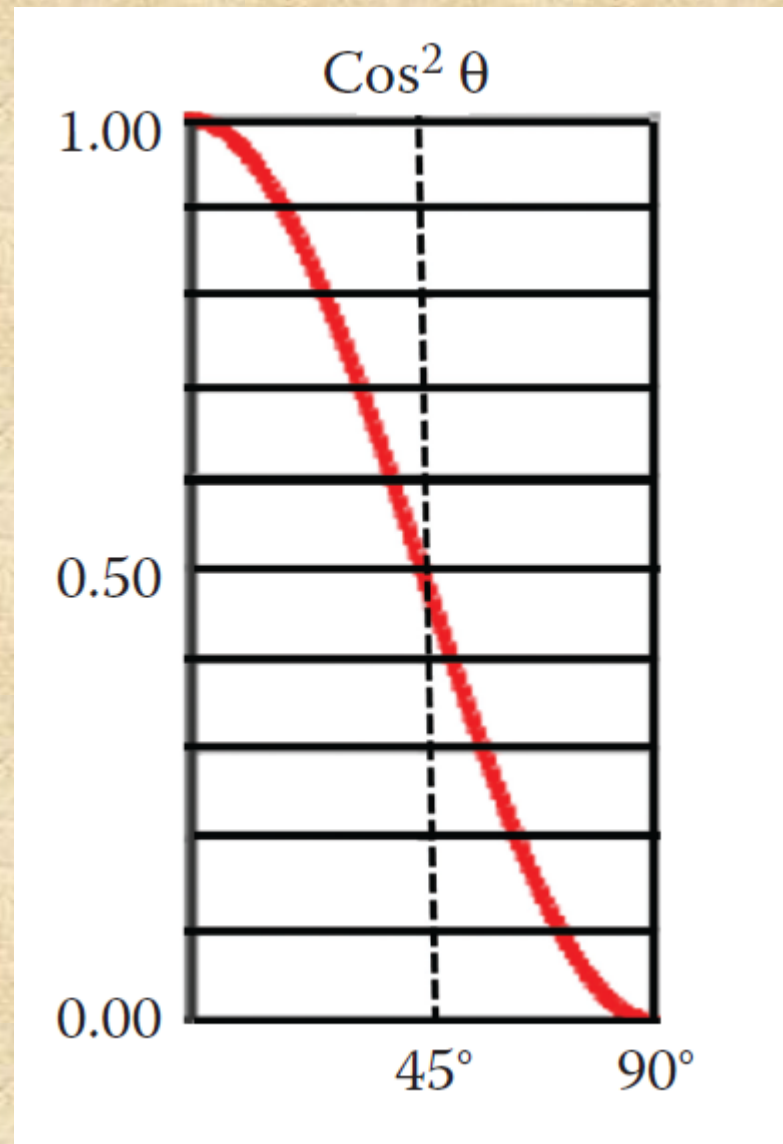
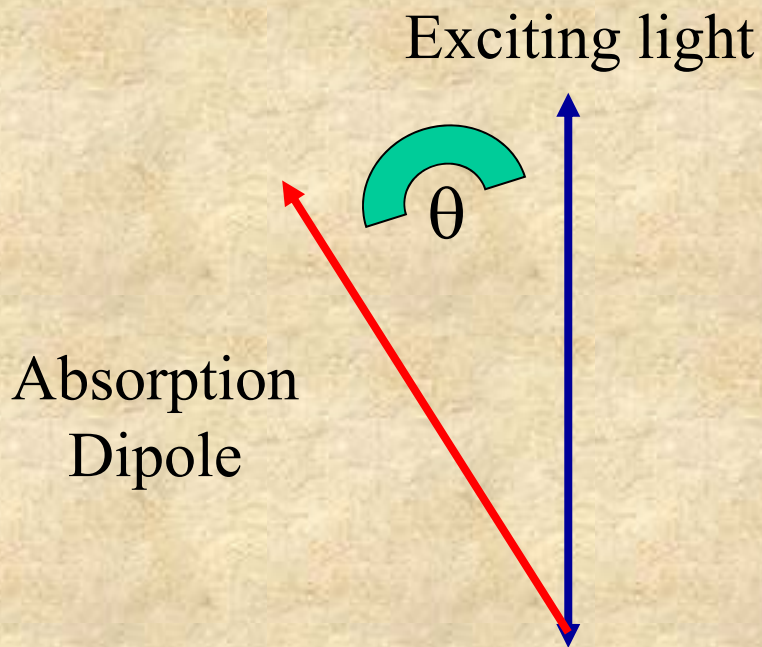
In solution these limits (e.g., +/-1) are not realized. Consider, as shown below, fluorophores at the origin of our coordinate system.

Upon absorption of an exciting photon a dipole moment is created in the fluorophore (usually of different magnitude and direction from the ground state dipole). The orientation of this dipole moment relative to the nuclear framework, and its magnitude, will be determined by the nature of the substituents on the molecule. This excited state dipole moment is also known as the transition dipole or transition moment.

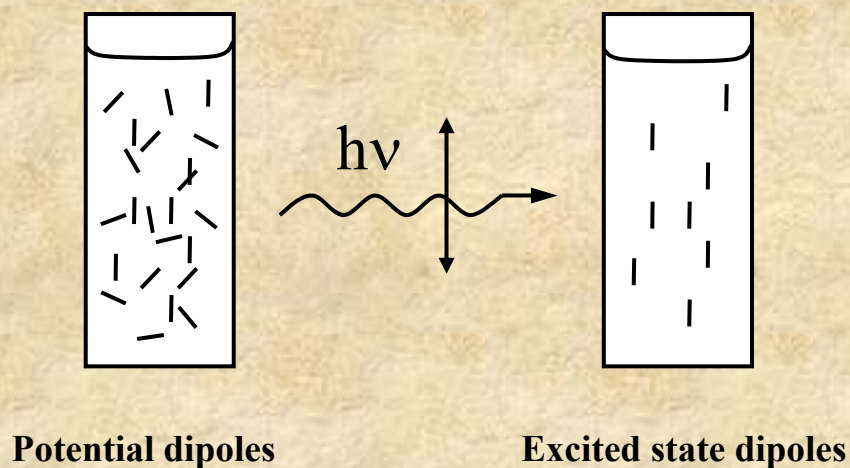


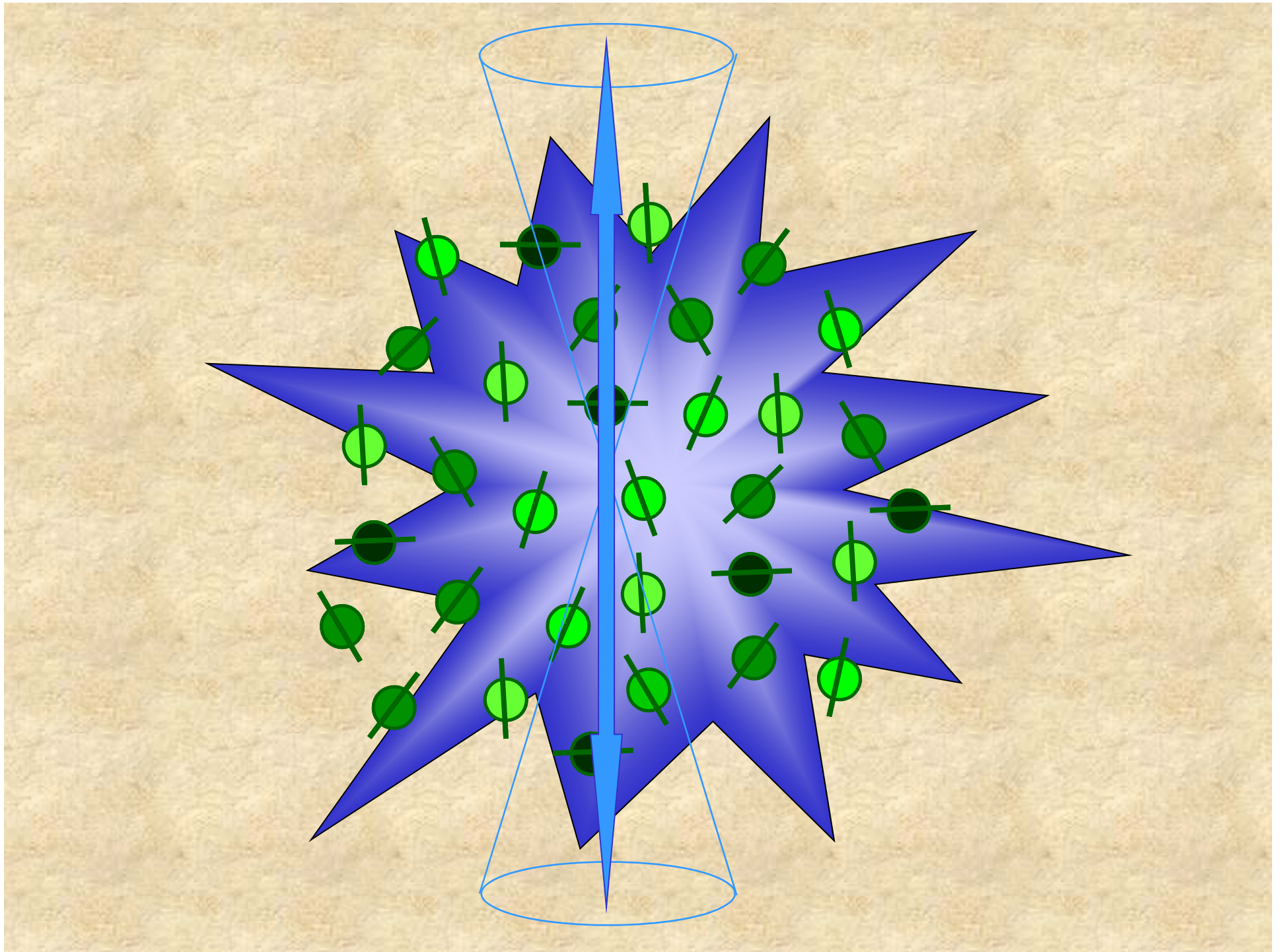
In fact, if light of a particular electric vector orientation (plane polarized light) impinges on a sample, only those molecules which are properly oriented relative to this electric vector can absorb the light.

Specifically, the probability of the absorption is proportional to the cosine squared ($\cos^2\theta$) of the angle θ between the exciting light and the transition dipole.

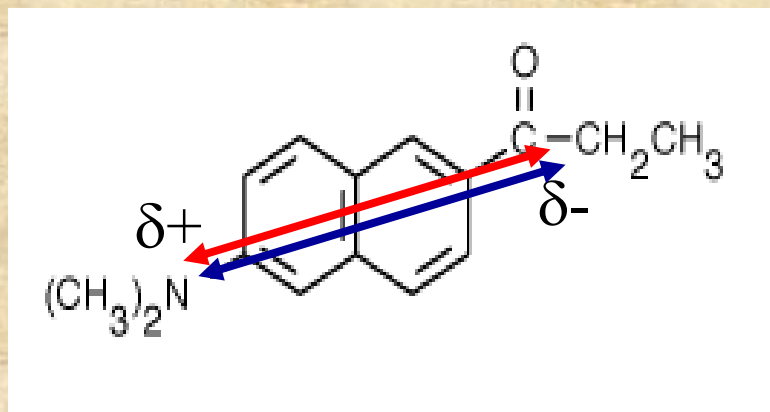


Hence, when we excite an ensemble of randomly oriented fluorophores with plane-polarized light we are performing a *photoselection* process, creating a population of excited molecules which nominally have their excited dipoles lined up with the polarization direction of the excitation. This process is illustrated below:

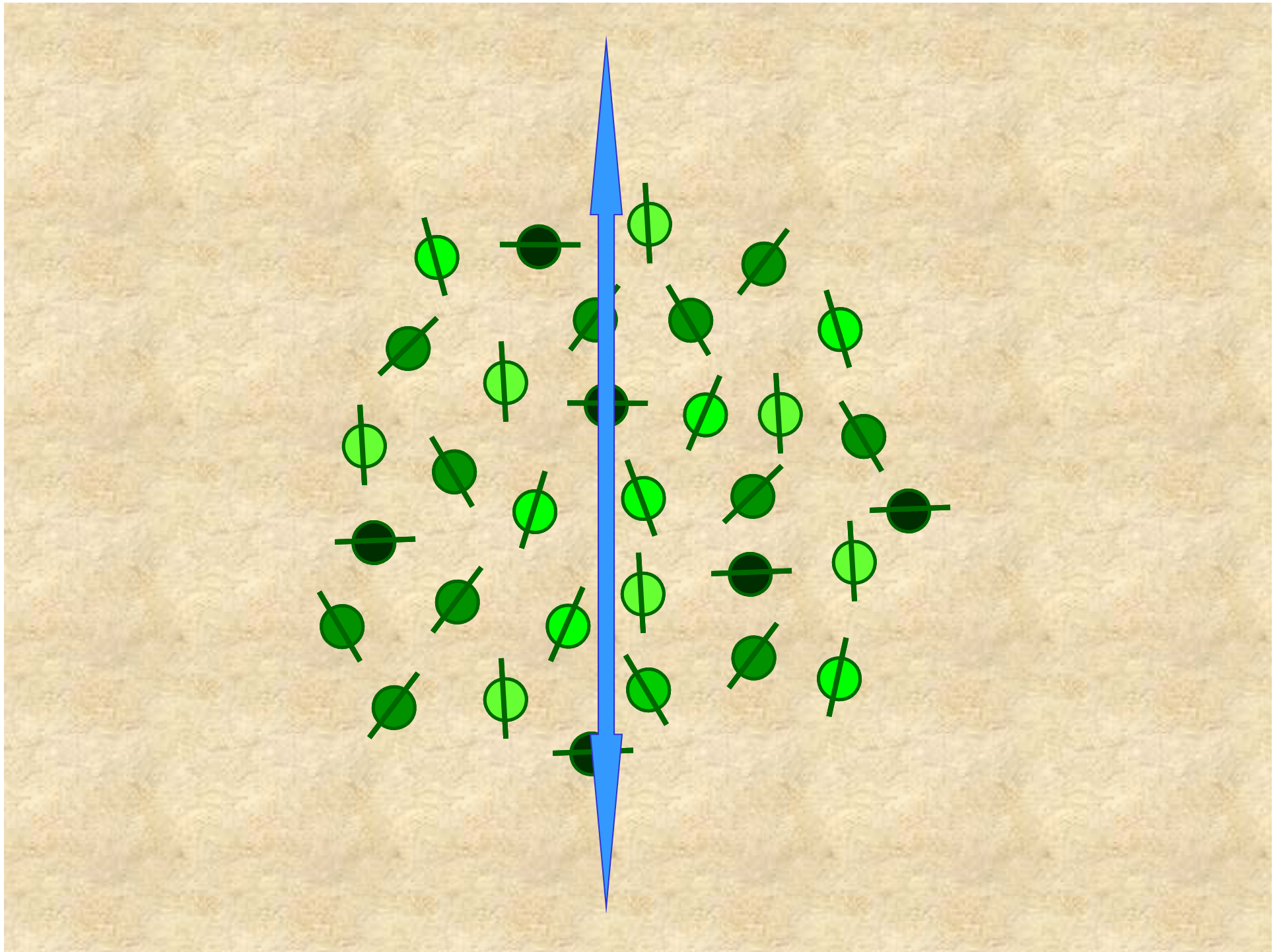




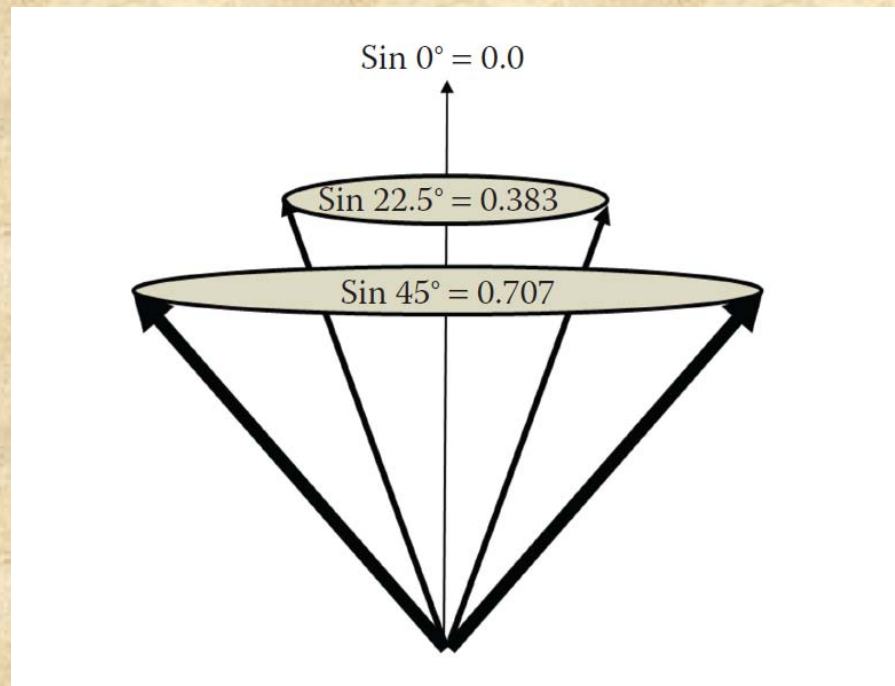
Consider now that the transition dipole corresponding to the emission of light from the excited fluorophore is parallel to the absorption dipole and that the excited fluorophore cannot rotate during the lifetime of the excited state (for example if the fluorophores are embedded in a highly viscous or frozen medium).



If we were to now measure the polarization of the emission it would be less than +1 since some of the dipoles excited will not be exactly parallel to the direction of the exciting light.



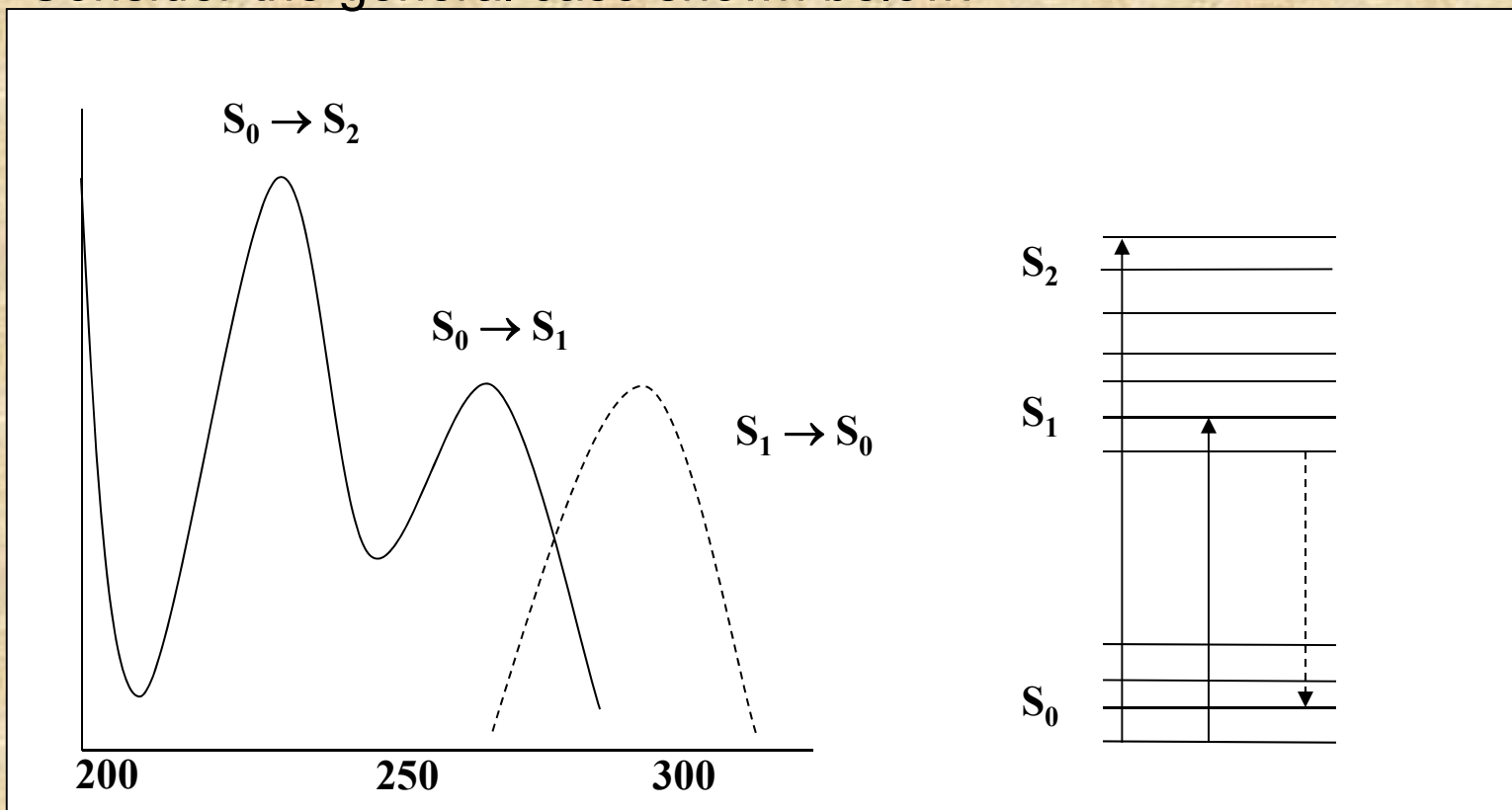
In fact, the number of potential dipoles making an angle θ with the vertical axis will be proportional to $\sin \theta$.



We can then calculate that the upper polarization limit for such a randomly oriented (but rigidly fixed, i.e., non-rotating) ensemble - with co-linear excitation and emission dipole - will be $+1/2$

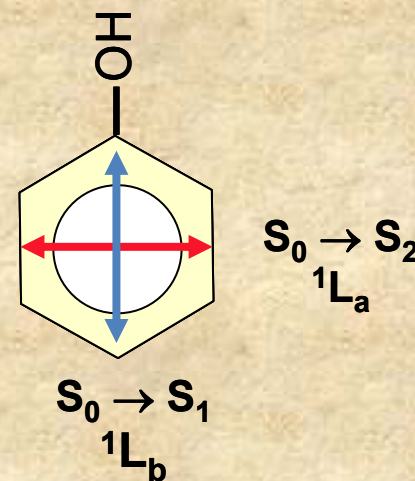
This case, however, assumes that the emission dipole is parallel (co-linear) to the absorption dipole.

Consider the general case shown below:



Here are depicted two principle absorption bands for phenol along with and the emission band. The energy level diagram corresponding to this system is also depicted.

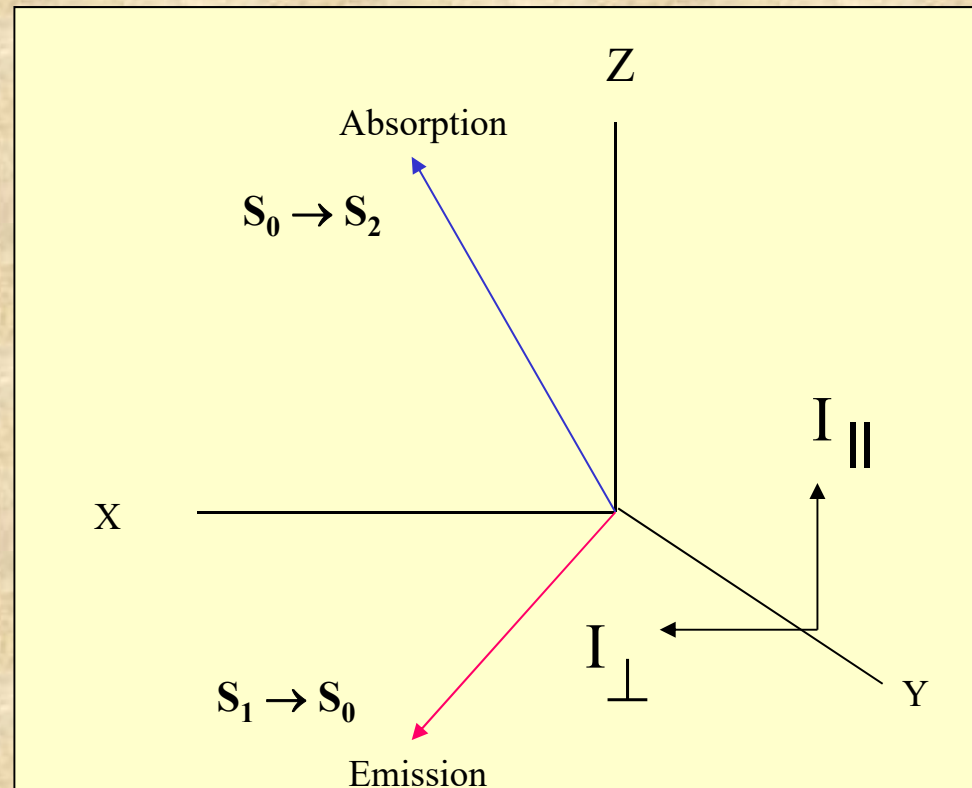
The directions of the absorption dipoles – relative to the nuclear framework – may differ greatly for the two transitions as illustrated on the right.



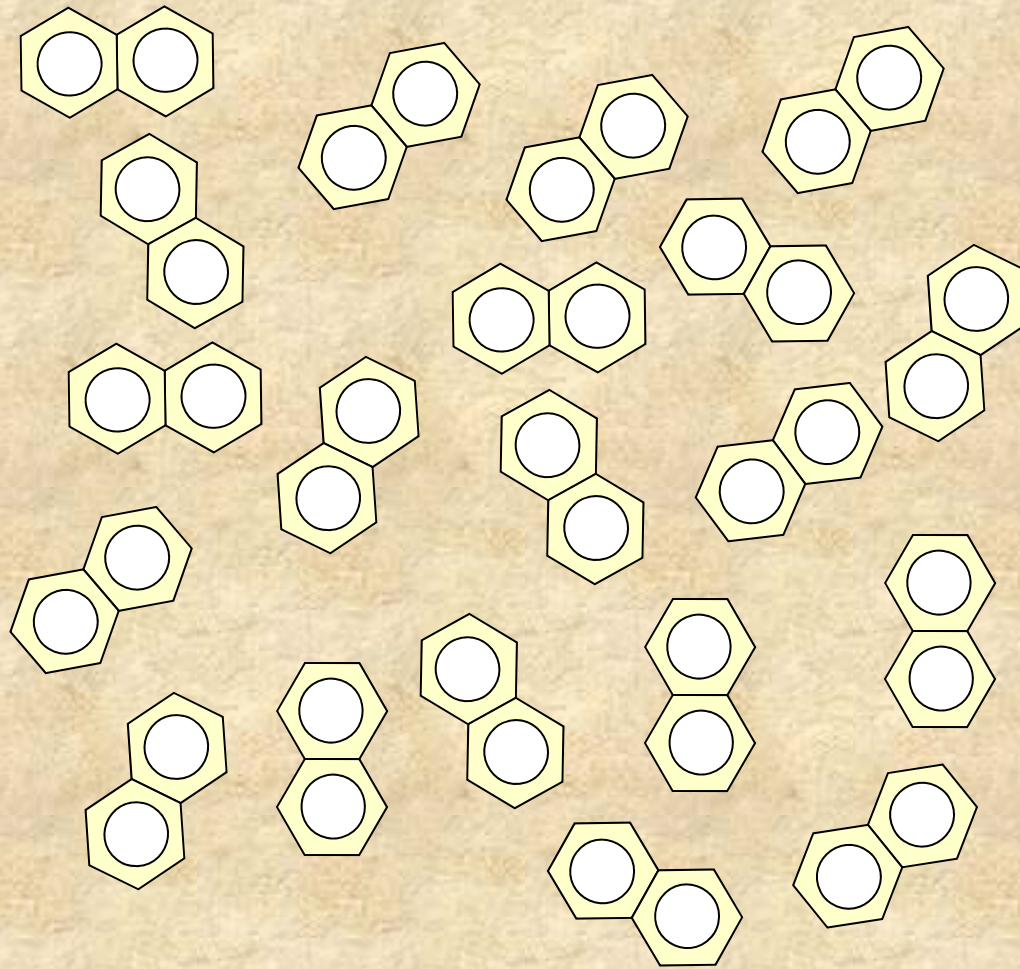
So we see that the two excited dipoles corresponding to the $S_0 \rightarrow S_1$ and the $S_0 \rightarrow S_2$ transitions may be oriented at an arbitrary angle - in the extreme case this angle could be 90° .

After the excitation process, however, regardless of whether the absorption process corresponded to the $S_0 \rightarrow S_1$ or the $S_0 \rightarrow S_2$ transition, rapid thermalization leaves the excited fluorophore in the S_1 level.

This situation is depicted below:

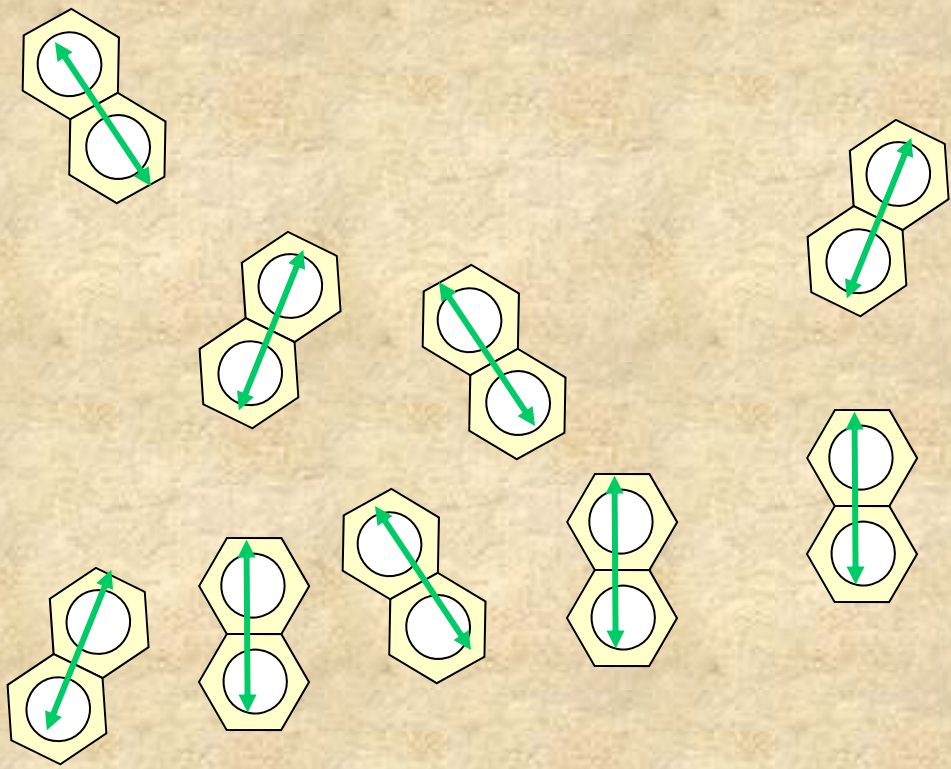


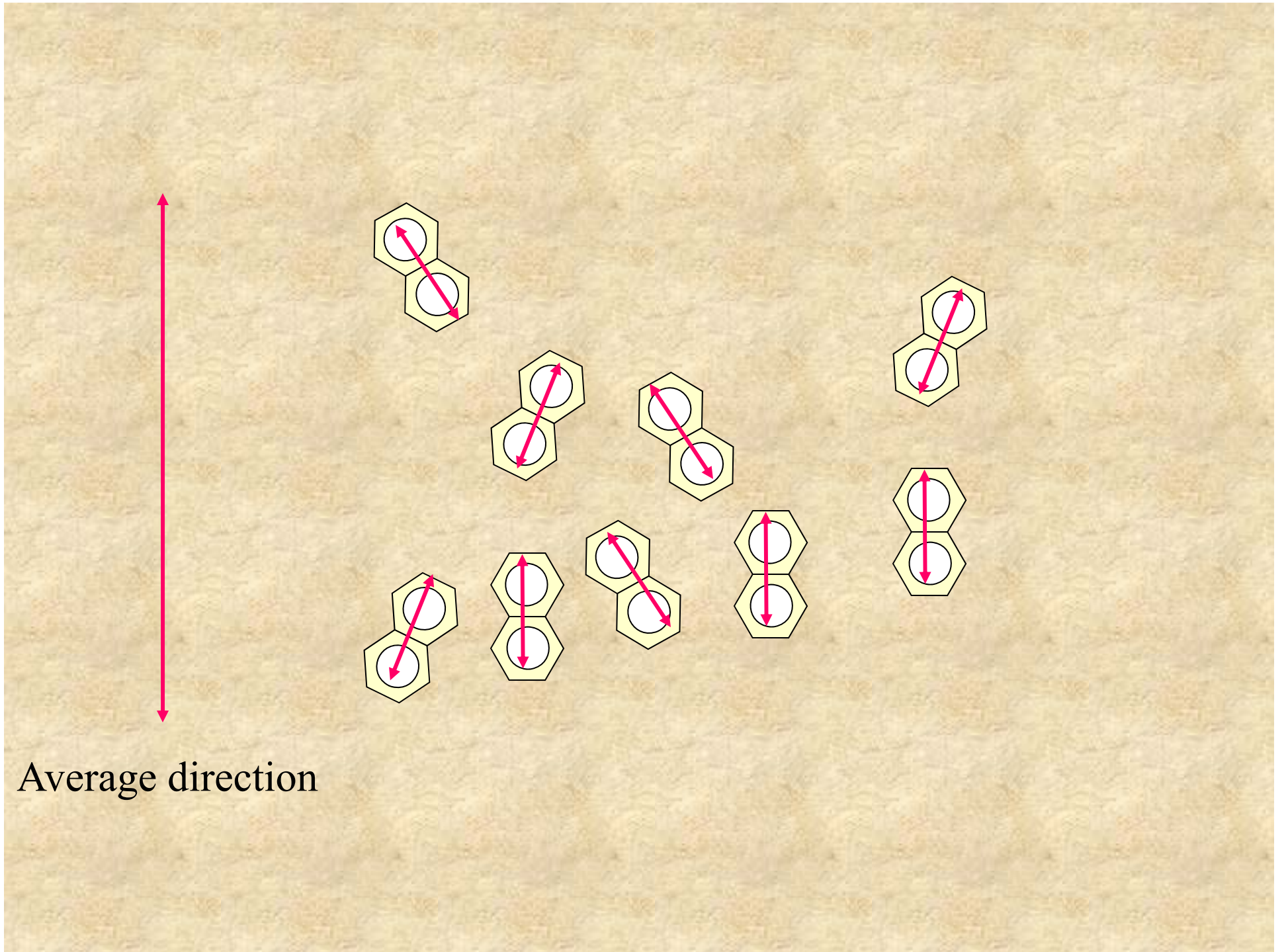
The orientation of the excited dipoles will thus now possess a different average orientation than the absorption dipoles originally photoselected by the exciting light.



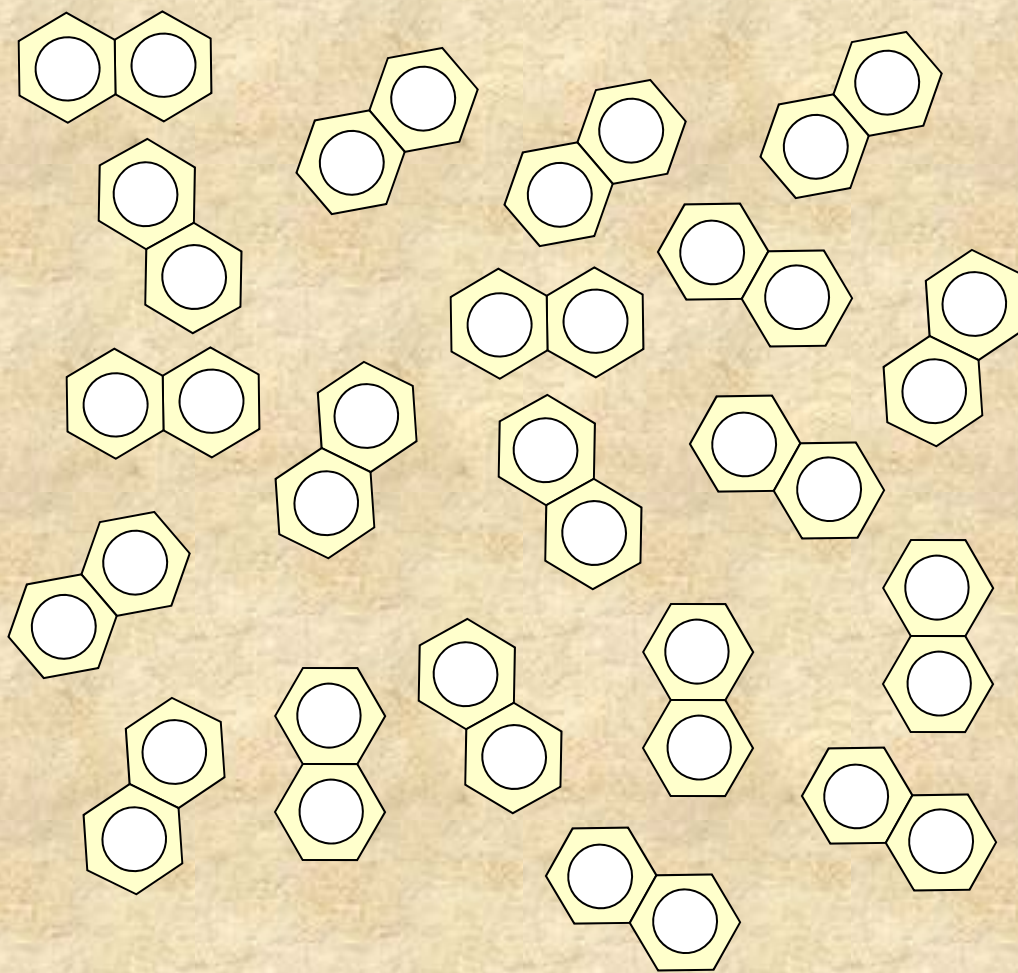


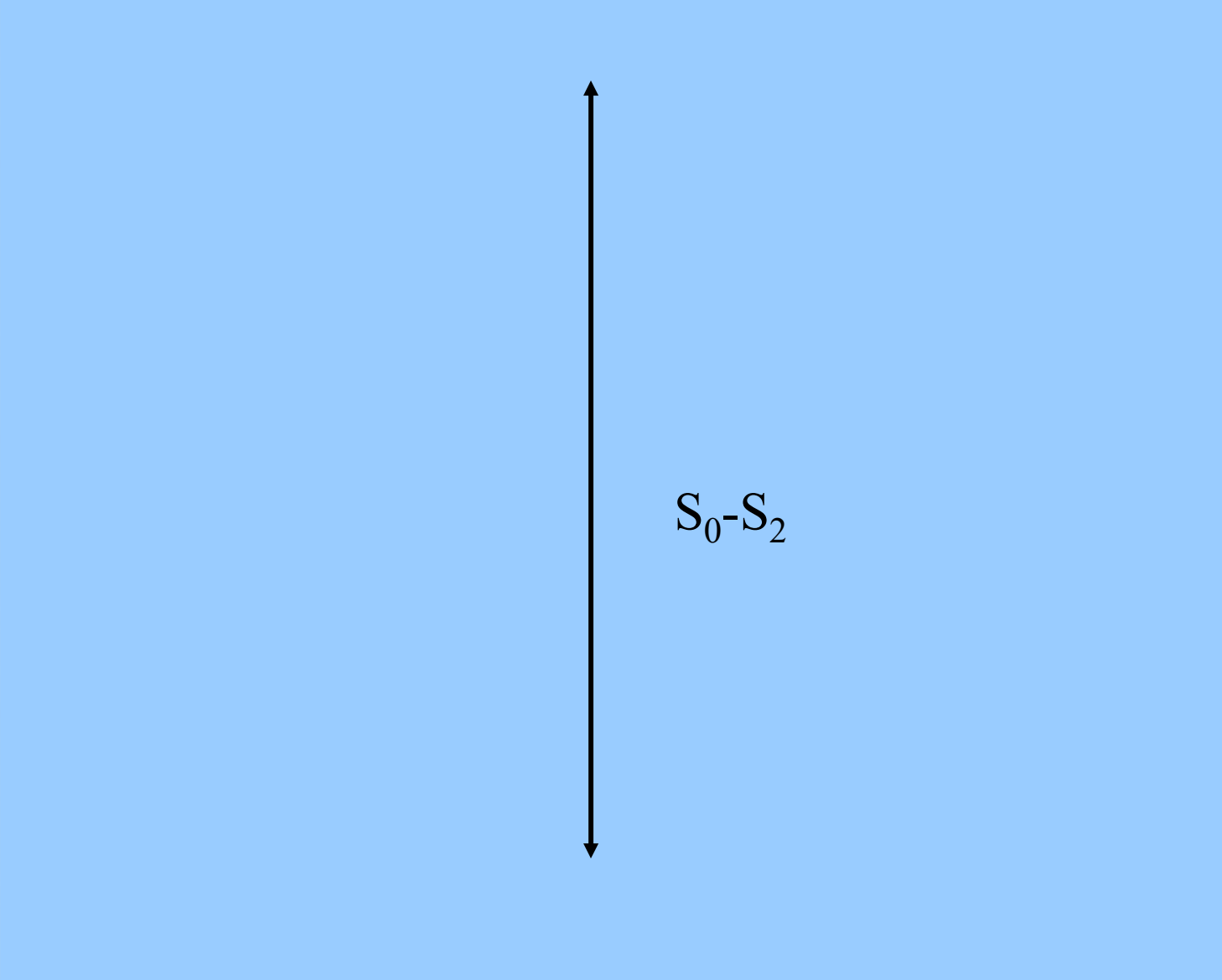
$S_0 - S_1$



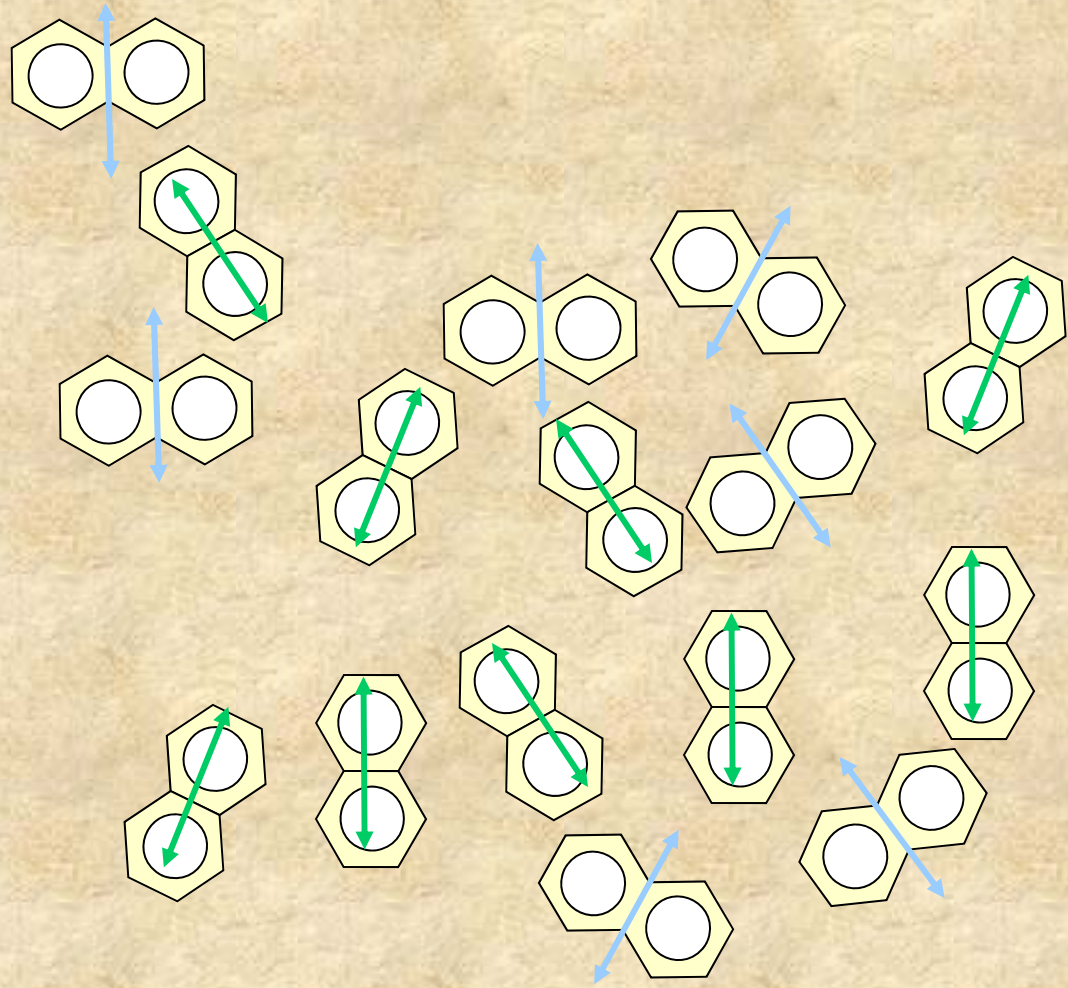


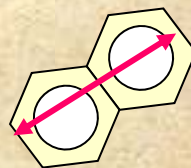
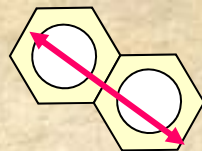
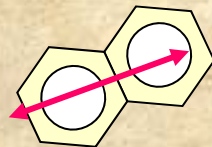
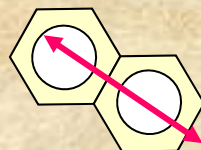
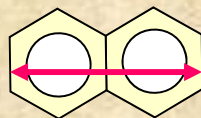
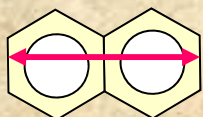
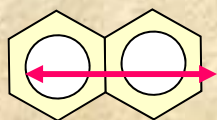
Average direction





S_0-S_2





Average direction

Hence we will observe more emission in the perpendicular direction than in the parallel direction and the resulting polarization will be negative. Considering the same $\cos^2 \theta$ photoselection rule and the $\sin \theta$ population distribution as before we can show that, if the absorption and emission dipoles are at 90° to each other, then $P = -1/3$.

These polarization values, in the absence of rotation, are termed limiting or intrinsic polarizations and are denoted as P_o . In general:

$$\frac{1}{P_o} - \frac{1}{3} = \frac{5}{3} \left(\frac{2}{3 \cos^2 \phi - 1} \right)$$

Where ϕ is the angle between absorption and emission dipoles.

We can then understand that the limiting polarization of a fluorophore will depend upon the excitation wavelength.

Consider the excitation polarization spectrum for phenol (in glycerol at -70 C).

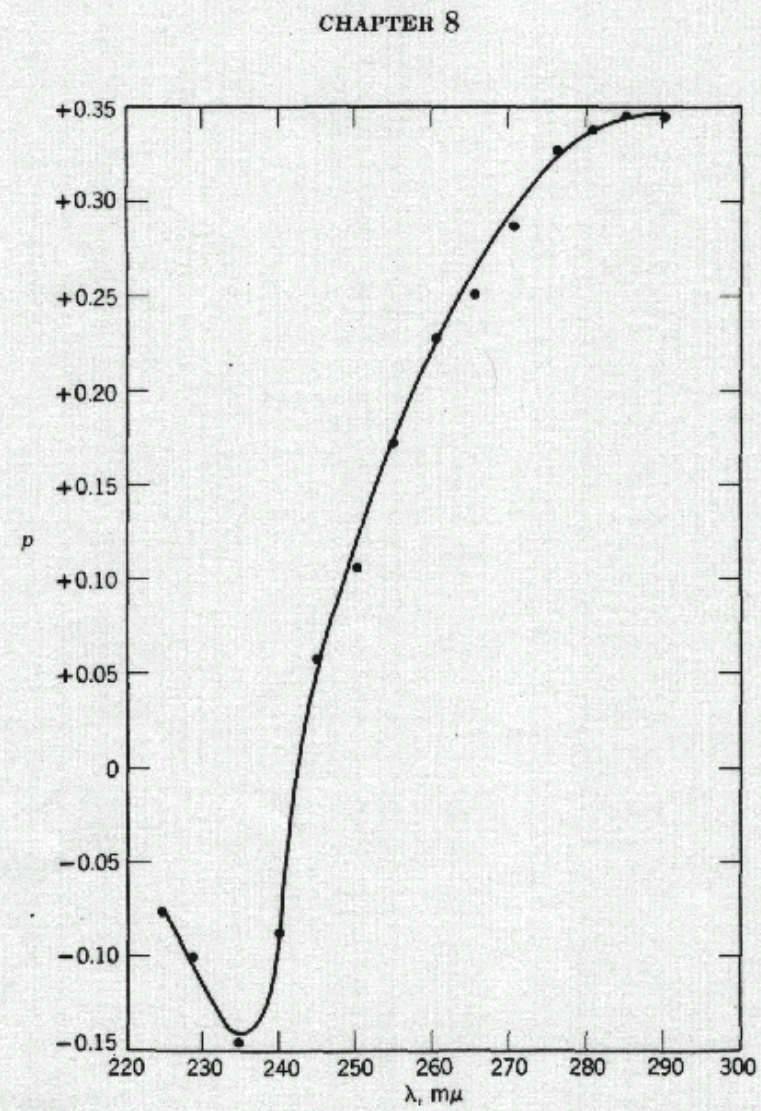
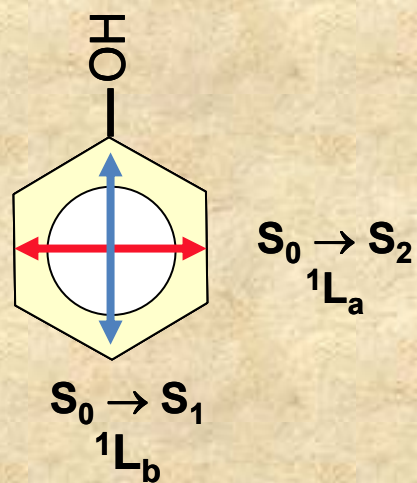
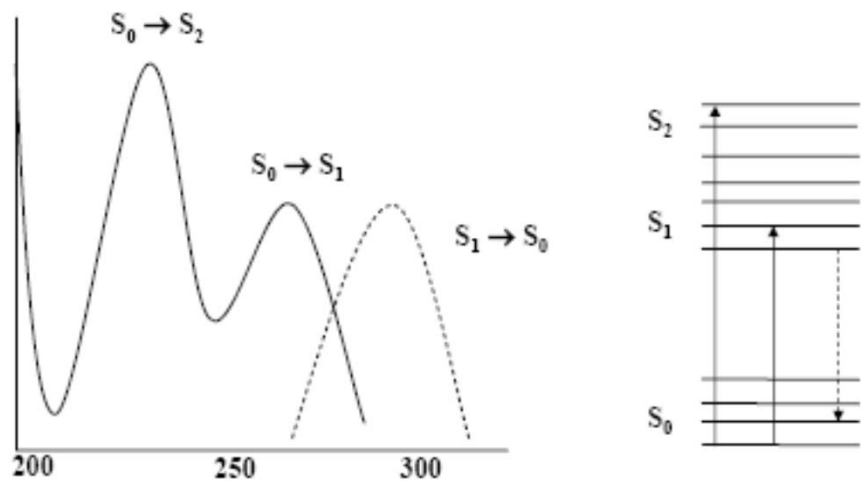
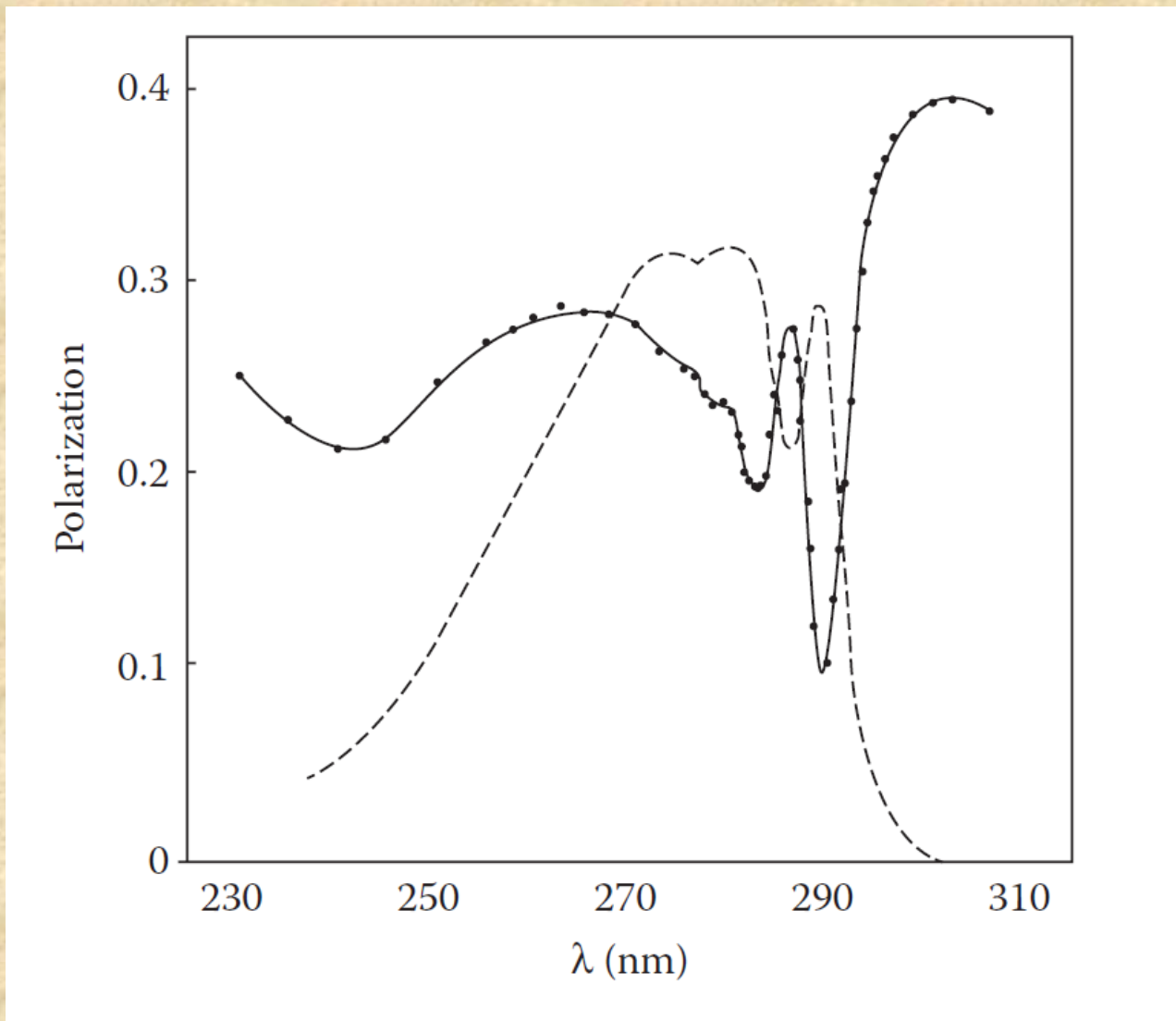
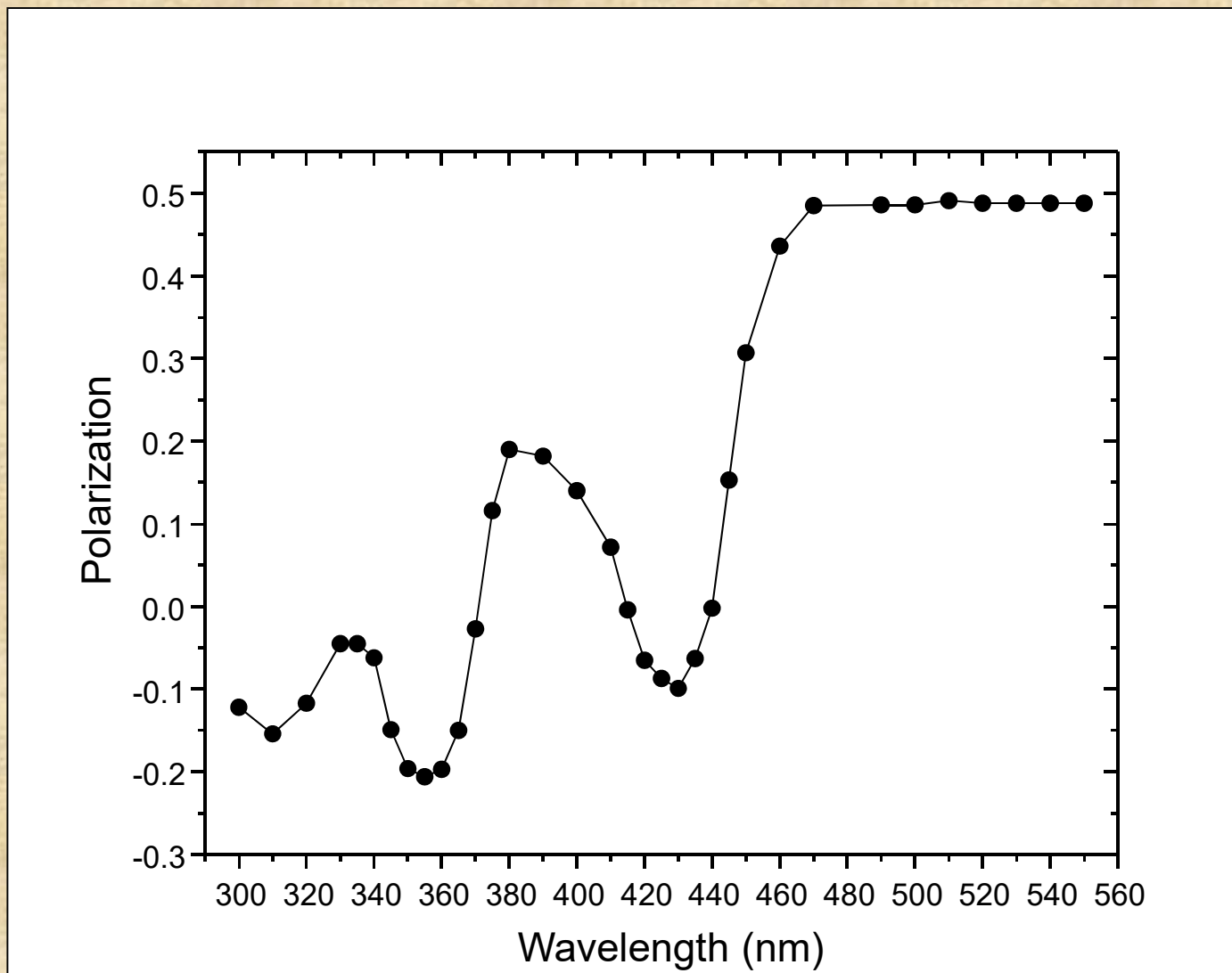


Fig. 8-5. Fluorescence polarization spectrum of phenol at -70°C in propylene glycol. Ordinate = polarization, p ; abscissa, exciting wavelength in $m\mu$. Redrawn from Weber (18).

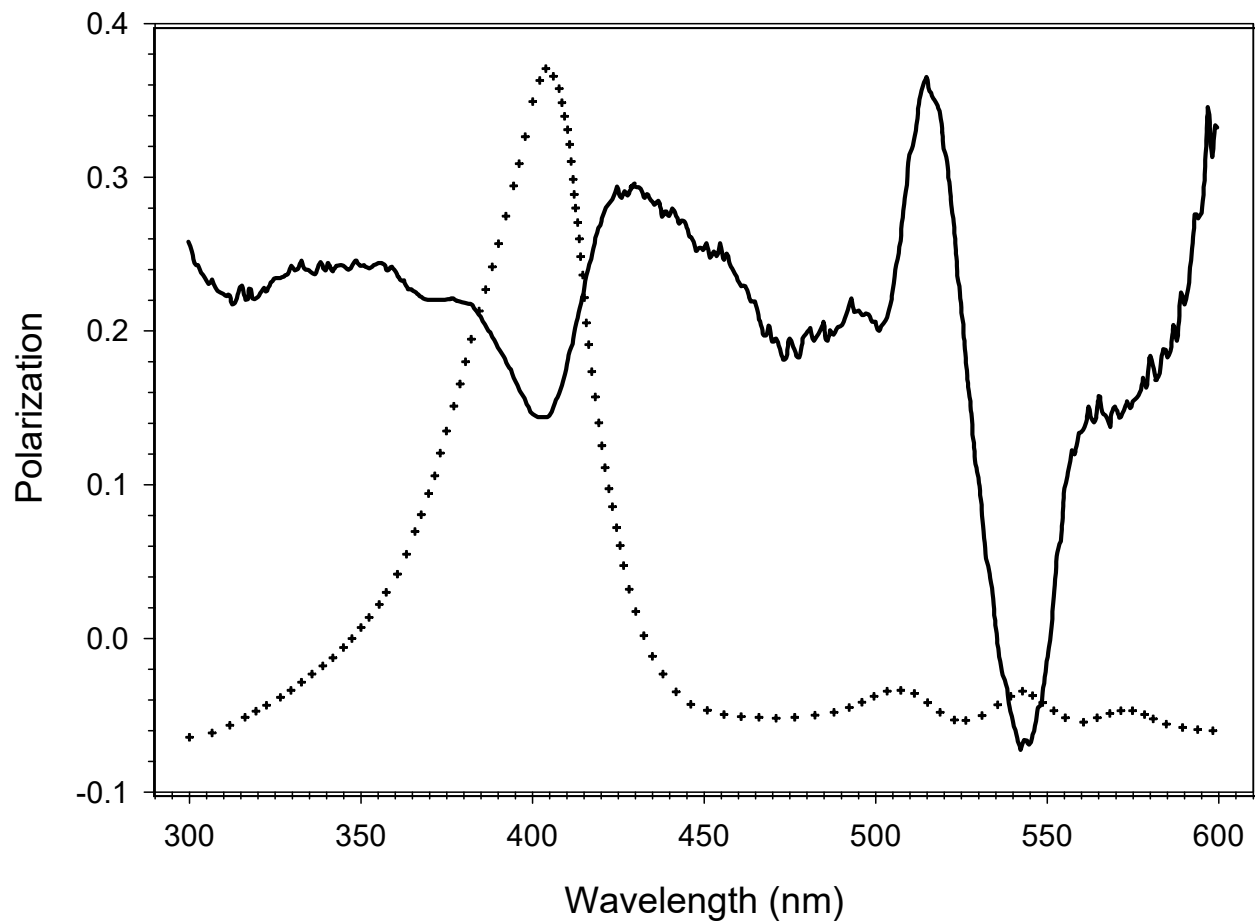
In cases where there are multiple overlapping absorption bands at various angles, the excitation polarization spectrum can be somewhat complex as shown below for indole.



Excitation polarization spectra of rhodamine B embedded in a Lucite matrix at room temperature. Emission was viewed through a cut-on filter passing wavelengths longer than 560nm; slits were ~4nm.

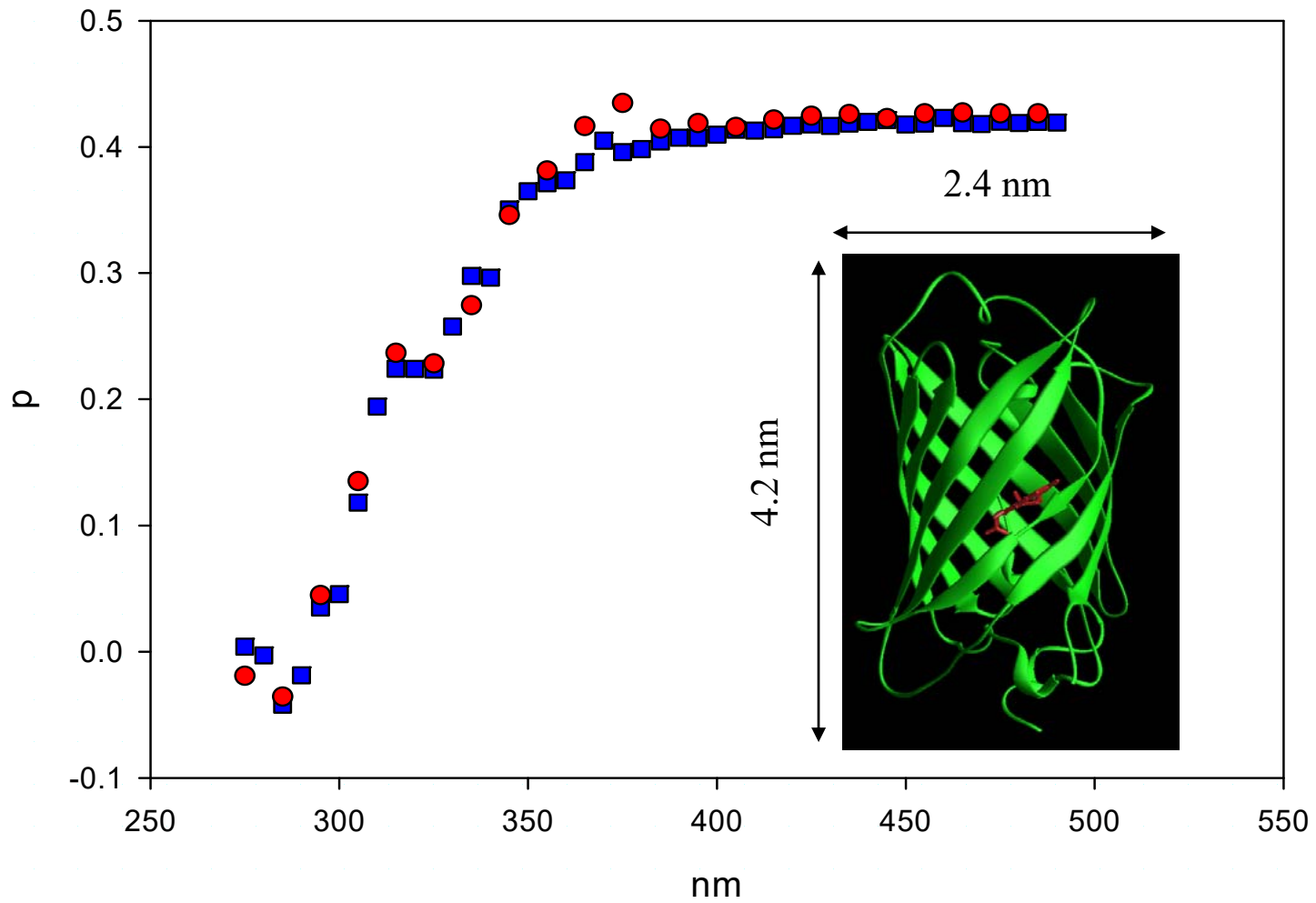


Another example is protoporphyrin IX in glycerol at -20°C



Excitation Polarization Spectrum of GFP

Emission 507nm



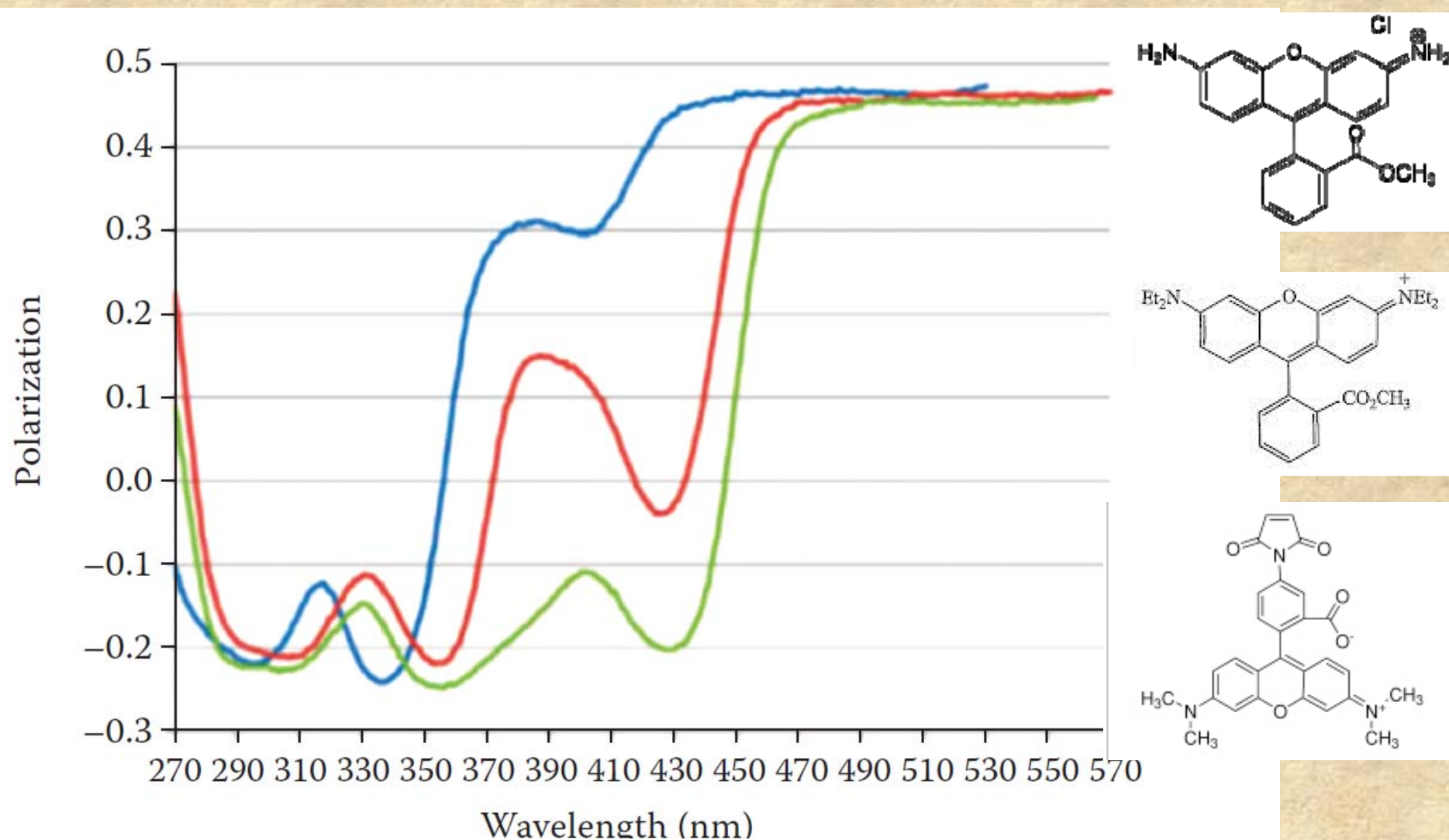
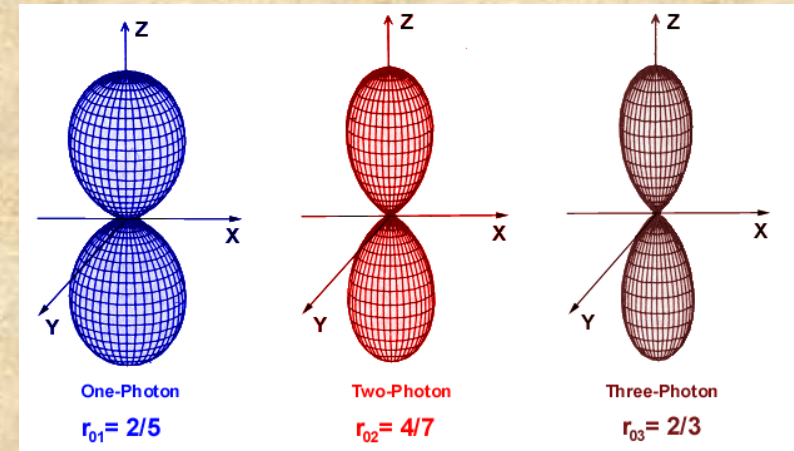
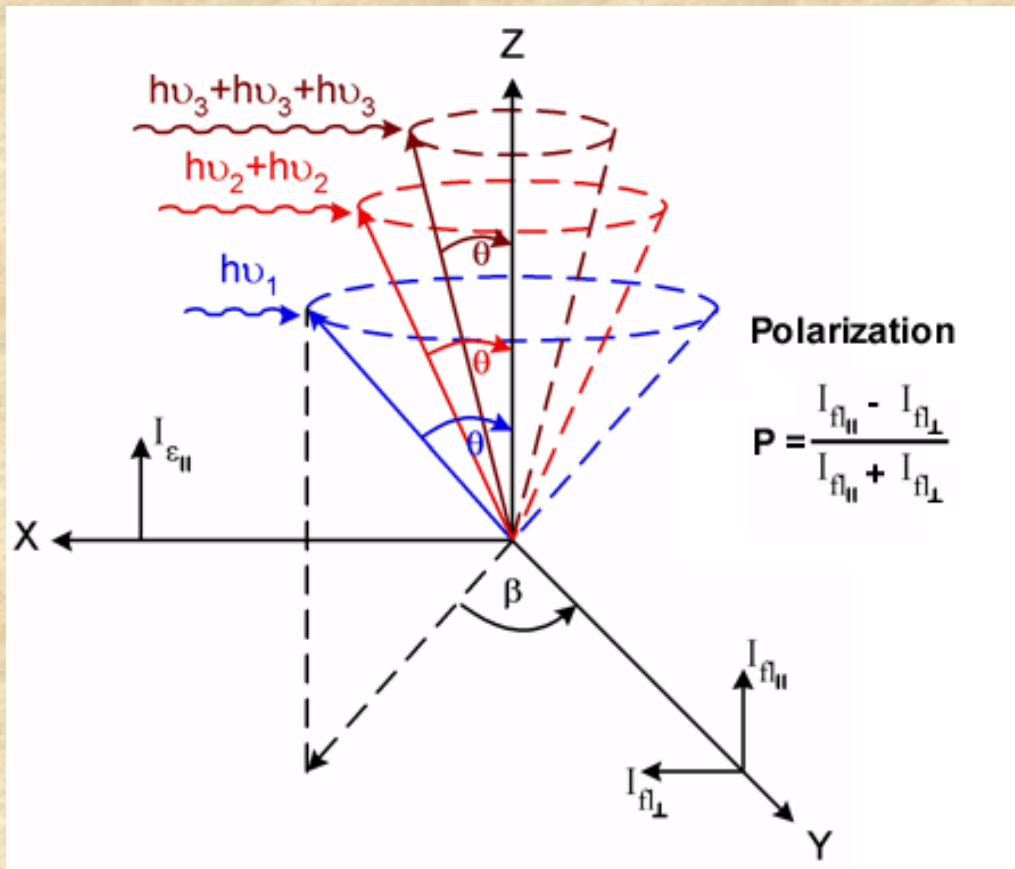
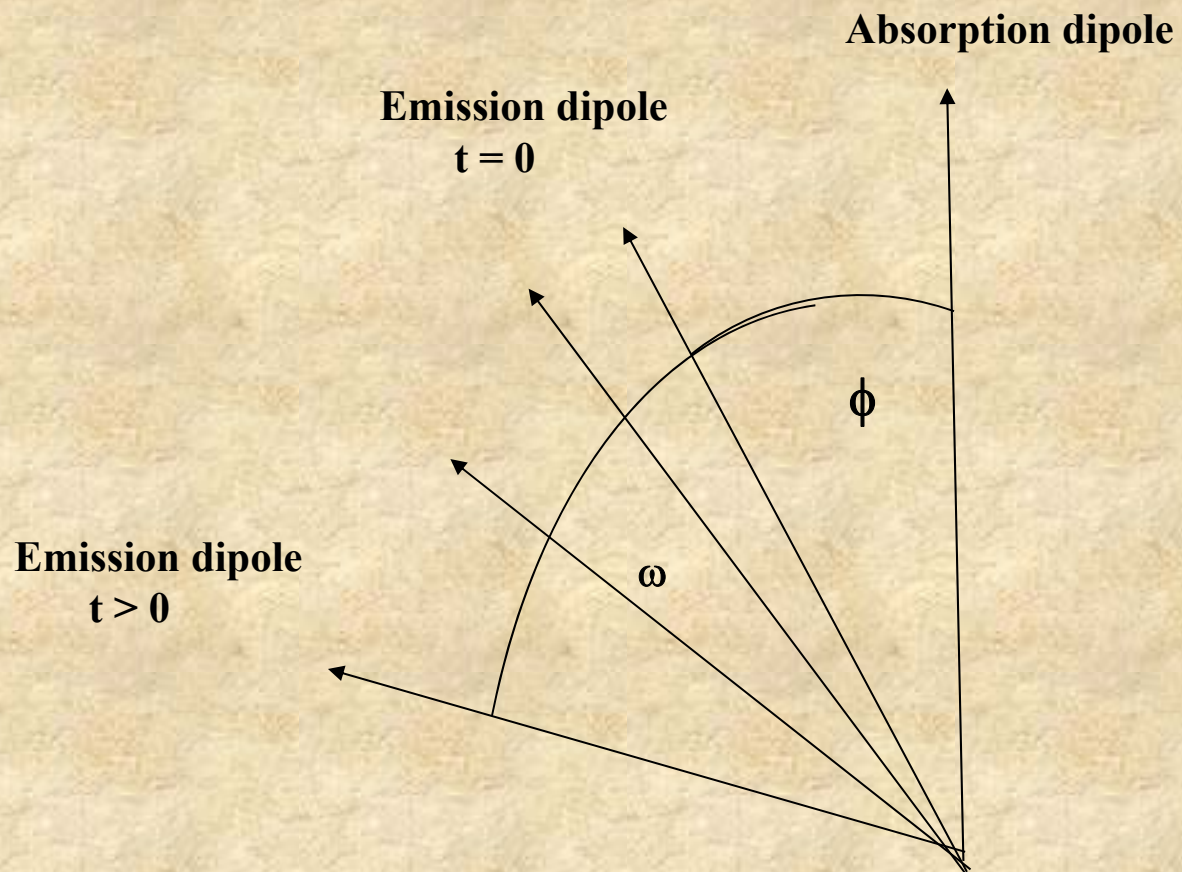


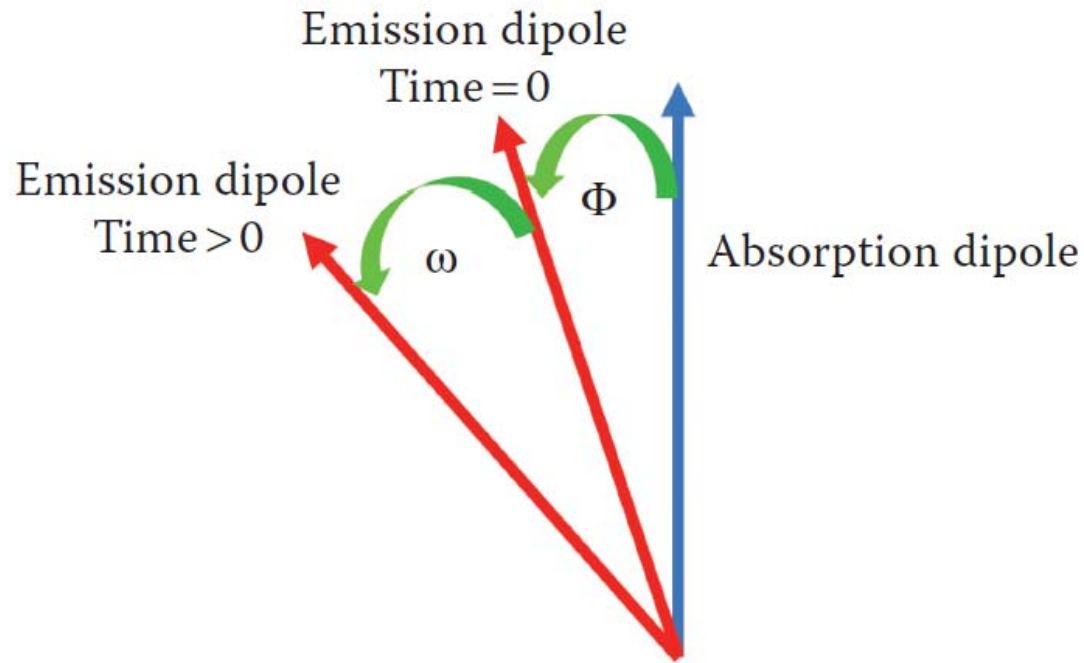
FIGURE 5.13 Excitation polarization spectra for several rhodamines in glycerol at 2°C. Rhodamine 123 (blue), Rhodamine B methyl ester (red), and tetramethylrhodamine maleimide reacted with free cysteine (green). (Reprinted with permission from D.M. Jameson and J.A. Ross, 2010. Fluorescence polarization/anisotropy in clinical diagnostics and imaging. *Chem. Rev.* 110: 2685–2708. Copyright (2010) American Chemical Society.)

Note: in the case of multi-photon excitation the limits differ



We may now consider the case where the fluorophore is permitted to rotate during the excited state lifetime.



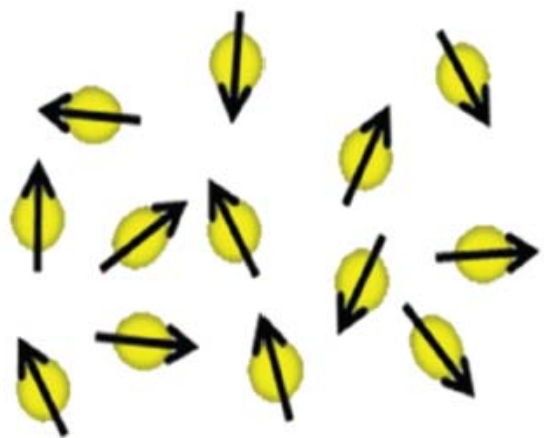


Additional depolarization occurs if the dipole rotates through an angle ω .

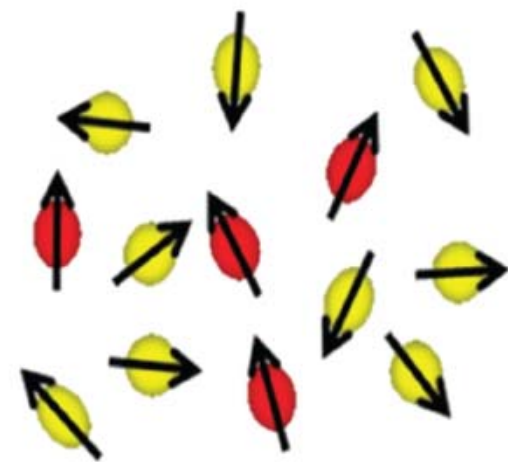
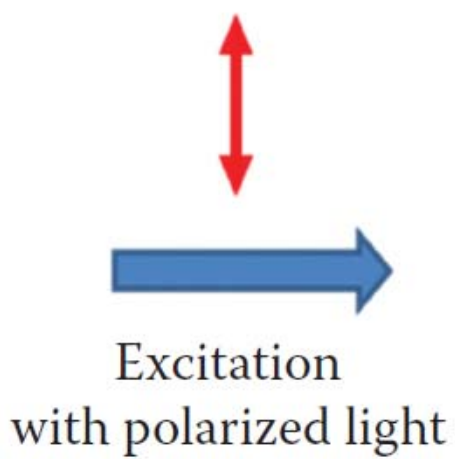
In fact:

$$\frac{1}{P} - \frac{1}{3} = \left(\frac{1}{P_0} - \frac{1}{3} \right) \left(\frac{2}{3 \cos^2 \omega - 1} \right)$$

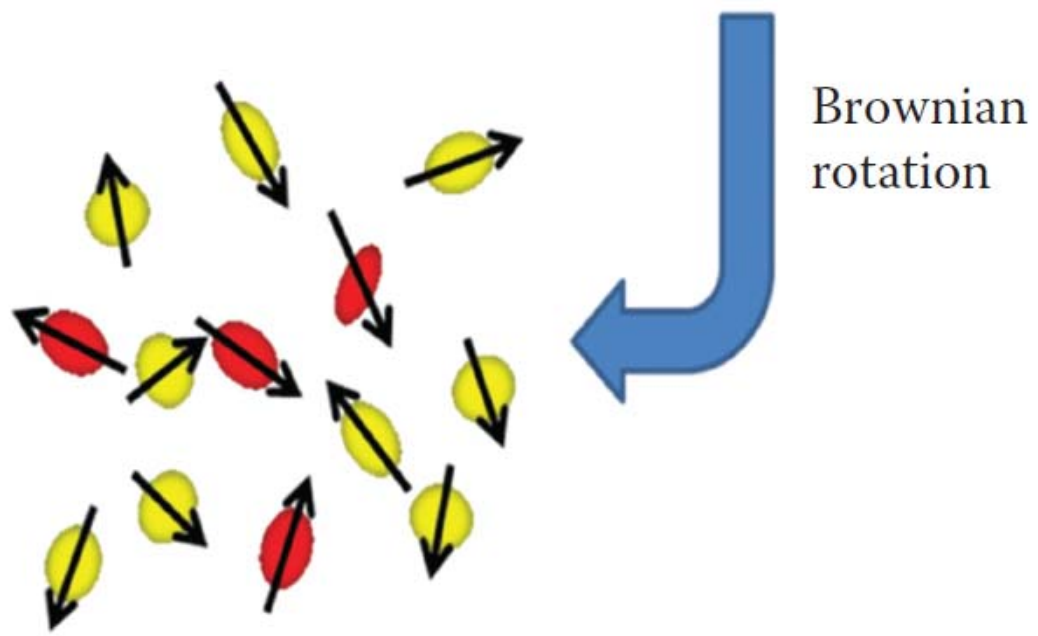
where P is the observed polarization. So the total depolarization is determined by an intrinsic factor (P_0) and an extrinsic factor (ω).



Isotropic distribution



Photoselection



Brownian rotation

F. Perrin related the observed polarization to the excited state lifetime and the rotational diffusion of a fluorophore: *Perrin, F. 1926. Polarisation de la Lumiere de Fluorescence. Vie Moyene des Molecules Fluorescentes. J. Physique. 7:390-401.*

Specifically:

$$\frac{1}{P} - \frac{1}{3} = \left(\frac{1}{P_0} - \frac{1}{3} \right) \left(1 + \frac{RT}{\eta V} \tau \right)$$

where V is the molar volume of the rotating unit, R is the universal gas constant, T the absolute temperature, η the viscosity and τ the excited state lifetime.

We can rewrite this equation as:

$$\frac{1}{P} - \frac{1}{3} = \left(\frac{1}{P_0} - \frac{1}{3} \right) \left(1 + \frac{3\tau}{\rho} \right)$$

Where ρ is the Debye rotational relaxation time which is the time for a given orientation to rotate through an angle given by the arccos e^{-1} (68.42°).

For a spherical molecule:

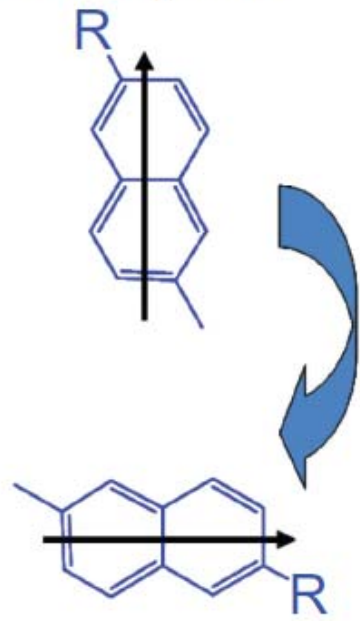
$$\rho_0 = \frac{3\eta V}{RT}$$

For a spherical protein,
it follows that:

$$\rho_0 = \frac{3\eta M(\nu + h)}{RT}$$

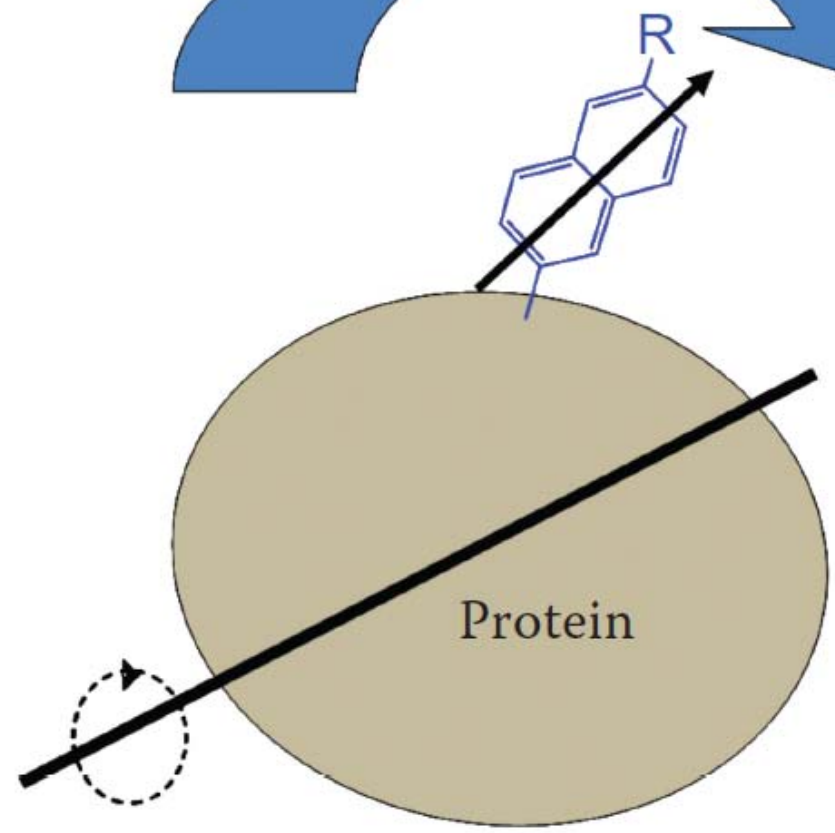
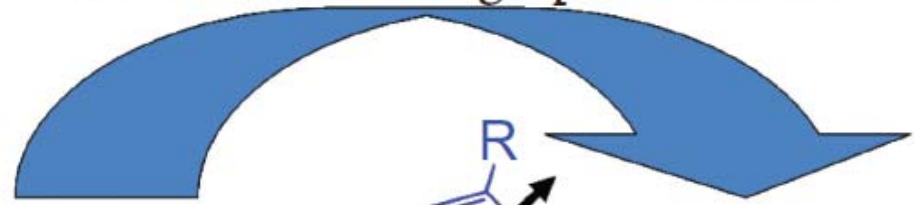
Where M is the molecular weight, ν is the partial specific volume and h the degree of hydration.

Fluorophore



Fast rotation
low polarization

Slow rotation: High polarization



Protein tumbling

* *Rotational relaxation time versus rotational correlation time.*

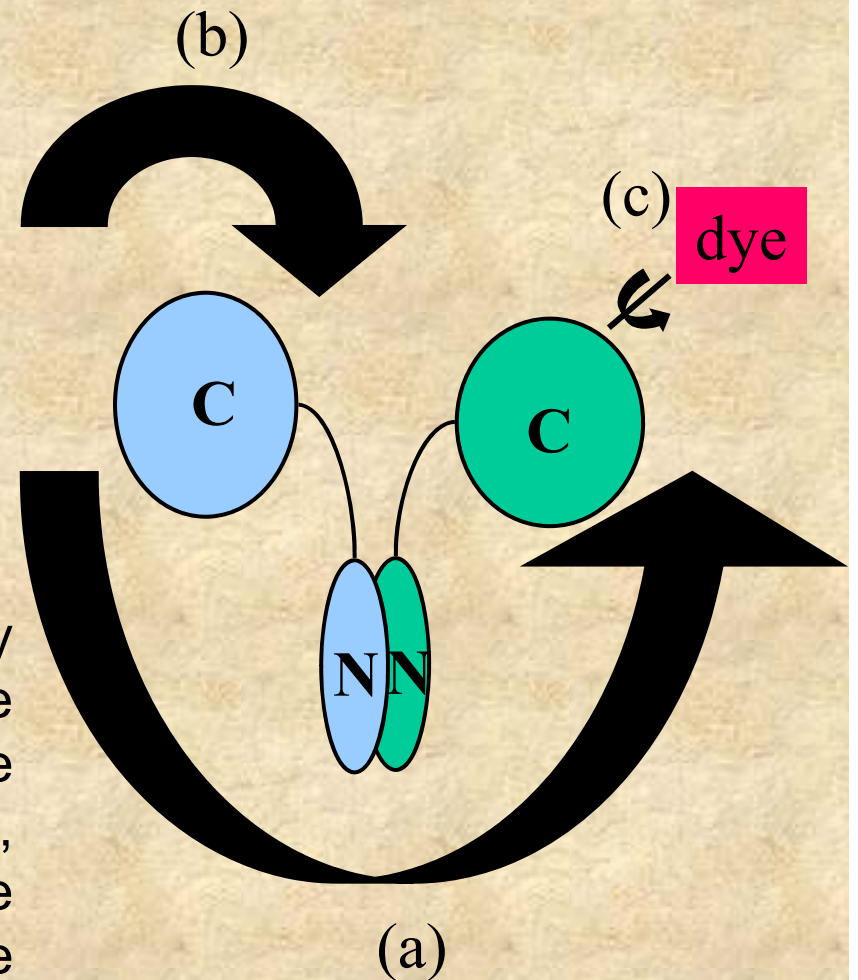
We should note that it is not uncommon to see the term “rotational correlation time”, often denoted as τ_c , used in place of the Debye rotational relaxation time. The information content of these terms is similar since $\rho = 3\tau_c$ but we have observed that some people become rather fervently attached to the use of one term or the other.

In the original development of the theories of rotational motion of fluorophores Perrin and others used the rotational relaxation time, as originally defined by Debye in his studies on dielectric phenomena. Only later (in the 1950's) during the development of nuclear magnetic resonance was the term rotational correlation time used by Bloch. It thus seems reasonable for fluorescence practitioners to use ρ but certainly adoption of either term should not lead to confusion. In terms of anisotropy and rotational correlation times, then, the Perrin equation would be:

$$\frac{r_0}{r} = \left(1 + \frac{\tau}{\tau_c} \right)$$

In the case of fluorescence probes associated non-covalently with proteins, (for example porphyrins, FAD, NADH or ANS to give but a few systems), the probe is held to the protein matrix by several points of attachment and hence its “local” mobility, that is, its ability to rotate independent of the overall “global” motion of the protein, is very restricted.

In the case of a probe attached covalently to a protein, via a linkage through an amine or sulfhydryl groups for example, or in the case of tryptophan or tyrosine sidechains, considerable “local” motion of the fluorophore can occur. In addition, the protein may consist of flexible domains which can rotate independent of the overall “global” protein rotation. This type of mobility hierarchy is illustrated on the right for the case of a probe covalently attached to a dimeric protein

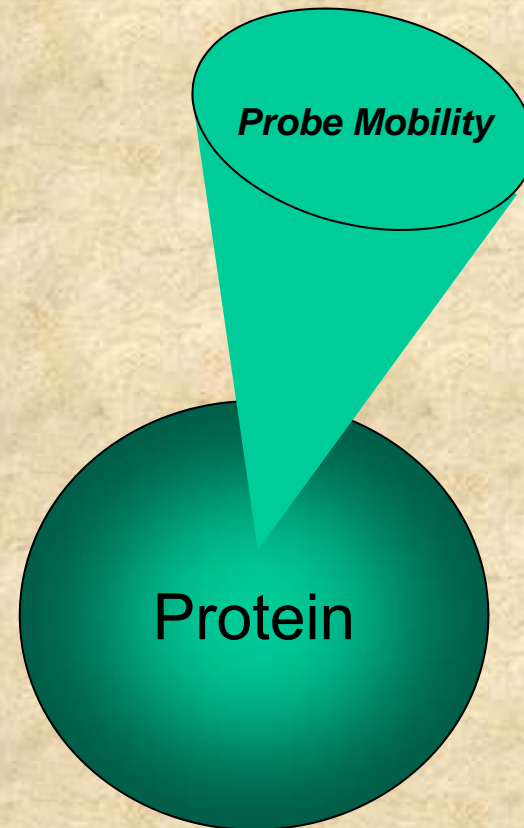


Rotational Modalities

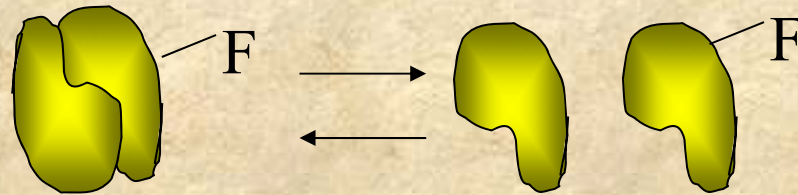
- (a) overall dimer rotation
- (b) movement of one C-domain relative to other domains
- (c) movement of dye molecule around its point of attachment

In the case of fluorescence probes associated non-covalently with proteins, (for example porphyrins, FAD, NADH or ANS to give but a few systems), the probe is held to the protein matrix by several points of attachment and hence its “local” mobility, that is, its ability to rotate independent of the overall “global” motion of the protein, is very restricted.

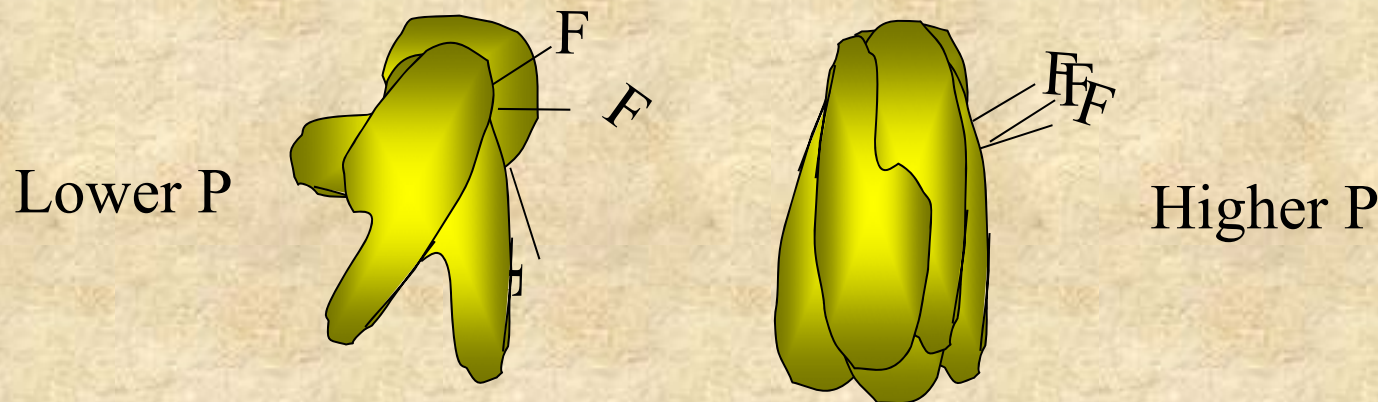
In the case of a probe attached covalently to a protein, via a linkage through an amine or sulfhydryl groups for example, or in the case of tryptophan or tyrosine sidechains, considerable “local” motion of the fluorophore can occur. In addition, the protein may consist of flexible domains which can rotate independent of the overall “global” protein rotation. This type of mobility hierarchy is illustrated on the right for the case of a probe covalently attached to a dimeric protein



Polarization methods are ideally suited to study the aggregation state of a protein. Consider, for example the case of a protein dimer - monomer equilibrium.



Following either intrinsic protein fluorescence (if possible) or by labeling the protein with a suitable probe one would expect the polarization of the system to decrease upon dissociation of the dimer into monomers since the smaller monomers will rotate more rapidly than the dimers (during the excited state lifetime).



Hence for a given probe lifetime the polarization (or anisotropy) of the monomer will be less than that of the dimer

In the concentration range near the dimer/monomer equilibrium constant, one expects to observe a polarization intermediate between that associated with either dimer or monomer. One can relate the observed polarization to the fraction of dimer or monomer using the additivity of polarizations first described by Weber (1952) namely:

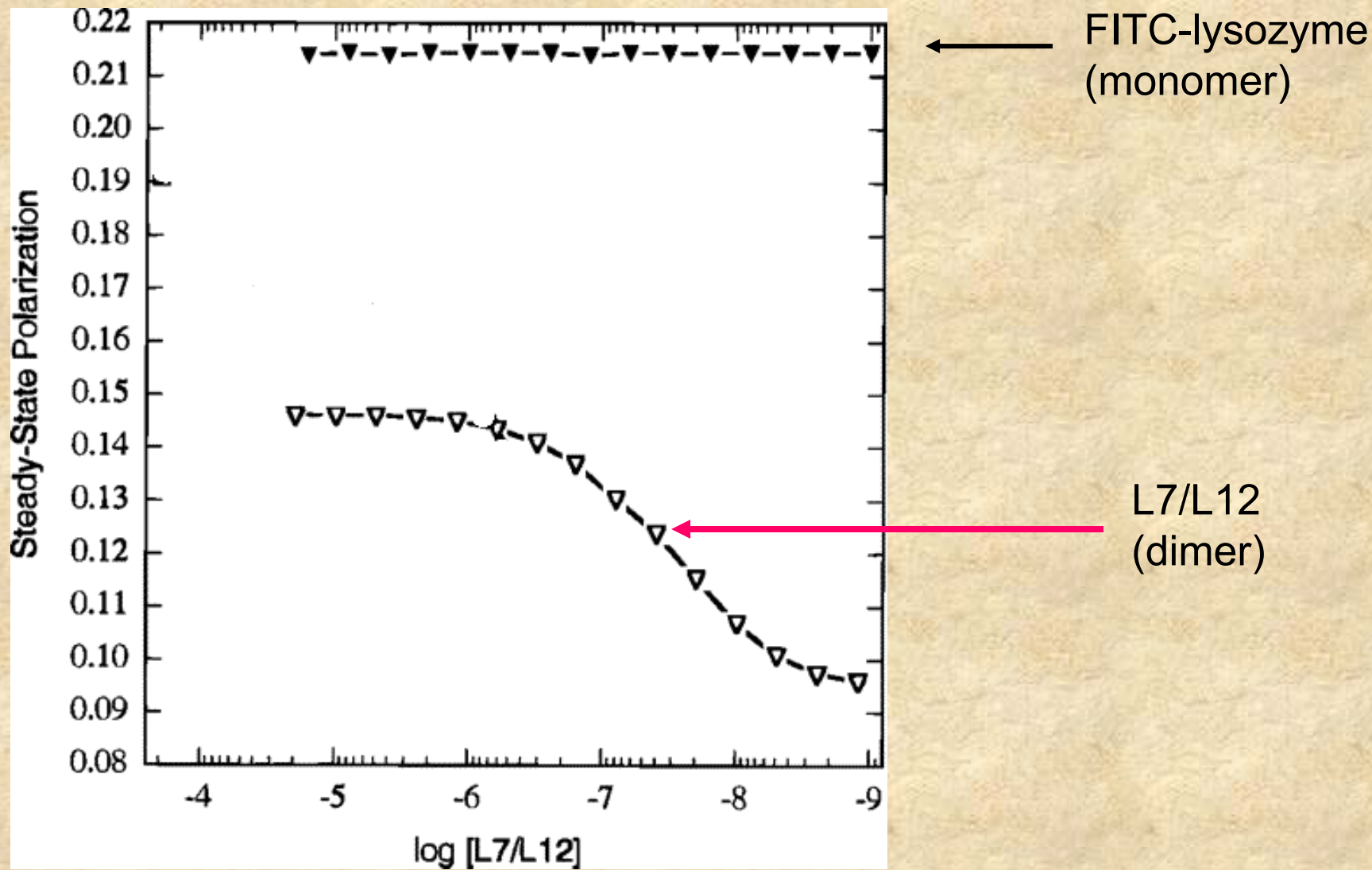
$$\left(\frac{1}{\langle P \rangle} - \frac{1}{3} \right)^{-1} = \sum f_i \left(\frac{1}{P_i} - \frac{1}{3} \right)^{-1}$$

where $\langle P \rangle$ is the observed polarization, f_i is the fractional intensity contributed by the i th component and P_i is the polarization of the i th component. One must then relate the fractional intensity contributions to molar quantities which means that one must take into account any change in the quantum yield of the fluorophore associated with either species.

The anisotropy function is directly additive (owing to the fact that the denominator represents the total emitted intensity) and hence:

$$\langle r \rangle = \sum f_i r_i$$

So to determine the dissociation constant, one can dilute the protein and observe the polarization (or anisotropy) as a function of protein concentration as shown below.



The polarization/anisotropy approach is also very useful to study protein-ligand interactions in general.

The first application of fluorescence polarization to monitor the binding of small molecules to proteins was carried out by D. Laurence in 1952 using Gregorio Weber's instrumentation in Cambridge. Specifically, Laurence studied the binding of numerous dyes, including fluorescein, eosin, acridine and others, to bovine serum albumin, and used the polarization data to estimate the binding constants.

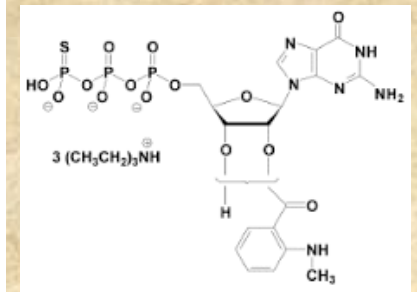
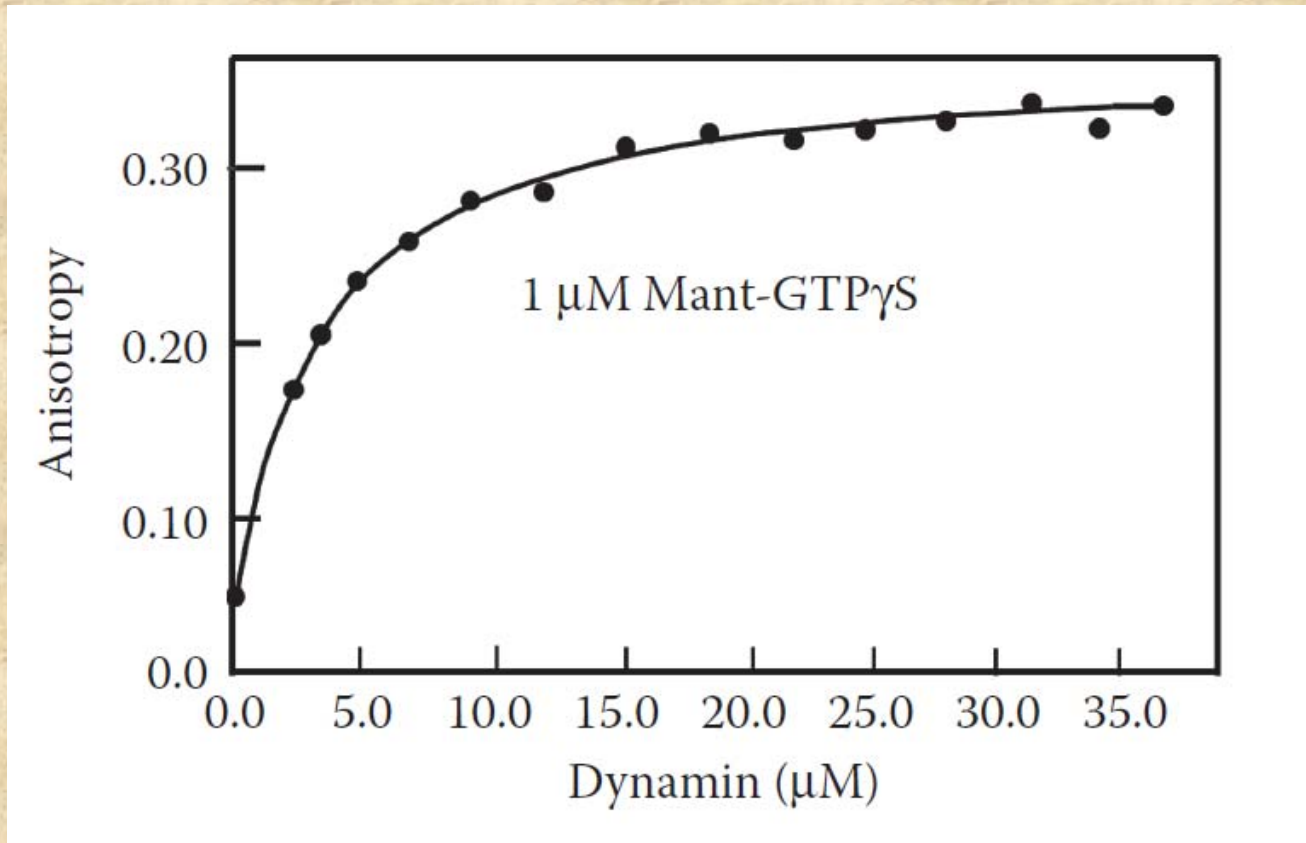
Although many probes (such as fluorescein) do not significantly alter their quantum yield upon interaction with proteins, one should not take this fact for granted and would be well advised to check. If the quantum yield does in fact change, one can readily correct the fitting equation to take the yield change into account. In terms of anisotropy the correct expression relating observed anisotropy (r) to fraction of bound ligand (x), bound anisotropy (r_b), free anisotropy (r_f), and the quantum yield enhancement factor (g) is:

$$x = \frac{r - r_f}{r_b - r_f + (g - 1)(r_b - r)}$$

In terms of polarization, the analogous equation is

$$x = \frac{(3 - P_b)(P - P_f)}{(3 - P)(P_b - P_f) + (g - 1)(3 - P_f)(P_b - P)}$$

A typical plot of polarization versus ligand/protein ratio is shown below:



In this experiment, 1 micromolar mant-GTP γ S (a fluorescent, very slowly-hydrolyzable GTP analog) was present and the concentration of the GTP-binding protein, dynamin, was varied by starting at high concentrations followed by dilution. The binding curve was fit to the anisotropy equation (in this case the yield of the fluorophore increased about 2 fold upon binding). The K_d was found to be 8.3 micromolar.

Proteolytic processing, mediated by proteolytic enzymes, or proteases, is critical to many vital biological processes, including post-translational protein processing, blood clotting, digestion, hormone processing, apoptosis, and many others, as well as many deleterious processes, such as those mediated by anthrax and botulinum neurotoxins.

Hence, an evaluation of protease activity is often a requirement for an understanding of a particular pathway or for development of novel therapeutic agents. Protease assays have been around for many decades but more recently the development of rapid and sensitive protease assays suitable for high-throughput screening has attracted considerable attention.

Fluorescence polarization lends itself very well to such assays since the essential aspect of a protease is to cleave a peptide bond which almost always results in smaller molecular weight species. Hence, if the target protein can be labeled with a fluorescence probe one would expect the polarization to decrease after proteolysis since the fluorophore will be able to rotate more rapidly after the protein mass to which it is tethered is reduced in size

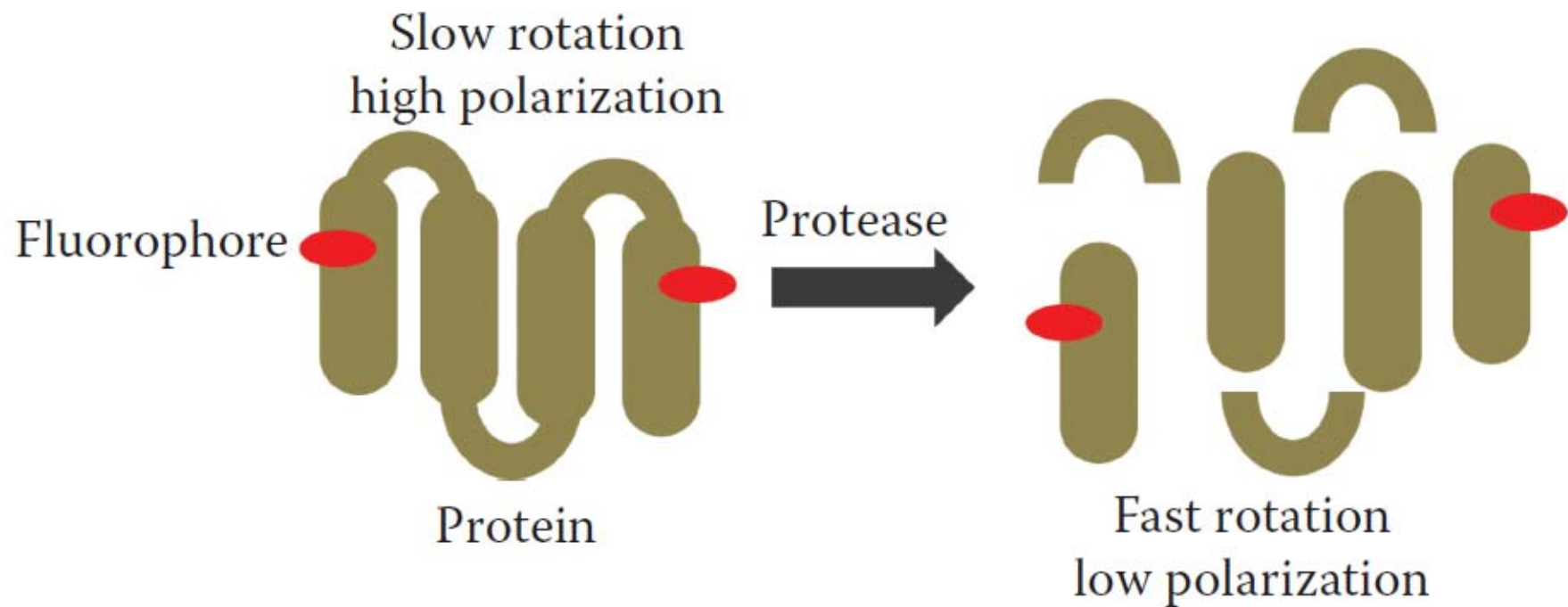


FIGURE 5.23 Depiction of the change in polarization as a fluorophore-labeled protein is treated with a protease.

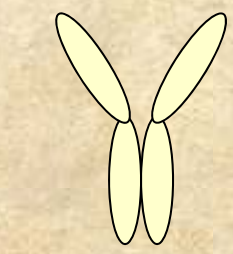
FPIA – Fluorescence Polarization ImmunoAssay

Among the first commercial instruments designed to use a fluorescence polarization immunoassay for clinical diagnostic purposes was the Abbott TDx – introduced in 1981.



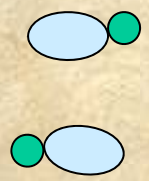
The basic principle of a polarization immunoassay is to:

- (1) Add a fluorescent analog of a target molecule – e.g., a drug – to a solution containing antibody to the target molecule
- (2) Measure the fluorescence polarization, which corresponds to the fluorophore bound to the antibody
- (3) Add the appropriate biological fluid, e.g., blood, urine, etc., and measure the decrease in polarization as the target molecules in the sample fluid bind to the antibodies, displacing the fluorescent analogs.

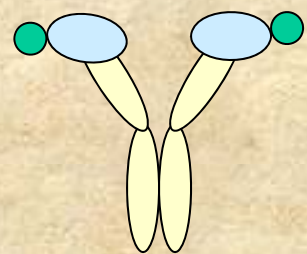


Antibody

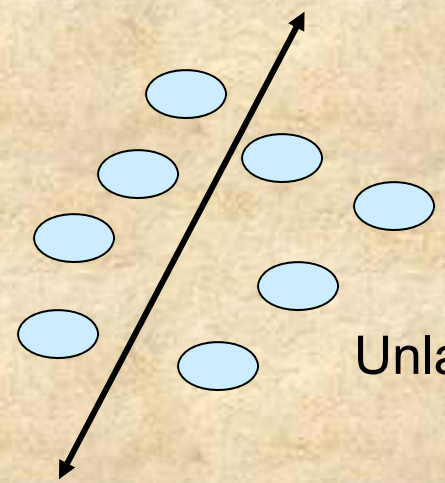
+



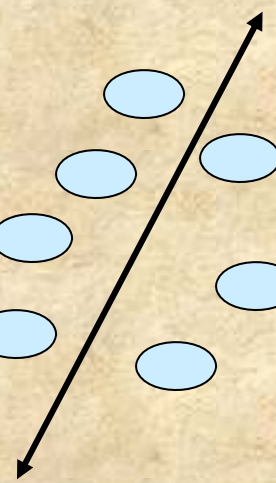
Fluorophore-linked antigen



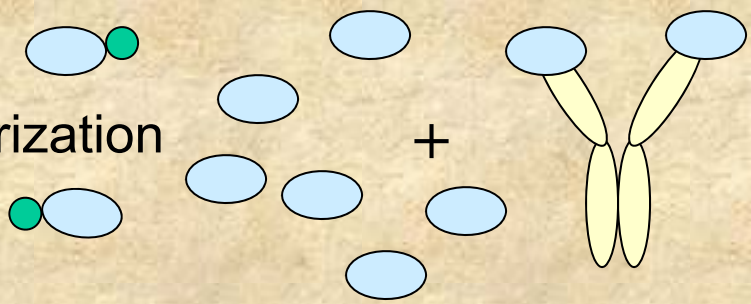
High Polarization



Unlabeled antigen



Low Polarization



+

7. Dandliker, W. B., Kelly, R. J., Dandliker, J., et al., Fluorescence polarization immunoassay. Theory and experimental method. *Immunochemistry* 10, 219–227 (1973).

CLIN. CHEM. 27/7, 1190–1197 (1981)

Fluorescence Polarization Immunoassay I. Monitoring Aminoglycoside Antibiotics in Serum and Plasma

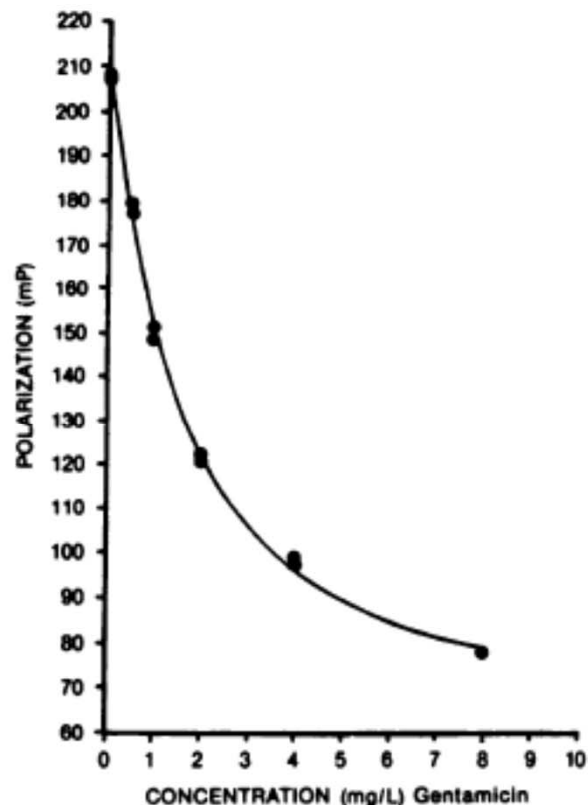
Michael E. Jolley, Stephen D. Stroupe, Chao-Huei J. Wang, Helen N. Panas, Candace L. Keegan, Robert L. Schmidt, and Kathryn S. Schwenzer

Special Apparatus

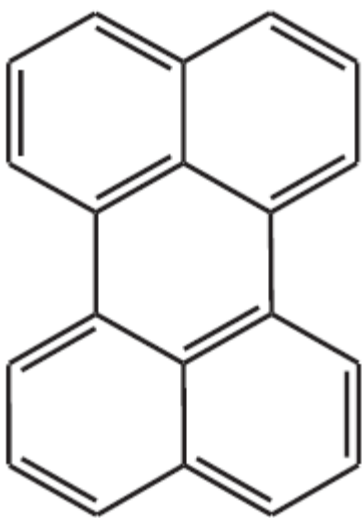
A microprocessor-controlled fluorometer was constructed in our laboratories (19). The instrument was designed to measure precisely the polarization of fluorescence emitted from the sample contained in a standard 12 × 75 mm disposable culture tube. Each determination was performed in 10 s, to a precision of ±0.001 polarization unit. The instrument determined fluorescence polarization (in arbitrary units) according to the equation (7):

$$P = \frac{I_{\text{parallel}} - I_{\text{perpendicular}}}{I_{\text{parallel}} + I_{\text{perpendicular}}}$$

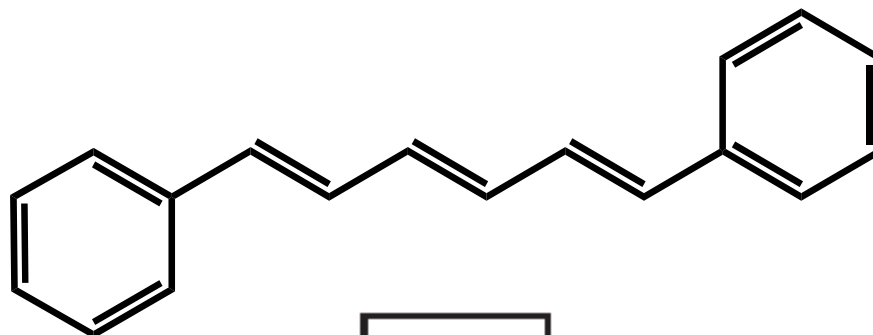
where I represents light intensity. For convenience, results are reported in millipolarization units (mP), where 1 mP = 0.001 P.



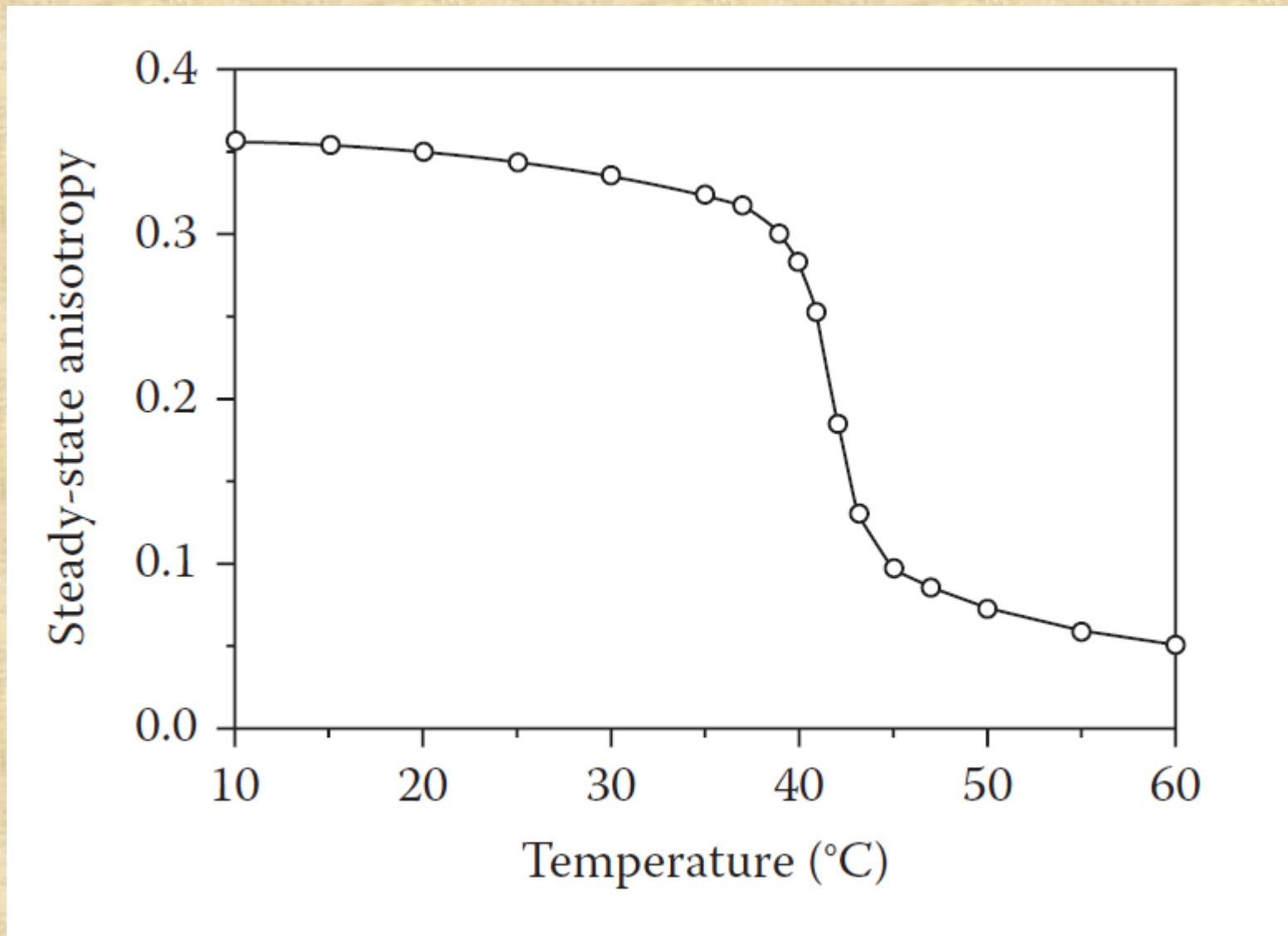
In 1971, Gregorio Weber and his colleagues introduced the use of polarization to study the physical state of lipids in model membrane systems (an idea he had actually mentioned in his PhD thesis of 1947). In that work they used perylene and a few other fluorescent dyes. A few years later Meir Shinitzky (who had been a postdoctoral fellow with Weber and a coauthor on the 1971 paper) and Yechezkel Barenholz introduced the probe diphenylhexatriene (DPH), which arguably became the most popular fluorescence polarization membrane probe of all time.



Perylene

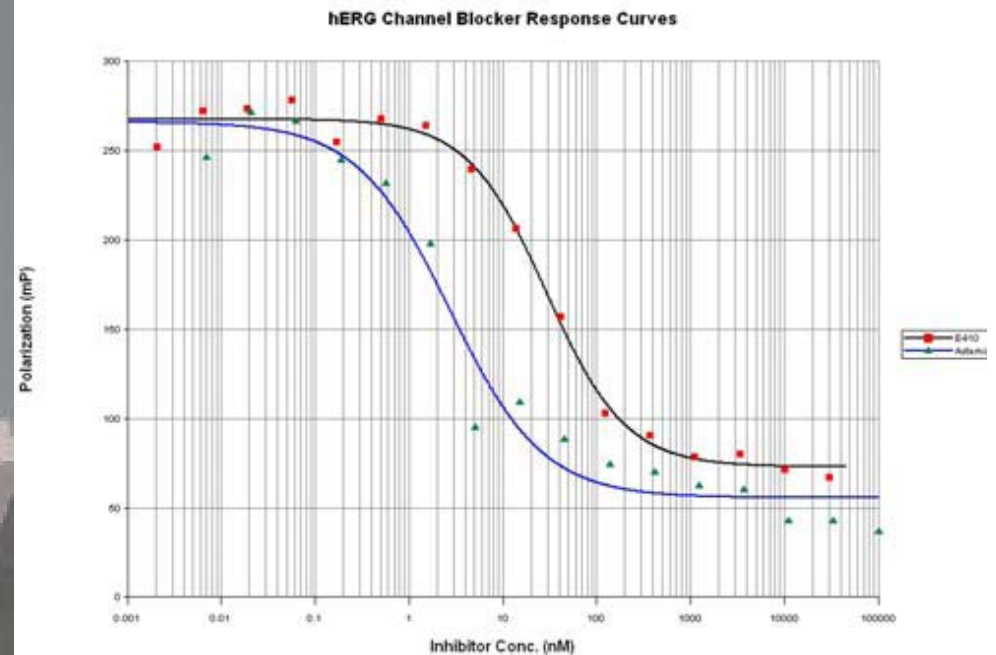


DPH

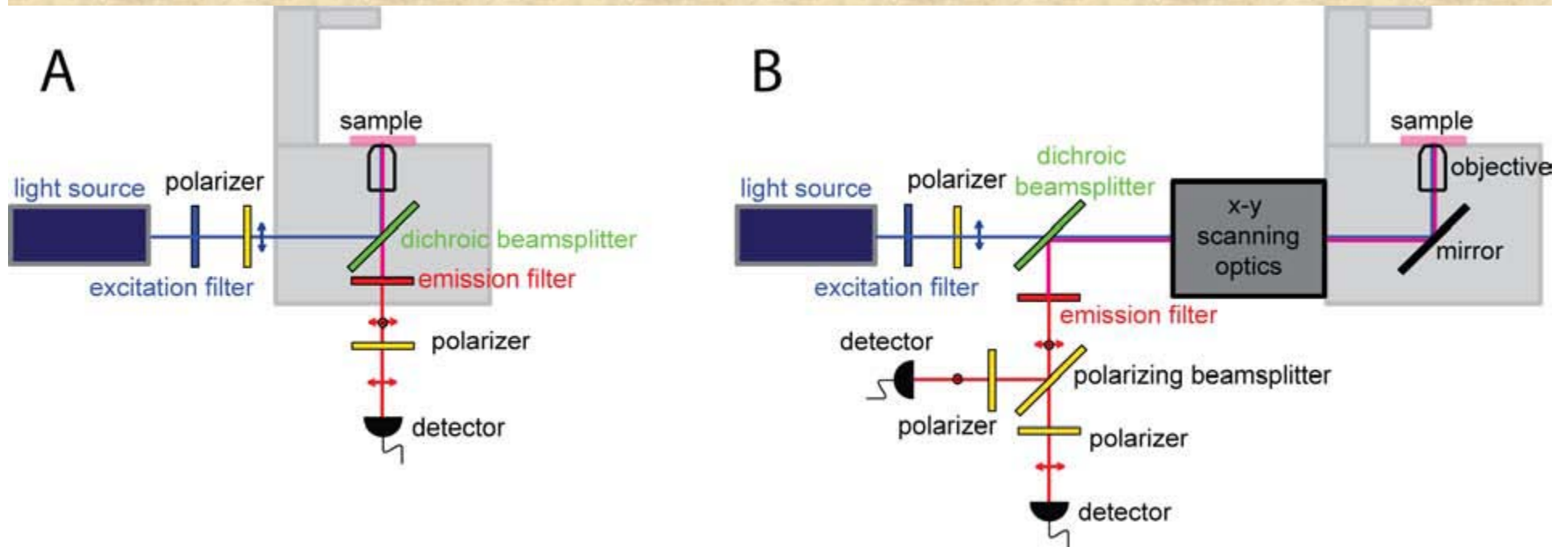


**Anisotropy of DPH in DPPC vesicles as a function of temperature
(courtesy of Ivo Konopasek from <http://web.natur.cuni.cz/~konop/gallery.php>)**

Fluorescence polarization platereaders are available for High Throughput Screening experiments



Fluorescence Polarization Microscopy



Numerical aperture effects will lower the measured polarization

Jameson and Ross

Chem. Rev. 2010, 110, 2685–2708

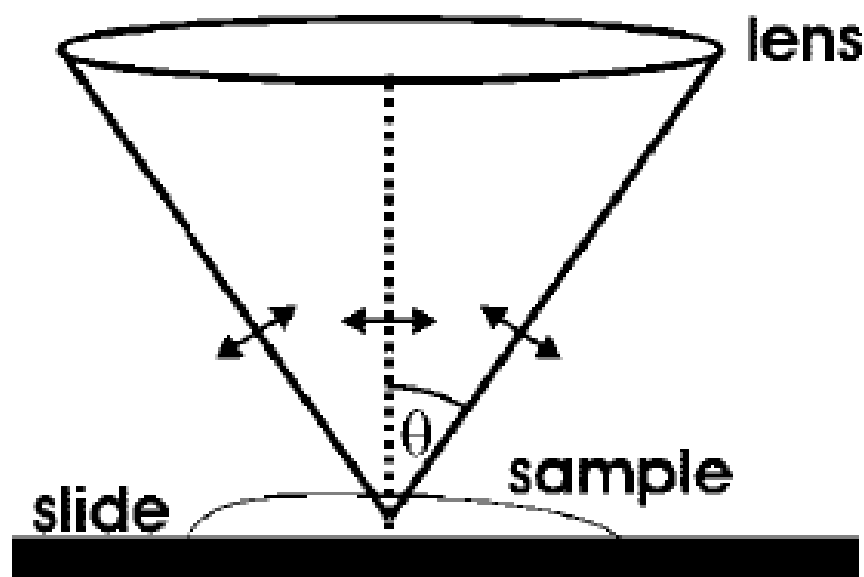


Figure 14. Diagram of light rays emitted from a lens focused on a sample with half angle θ . Arrows indicate the orientation of the electric field vector of the incident light.

CARBOCYANINE DYE ORIENTATION IN RED CELL MEMBRANE STUDIED BY MICROSCOPIC FLUORESCENCE POLARIZATION

DANIEL AXELROD, *Biophysics Research Division and Department of Physics, The University of Michigan, Ann Arbor, Michigan 48109 U.S.A*

Biophys J. 1979 Jun;26(3):557-73

APPENDIX

High Aperture Correction of Fluorescence Polarization

We must first define two right-handed coordinate systems (Fig. 7): one (the X system) is a microscope-fixed reference frame; the other (the X^0 system) is a nonfixed frame convenient for analyzing the polarization of rays in object space. Both of these systems share the same origin at which is located the transition dipole moments of the fluorescent sample under view in the object space of the objective. We assume for simplicity of units that the adsorption and emission dipole moments are of unit magnitude.

In the X system, X_1 is parallel to the optical axis of the microscope and the X_3 axis is parallel to the electric field vector of the polarized excitation light. An emission dipole has components along these axes denoted by (x_1, x_2, x_3) . A typical emitted fluorescence ray propagates toward the objective in a direction given by polar angle, σ , and azimuthal angle, ϕ , with respect to the X_1 and X_3 axes, respectively. Because

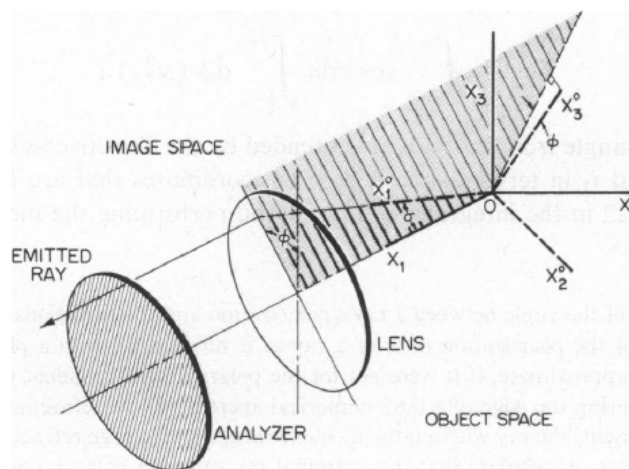
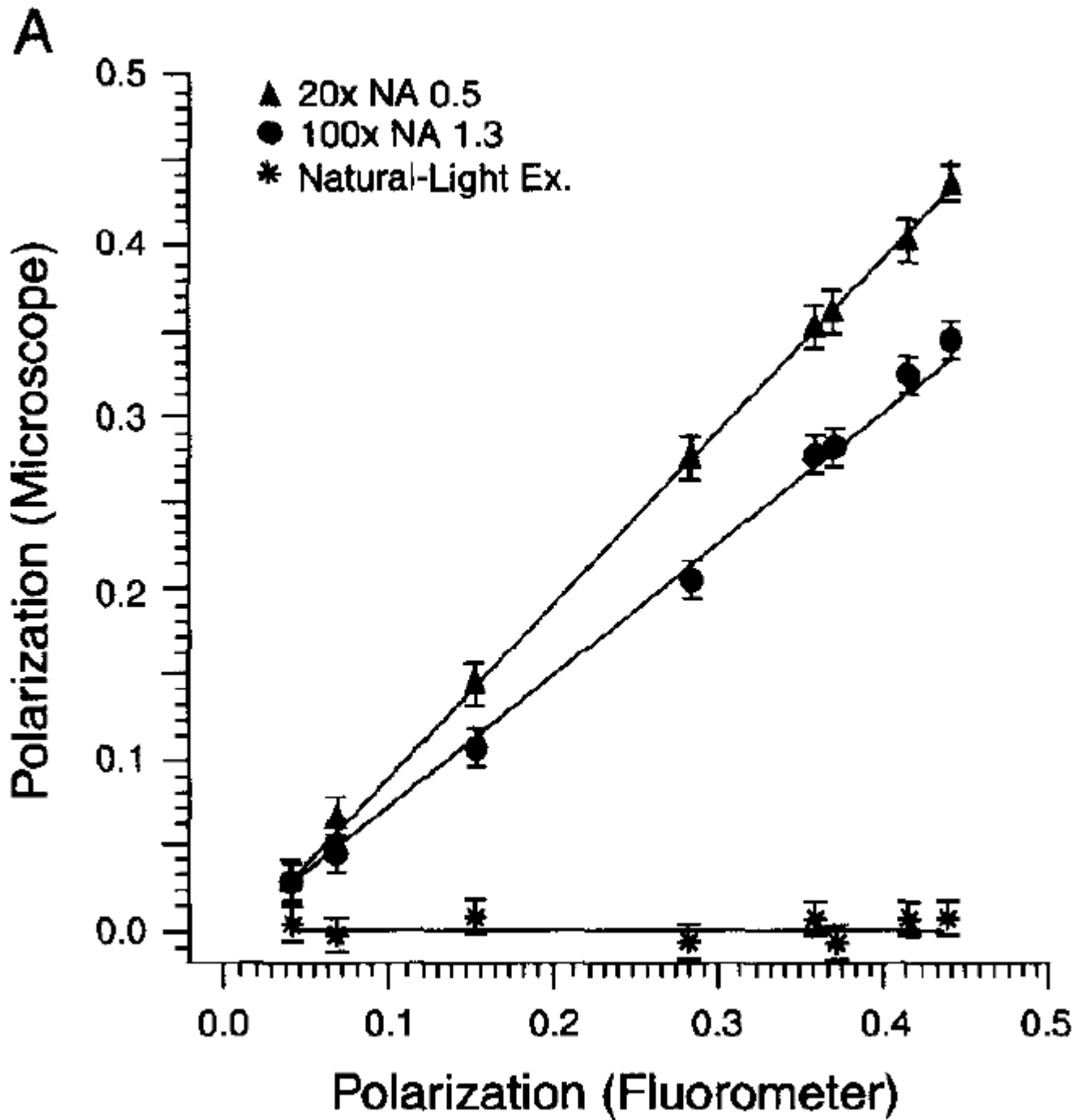


FIGURE 7 Coordinate systems X (microscope-fixed) and X^0 (emitted ray-fixed). The fluorescent sample is at origin O . The meridional plane is shaded. The emitted ray travels along X_1^0 in object space and then parallel to X_1 in image space. Axis X_3 is the direction of the excitation light polarization. Axes X_3 and X_3^0 both make the same angle ϕ with the meridional plane.



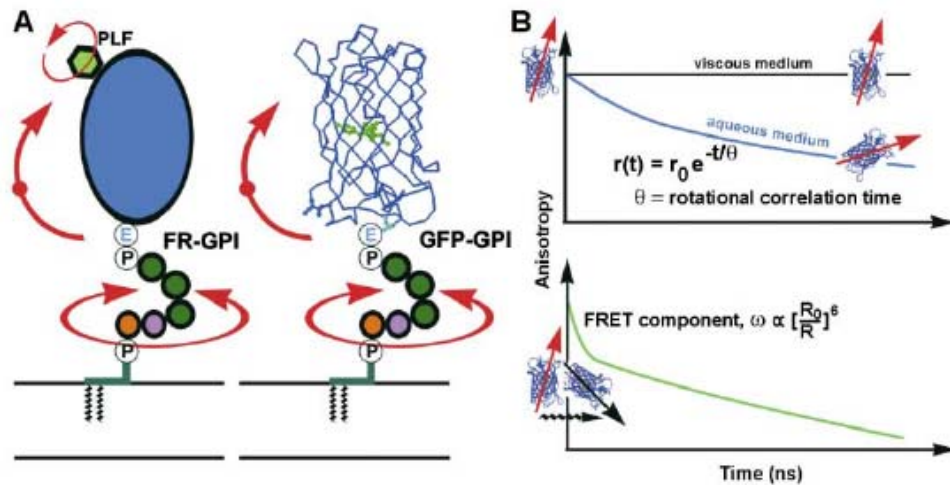
Yan and Marriott:

Methods in Enzymology,
Volume 360, 2003, Pages
561-580

Nanoscale Organization of Multiple GPI-Anchored Proteins in Living Cell Membranes

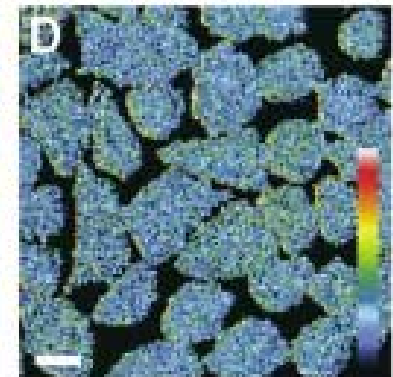
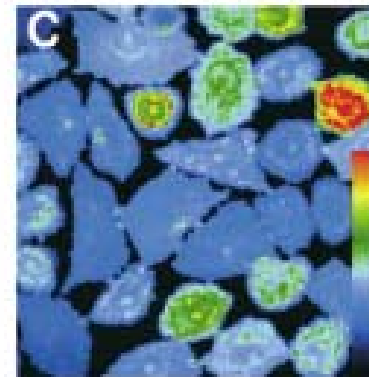
Pranav Sharma,^{1,4} Rajat Varma,^{1,4,5} R.C. Sarasij,^{2,4}
Ira,^{3,6} Karine Gousset,⁶ G. Krishnamoorthy,³
Madan Rao,^{1,2,*} and Satyajit Mayor^{1,*}

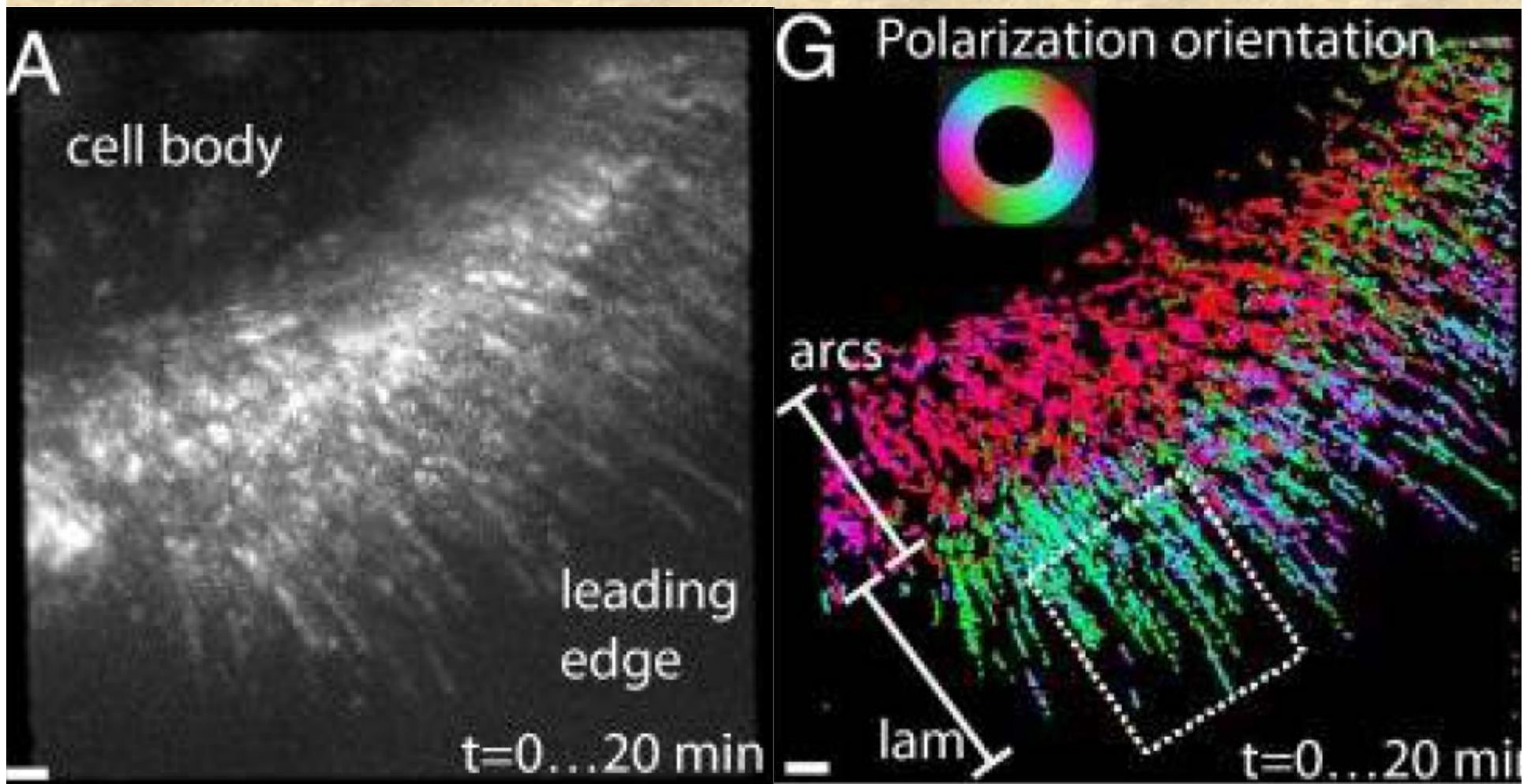
son, 2002; Jacobson and Dietrich, 1999; Simons and Ikonen, 1997; Simons and Toomre, 2000). Two major hypotheses regarding the nature of cell membrane rafts



Total intensity image

Anisotropy image





AF488-phalloidin bound to F-actin during retrograde flow in live cells

Mehta S, McQuilken M, La Riviere P, Occhipinti P, Verma A, Oldenbourg R, Gladfelter A, Tani T. Dissection of molecular assembly dynamics by tracking orientation and position of single molecules in live cells. 2016. PNAS.